THE DESIGN MULTIANIONIC CHELATING LIGANDS FOR THE PRODUCTION

OF INORGANIC OXIDIZING AGENTS. SYNTHESIS, STRUCTURE AND

REACTIVITY OF OSMIUM COMPLEXES DERIVED FROM

A TETRADENTATE TETRAANIONIC LIGAND

Thesis by

Terry Edward Krafft

In Partial Fulfillment of the Requirements

for the Degree of

Doctor of Philosophy

California Institute of Technology

Pasadena, California

1985

(Submitted February 7, 1985)

ACKNOWLEDGMENTS

Much of this project has been a collaborative effort with Steve Gipson in Fred Anson's group. Steve performed all of the electrochemistry reported in this thesis and he did other experiments as well. The somewhat convoluted way in which our results unfolded required that a significant amount of Steve's work be included here for the sake of continuity. I have tried to acknowledge Steve when appropriate, either in the text or by footnote. Any omissions are unintentional. The interaction with Steve and Fred Anson has been both productive and instructive.

A special thanks to my advisor Terry Collins. The conception of this project was his alone and throughout it he has been an excellent resource.

I would like to acknowledge Judy Christie (now Judy Audett) who began working on the osmium "ligand project." She first used what later proved to be the magic starting material and she had already made and partially characterized two of the osmium ligand complexes when I moved to this project.

Many thanks to George Spies and Bernard Santarsiero for their efforts in teaching me X-ray crystallography. Both were instrumental in helping solve the structure of the "bis pyridine" complex. Bob Coots performed two crystal structures and George Spies performed the structure of my "asymmetric complex." Their contributions are greatly appreciated. George also played a big role in the early development of the "ligand project." Other members of the Kiwi group also had considerable impact on my aspect of the project. Doug Meinhart, John Keech and the staff at the Southern California Regional NMR facility provided valuable assistance with my NMR

ABSTRACT

The design of multianionic chelating ligands for use in high valent transition metal chemistry is discussed. Possible application of such ligands to problems in inorganic oxidation chemistry is addressed. A class of potentially tetradentate tetraanionic ligands was synthesized. The ligand 1,2 -bis(3,5-dichloro-2-hydroxybenzamido)ethane (H_4CHBA-Et), 1, was found to coordinate to osmium as a tetradentate tetraanion in the oxidation states (II), (III), (IV), (V), and (VI). X-ray crystal structures of two osmium(IV) complexes of this ligand are reported. The μ-oxo dimer, $K_2(\{Os(\eta^4$-CHBA-Et)(OPPh_3)\}_2$-O), 3, features octahedral osmium with the tetradentate tetraanionic ligand 1 coordinated to the equatorial positions and the potassium ions in unusual coordination environments. The structure of octahedral $Os(\eta^4$-CHBA-Et)(py)$_2$, 5, shows the ligand 1 coordinated in the same fashion with pyridines in the axial positions.

Compound 5 and all of the osmium(IV) compounds reported here exhibit well-resolved paramagnetically shifted NMR spectra. The ^{1}H NMR data suggest the possibility of an unusual π-backbonding interaction from osmium(IV) to pyridine. Electrochemical data indicate that ligand 1 and related ligands have a profound effect on the osmium redox couples which are found at significantly lower potentials than with other ligands.

Controlled potential oxidation of 5 in the presence of water or alcohol was found to trigger a series of irreversible chemical and electrochemical transformations in which the ethane backbone of the ligand is oxidized in a selective and stepwise fashion. Several key intermediates have been isolated, independently synthesized and characterized. The first intermediate

isolated, $Os(\eta^4\text{-CHBA-ethylene})(py)_2$, **7**, results from dehydrogenation of the ligand bridge. An X-ray crystal structure of this material is reported and significant features are discussed. In the second isolated intermediate the unsaturated ethylene bridge of **7** has been oxidized to a <u>trans</u>-1,2-diether in compound **8**. A crystal structure of the related <u>trans</u>-1,2-hydroxy-alkoxy complex, **8***, has been performed. Cleavage of the bridge carbon-carbon bond in **8** yields the final oxidation products <u>cis-α</u>- and <u>trans</u>-$Os(\eta^2\text{-Fo-CHBA})_2$-$(py)_2$, **9** and **9'**, in which the amide nitrogen of each bidentate ligand is substituted with a formyl group. <u>t</u>-Bupy derivatives of both isomers have been characterized by X-ray crystal structure determinations. The diastereomeric distribution is determined by the nature of the alcohol in solution during the electrolysis. Mechanistic aspects of the ligand oxidation process are addressed.

Compounds **9** and **9'** can be converted to catalysts for the electrochemical oxidation of alcohols. The catalysts were found to be the osmium(IV) compounds <u>cis-α</u>- and <u>trans</u>-$Os(\eta^2\text{-CHBA})_2(\underline{t}\text{-Bupy})_2$, **11** and **11'**, which are formed by a selective stepwise hydrolysis of the two formyl groups in **9/9'**. A crystal structure of **11'** shows the primary amide group of 3,5-dichloro-2-hydroxybenzamide, H_2CHBA, to be coordinated through nitrogen. Chemical synthesis of the catalysts was pursued by coordination of H_2CHBA to osmium. Two of the ligands coordinate to osmium(VI) as bidentate dianions in the complex $K_2\{Os(\eta^2\text{-CHBA})_2(O)_2\}$, **12**, which can be converted to **11'**, **15** and the compounds <u>trans</u> and <u>cis</u>-$Os(\eta^2\text{-CHBA})_2(\underline{t}\text{-Bupy})(Ph_3P{=}O)$, **13** and **14**. Compound **15** has been formulated as the dimer $Os_2(\eta^2\text{-CHBA})_4(\underline{t}\text{-Bupy})_4$.

Compounds **11**, **11'**, **13** and **14** are catalysts for the electrochemical

oxidation of alcohols. The catalytic system selectively oxidizes benzyl alcohol to benzaldehyde without further oxidation to benzoic acid or benzyl esters. Approximately 150 molecules of benzyl alcohol are oxidized during the lifetime of the catalyst, 11, but activity with other alcohols is quite low. The synthesis, characterization and properties of the above osmium compounds and significant features of the catalytic system are reported.

TABLE OF CONTENTS

Page

LIST OF FIGURES

LIST OF FIGURES (continued)

LIST OF FIGURES (continued)

LIST OF TABLES

LIST OF TABLES (continued)

LIST OF SCHEMES

ABBREVIATIONS

Infrared Spectroscopy (IR)

m	medium
s	strong
vs	very strong
w	weak

Nuclear Magnetic Resonance Spectroscopy (NMR)

d	doublet
dd	doublet of doublets
dq	doublet of quartets
dt	doublet of triplets
m	multiplet
s	singlet
t	triplet
tt	triplet of triplets

Other

acac	acetylacetonate
BPG	basal plane pyrolytic graphite
bpy	bipyridine
DDQ	2,3-dichloro-5,6-dicyano-1,4-benzoquinone
E^f	formal potential of a reversible redox couple
E_p	peak potential of an irreversible oxidation
F_c	ferrocene
HBA	generic bis-o-hydroxybenzamide ligand
H_2CHBA	3,5-dichloro-2-hydroxybenzamide
H_4CHBA-DCB	1,2-bis(3,5-dichloro-2-hydroxybenzamido)-4,5-dichlorobenzene
H_4CHBA-DMBu	1,2-bis(3,5-dichloro-2-hydroxybenzamido)-2,3-dimethylbutane
H_4-CHBA-Et	1,2-bis(3,5-dichloro-2-hydroxybenzamido)ethane
H_4-CHBA-Pr	1,3-bis(3,5-dichloro-2-hydroxybenzamido)propane

Others (continued

H_2Fo-CHBA	N-formyl-3,5-dichloro-2-hydroxybenzamide
H_4-HBA-oBZ	1,2-bis(2-hydroxybenzamido)benzene
H_4HBA-Et	1,2-bis(2-hydrocybenzamido)ethane
HPLC	high pressure liquid chromatography
i	iso
L	ligand
LUMO	lowest unoccupied molecular orbital
n	normal
py	pyridine
R	alkyl group
salen	bis-salicylaldehyde-ethylenediamine
SCE	saturated calomel electrode
t	tert
t-Bupy	4-tert-butylpyridine
TBAP	tetrabutylammonium perchlorate
THAP	tetrahexylammonium perchlorate
THF	tetrahydrofuran
TLC	thin layer chromatography
trpy	terpyridine
X	halogen

CHAPTER 1

Introduction and Ligand Design

The principal idea underlying this project is that the use of appropriate multianionic chelating ligands should permit the exploration of transition metal chemistry in high oxidation states which are not normally accessible.[1] This work is part of a general interest in oxidation chemistry. The motivation for working in this area stems from two facts. The first is that high valent transition metal chemistry has been poorly developed compared with the chemistry of the lower oxidation states. The second is that there is a general need for better and more selective oxidizing agents. The successful development of new high valent transition metal species could make a significant contribution to both of these areas.

Oxidation chemistry is a broad and complex field with a long history.[2] It encompases a wide range of electron transfer and atom transfer processes. Oxygenation of hydrocarbons is of major significance to the industrial synthesis of many commodity chemicals from petroleum feedstocks.[3] Much of this chemistry involves heterogeneous catalysts, but the oxidation of organic compounds is also an important area of transition metal homogeneous catalysis.[4] Notable examples include the Wacker process[5] for oxidation of ethylene to acetaldehyde, the Mid-Century process[6] for the production of terephthalic acid and the Halcon or Oxirane process[7] for epoxidation of olefins. Oxidation is widely used in laboratory scale organic synthesis and in the manufacture of drugs. It is also an integral part of many important biochemical processes.[8] Inorganic, and particularly transition metal based oxidants feature prominently in all of these areas.

Despite the broad application of oxidative transformations to chemical synthesis, there is a notable lack of mechanistic understanding in this

chemistry.[9] Detailed mechanistic studies are often difficult or impossible for systems that involve transition metal oxidants because the reactions tend to be very rapid and complex, and often involve a considerable number of highly reactive intermediates. Inorganic oxidizing systems can be further complicated by the presence of paramagnetic species which often preclude the useful application of NMR spectroscopy. Oxidation has received little attention from inorganic chemists over the last thirty years. As a result, the role of the metal is usually poorly defined.

Another general problem in oxidation chemistry is poor selectivity.[9] This can often be traced to free radical chemistry which accompanies one electron change at the metal center. Generation of multiple oxidants in situ can also cause a mixture of products. High valent oxo compounds of chromium and manganese, which are among the most common reagents used in organic oxidation,[10] serve to illustrate these problems.

Most oxidations with permanganate, MnO_4^-,[11] are not very selective. For example, oxidation of isopropanol produces acetone, acetic acid, formic acid and carbon dioxide. The products in olefin oxidations[12] can be controlled to some extent by varying the pH, but mixtures of diols, α-hydroxy ketones and cleavage products are usually obtained. The final inorganic product is Mn(II), (III) or (IV) and depends on the conditions of the reaction. The intermediate oxidation states have been implicated as separate and distinct oxidizing agents. Poor selectivity in these systems is probably due to the presence of a number of different oxidants, each with its own unique oxidizing properties.

One system in which the multicomponent nature of the oxidizing agent has been clearly demonstrated is the Cr(VI) oxidation of secondary alcohols.[13]

Studies by Rocĕk, Wiberg and Westheimer have established the mechanism shown in Scheme 1.1 for the oxidation of isopropanol to acetone. Three separate oxidants and radical species are involved. Although the reaction is

Scheme 1.1

$$(CH_3)_2CHOH + Cr(VI) \longrightarrow (CH_3)_2C=O + Cr(IV)$$

$$2(CH_3)_2CHOH + 2Cr(IV) \longrightarrow 2(CH_3)_2\dot{C}OH + 2Cr(III)$$

$$2(CH_3)_2\dot{C}OH + 2Cr(VI) \longrightarrow 2(CH_3)_2C=O + 2Cr(V)$$

$$2Cr(V) \longrightarrow Cr(IV) + Cr(VI)$$

$$3(CH_3)_2CHOH + 2Cr(VI) \longrightarrow 3(CH_3)_2C=O + 2Cr(III)$$
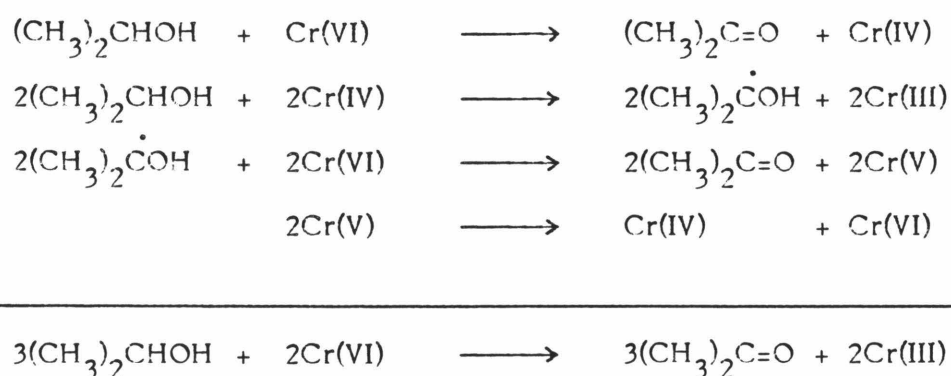
very selective for conversion of isopropanol to acetone, the one electron oxidations by Cr(IV) lead to multiple products with most other substrates. For example, in the chromic acid oxidation of cyclobutanol the Cr(VI) cleanly produces cyclobutanone (eq. 1) but the Cr(IV) generated in this process then oxidizes the substrate in a different fashion to give the cleavage product

$$(1.1)$$

$HO(CH_2)_3CHO$ (eq. 2).[13c] Each is a highly selective transformation but, since both occur, the overall reaction is nonselective.

$$\text{(1.2)}$$
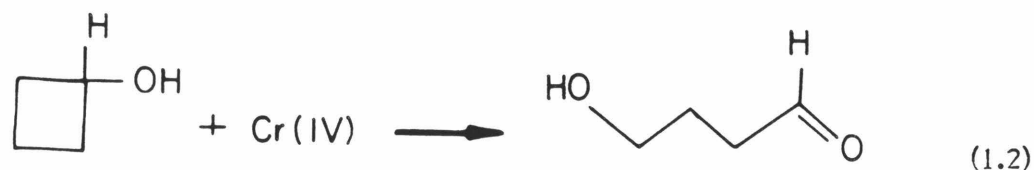
Modification of permanganate[14] and the Cr(VI) reagents[15] can lead to improved selectivity. These efforts have been rather empirical in nature and have principally involved changes in the solvent system. Although this approach has met with some success, it is rather limited in scope.

Poor selectivity and lack of mechanistic understanding are common problems in oxidation chemistry. Both of these limitations might be addressed in transition metal systems by developing ligands which provide greater control over the reactivity of the metal. We believe that high valent transition metal chemistry has been limited by the small number of suitable ligands. A survey of high valent manganese compounds[16-19] provides an illustration of this point.

Only nine Mn(V), (VI) and (VII) compounds have been well characterized (Table 1.1).[20] This is a sharp contrast with the thousands of manganese complexes that are known for the lower oxidation states.[16] The coordinating atoms are restricted to the highly electronegative elements oxygen, nitrogen, fluorine and chlorine and, with the exception of the one porphyrin nitrido complex, all of the ligands are monodentate and monatomic species. The same limitations apply to other very highly oxidized metals. In the absence of additional ligands, diversification of this chemistry is severely confined.

Our approach has been to develop new multianionic chelating ligands which are compatible with highly oxidized metal centers. The use of appropriate ligands should allow synthesis of new high valent transition metal

Table 1.1. Known high valent manganese compounds.[16-19]

Mn(V)	Mn(VI)	Mn(VII)
MnO_4^{3-}	MnO_4^{2-}	MnO_4^-
$MnOCl_3$	MnO_2Cl_2	MnO_3Cl
		MnO_3F
		Mn_2O_7

(TpMPP)MnN

aSee references 19 and 20. TpMPP = tetrakis(p-methoxyphenyl)porphyrinato dianion.

complexes. By expanding this class of compounds, we expect to uncover new structural types and new modes of reactivity. A chelating ligand which is resistant to oxidation, which coordinates through strong σ donation and which carries sufficient negative charge could lead to complexes of the type shown schematically in Figure 1.1.
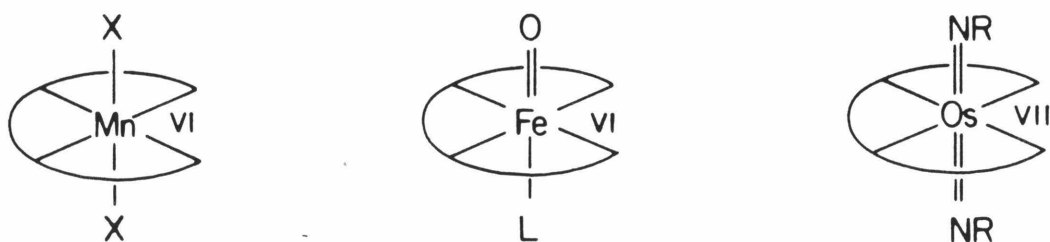
Figure 1.1.   Potential high valent chelate complexes with schematic tetradentate tetraanionic ligands.

These new ligands could provide the means to control reactivity and improve selectivity. For example, a clean oxo transfer reagent might be

developed in which the reduced inorganic product is rendered unreactive by stabilization from the ligand (eq. 1.3). The ligands could permit development of new electrochemical oxidations and could provide a means to control reactivity by varying the redox potentials of the complexes. Incorporation of

$$\overset{O}{\underset{L}{\parallel}}\,M^{n} + S \longrightarrow M^{n-2} + SO \qquad (1.3)$$
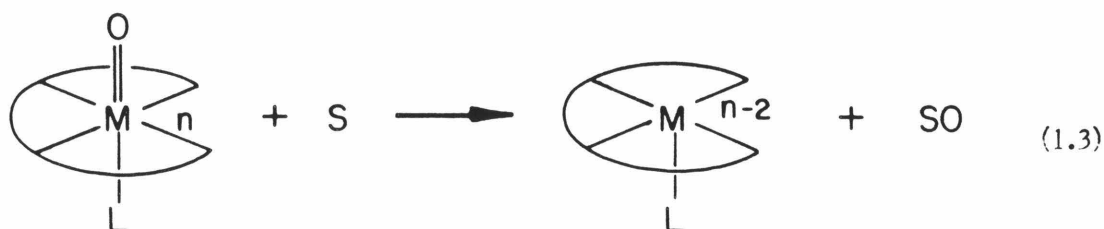
steric bulk or stereochemical features on the ligand could be used to produce selective systems. Mechanistic work might also be aided by higher stability of intermediates.

The development of ligands which are suitable for use in high valent transition metal chemistry requires consideration of the following. The use of strong σ donors is necessary to stabilize metals in high oxidation states. Coordinating atoms must be restricted to highly electronegative elements to prevent their oxidation by the metal. Chelation by the ligand is desirable since it should impart added stability to the complexes. This feature requires the ability to build on to the coordinating atoms which leaves oxygen and nitrogen as the two best choices. The following design features are considered necessary for chelating ligands used in high valent metal chemistry:

1. incorporation of O and/or N as the coordinating atoms;

2. sufficient negative charge to help counter the high positive charge on the metal center;

3. resistance to oxidation throughout the entire ligand;

4. formation of five or six membered metallacycles on coordination;

5. chemically and substitutionally inert binding sites;

6. a means of derivatization to change donor properties of the ligand or to incorporate steric and stereochemical features;

7. sufficient flexibility to aid in coordination;

8. simple and economic syntheses.

A number of ligand systems which incorporate these features can be envisaged. The system we have chosen to work with as a starting point in this project is based on a bis o-hydroxybenzamido (HBA) framework (Fig. 1.2).[21] The HBA ligand can function as a tetradentate tetraanion when coordinated through deprotonated amido nitrogens and phenoxy oxygens. Both the phenoxy[22] and amido*[23] groups are strong σ donors. The deprotonated amide in particular is known to be an excellent σ donor when coordinated through nitrogen.[23-26]

Margerum et al. synthesized a series of copper(III) and nickel(III) com-plexes[24] with chelating polypeptide ligands which coordinate through amines, carboxylates and deprotonated amides in various combinations. The study

---

*Unless otherwise noted, amide or amido refer to the organic amide group (e.g., RCONHR), not to the deprotonated amino group (e.g., R_2N^-), which has the same name in transition metal chemistry.
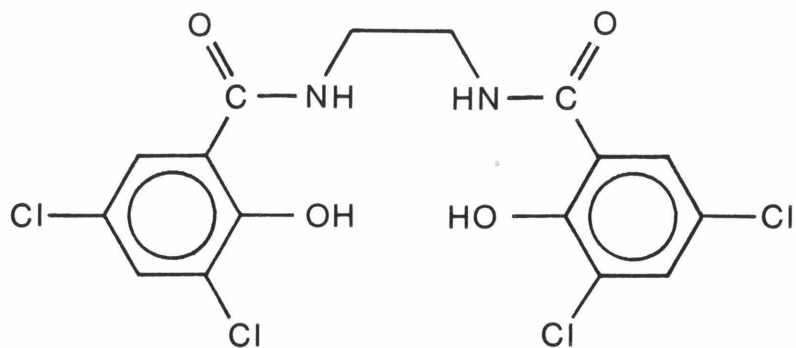
1,2-bis(3,5-dichloro-2-hydroxybenzamido)ethane (H$_4$CHBA-Et)
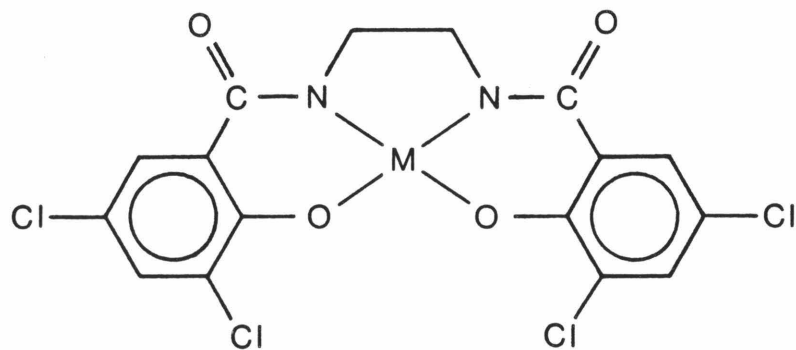
Figure 1.2.   An HBA ligand and its coordination as a tetradentate tetra-anion.

showed that the copper(III/II) couple is significantly reduced when a carboxylate

or amine is replaced with a deprotonated amide. The accessibility of these

relatively high oxidation states and the stability of the complexes has been

attributed, in large part, to the strong donation from the amido ligands.

Copper(III) and nickel(III) complexes can be produced with certain other

amide containing ligands.[25] A silver(III) polypeptide complex has also been

reported.[26] The production of cobalt(IV)[1b] and osmium(V)[1a] HBA complexes

in this group has further substantiated the unique ability of deprotonated

amides to stabilize high oxidation states.

Considerable oxidative resistance of the HBA ligands can be achieved by appropriate substitution. Margerum's work[27] has shown that a methylene unit adjacent to an amide in polypeptide ligands is a potential site of ligand decomposition. We have documented in some detail the sensitivity of the methylene units in our ligand, 1,2-bis(3,5-dichloro-2-hydroxybenzamido) ethane, H_4CHBA-Et (see Chapter 3). This problem can be avoided by substitution of alkyl groups for the methylene hydrogens.[28] Alternatively, in our system an arene ring can be used in place of the alkyl bridge.[1a] Substitution can also be included at the oxidatively sensitive sites on the phenolic rings.

The HBA ligand forms a 6,5,6 chelate ring system when coordinated to a single metal center (Fig. 1.2). The framework is similar to that found in certain schiff base ligands like salen, which are known to coordinate easily to many different metals. Both the phenolic rings and the ligand backbone provide substitutional sites through which the donor properties of the ligand can be systematically varied. They also provide the means to incorporate steric bulk or chiral centers into HBA complexes.

Numerous HBA ligands have now been prepared (Table 1.2). These form a family of potentially tetradentate tetranionic ligands which generally meet the design criteria listed above. The combination of high negative charge and strong σ donation from the phenoxy and amido groups makes these excellent ligands for stabilizing high oxidation states. The use of some of the ligands is limited by insufficient resistance to oxidation, but those which are protected against oxidation are suitable for coordination to strongly oxidizing

Table 1.2. Some representative HBA ligands.[a]
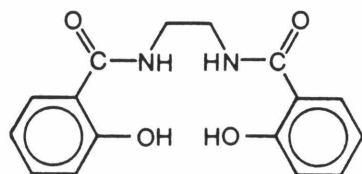
1,2-bis(2-hydroxybenzamido)-ethane
(H$_4$HBA-Et)[b]
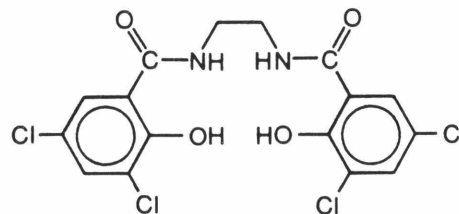
1,2-bis(3,5-dichloro-2-hydroxybenzamido)-
ethane   (H$_4$CHBA-Et)[c]
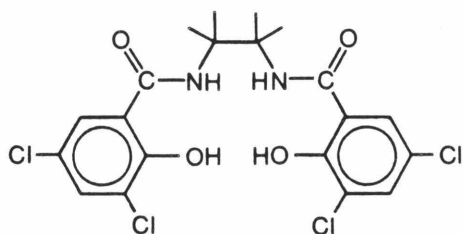
1,2-bis(3,5-dichloro-2-hydroxybenzamido)-
2,3-dimethylbutane   (H$_4$CHBA-DMBu)[c]
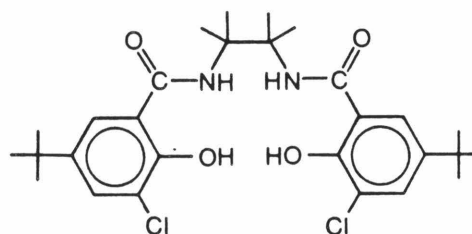
1,2-bis(5-t-butyl-2-hydroxybenzamido)-2,3-
dimethylbutane   (H$_4$-t-BuHBA-DMBu)[c]
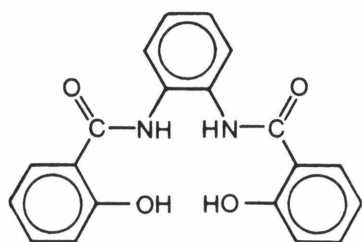
1,2-bis(2-hydroxybenzamido)-benzene
(H$_4$HBA-o-Bz)[b]
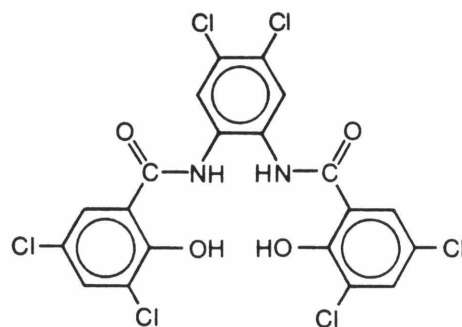
1,2-bis(3,5-dichloro-2-hydroxybenzamido)-
4,5-dichlorobenzene   (H$_4$CHBA-DCB)[d]

[a]The nomenclature has been chosen to emphasize the hydroxybenzamido
group. [b]Reference 29. [c]See Chapter 2. [d]Reference 1a.

metal centers. A variety of osmium, cobalt, rhodium, nickel and copper complexes have been synthesized with these ligands[1,30] and it appears that considerable diversification of this chemistry is possible.

Extension to the early transition metals may be hindered by their apparent preference for binding the amide carbonyl oxygen rather than the amide nitrogen.[23,29] Siegel and Martin[23] suggest that deprotonation of the amide nitrogen is promoted by the presence of later transition metal ions which can bind to the deprotonated amide nitrogen. They further suggest that the early transition metals are ineffective at replacing the amide proton. These conclusions are based on results obtained with divalent ions and may not be valid for metals in high oxidation states. The absence of early transition metal N-bound amides may be due to kinetic rather than thermodynamic problems. Several chromium complexes which contain deprotonated N-bound amides have been characterized[1d,31] indicating that additional chemistry with the early transition metals may be possible. Attempts to enter into the maganese chemistry of HBA ligands have not yet been successful.[32]

Precedents exist for high valent chemistry with certain other chelating ligands (Fig. 1.3). The most notable example is the porphyrin ligand.[8,33] A number of high valent porphyrin complexes, such as $(TPP)Cr^{IV}O$[34] and $(TpMPP)Mn^{V}N$,*[19] have been structurally characterized. Several metalloporphyrin complexes form the basis of catalytic systems which oxidize organic substrates. For example, $(TPP)CrCl$,[35] $(TPP)MnCl$[36]

---

*TPP = tetraphenylporphyrinato dianion. TpMPP = tetrakis(p-methoxyphenyl)-porphyrinato dianion.
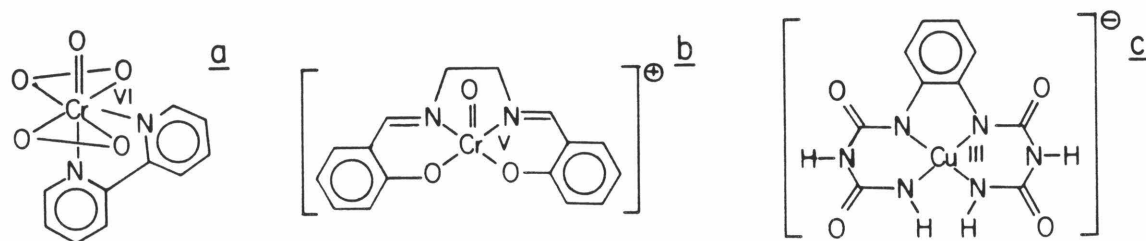
<u>Figure 1.3.</u>   Some structurally characterized high valent chelate complexes. [a]Reference 43a. [b]Reference 42. [c]Reference 25b.

and (TPP)FeCl[36a,37] catalyze the oxidation of organic substrates by oxidants such as iodosobenzene or tosylimidoiodobenzene. High valent chromium, manganese and iron complexes have been implicated as the active species in these systems. A considerable degree of selectivity can be achieved with certain metalloporphyrin catalyzed oxidations.[37b] The oxidative sensitivity of the ligand is ultimately the limiting factor in this chemistry. Efforts have recently been undertaken to address this problem.[38]

Other chelating ligands found in high valent transition metal chemistry include corroles (e.g. (corrolato)Cr^{V}O),[39] schiff bases (e.g., PF$_6$((salen)Cr^{V}O)),[40] peroxide (e.g. (bipy)(O$_2$)$_2$Cr^{VI}O),[41] oximines (e.g., ClO$_4$(R(dioximato)$_2$Co^{IV}L)),[42] α-hydroxy carboxylates (e.g., Na((O$_2$COCR$_2$)$_2$Cr^{V}O)),[43] polypeptides and related amide containing ligands[23-26] (e.g. (n-Bu)$_4$N (o-phenylenebis(biuretato)Cu^{III})),[25b] macro-cyclic cyclams (e.g. (cyclamato)Ag^{III})[44] and neutral aromatic complexes such as phenanthroline and bipyridine.[45]

All of these ligands, with the exception of peroxide, suffer to varying

degrees from oxidative sensitivity. Many of the complexes mentioned above
are stable only at low temperature and some of the peroxide complexes are
explosive. Nevertheless, the successful production of certain high valent
complexes and the development of oxidizing systems with some of these
ligands are encouraging results suggesting that further pursuits are
warranted. The deliberate design and synthesis of more suitable ligands will
undoubtedly widen the scope of this chemistry.

References and Notes

(1)   (a) Anson, F. C.; Christie, J. A.; Collins, T. J.; Coots, R. J.;
Furutani, T. T.; Gipson, S. L.; Keech, J. T.; Krafft, T. E.;
Santarsiero, B. D.; Spies, G. H. J. Am. Chem. Soc. (1984), 106, 4460.
(b) Anson, F. C.; Collins, T. J.; Coots, R. J.; Gipson, S. L.; Richmond,
T. G. Ibid. (1984), 106, 5037. (c) Collins, T. J.; Krafft, T. E.;
Santarsiero, B. D.; Spies, G. H. J. Chem. Soc., Chem. Commun.
(1984), 198. (d) Collins, T. J.; Santarsiero, B. D.; Spies, G. H. Ibid.
(1983), 681.

(2)   Wiberg, K. W., Ed. "Oxidation in Organic Chemistry, Part A"; Academic
Press, Inc.: New York, 1965. (b) Trahanovsky, W. S., Ed. "Oxidation
in Organic Chemistry, Part B"; Academic Press, Inc.: New York,
1973. (c) Trahanovsky, W. S., Ed. "Oxidation in Organic Chemistry,
Part C"; Academic Press, Inc.: New York, 1978. (d) Benson, D.
"Mechanism of Oxidations by Metal Ions"; Elsevier: New York, 1976.
(e) House, H. O. "Modern Synthetic Reactions"; Benjamin/Cummings:
Menlo Park, 1972.

(3)   Dumas, T.; Bulani, W. "Oxidation of Petrochemicals: Chemistry and
Technology"; John Wiley and Sons: New York, 1974.

(4)   (a) Parshall, G. W. "Homogeneous Catalysis"; John Wiley and Sons:
New York, 1980, pp. 185-207. (b) Sheldon, R. A.; Kochi, J. A. "Metal-
Catalyzed Oxidation of Organic Compounds"; Academic Press: New
York, 1981, pp. 17-32.

(5)   Parshall, G. W. "Homogeneous Catalysis"; John Wiley and Sons: New
York, 1980, pp. 101-104.

(6)   Dumas, T.; Bulani, W. "Oxidation of Petrochemicals: Chemistry and Technology"; John Wiley and Sons: New York, 1974, pp. 39-47.

(7)   (a) Sharpless, K. B.; Verhoeven, T. R. Aldrichimica Acta (1979), 12, 63. (b) Landau, R.; Sullivan, G. A.; Brown, D. Chemtech (1979), 602.

(8)   Spiro, T. G., Ed. "Metal Ion Activation of Dioxygen"; John Wiley and Sons: New York, 1980.

(9)   Collins, T. J., Ed. Report of the International Workshop on "Activation of Dioxygen Species and Homogeneous Catalytic Oxidations"; Galzignano (Padova), Italy, June 28-29, 1984.

(10)   Lee, D. G. "The Oxidation of Organic Compounds by Permanganate Ion and Hexavalent Chromium"; Open Court: La Salle, Illinois, 1980.

(11)   Stewart, R. In "Oxidation in Organic Chemistry, Part A," Wiberg, K. W., Ed.; Academic Press, Inc.: New York, 1965, pp. 1-68.

(12)   (a) Wiberg, K. B.; Saegebarth, K. A. J. Am. Chem. Soc. (1957), 79, 2822. (b) Lee, D. G.; Brownridge, J. R. Ibid. (1974), 96, 5517. (c) Simándi, L. I.; Jáky, M. Ibid. (1976), 98, 1995. (d) Wolfe, S.; Ingold, C. F.; Lemieux, R. U. Ibid. (1981), 103, 938. (e) Wolfe, S.; Ingold, C. F. Ibid. (1981), 103, 940. (f) Simándi, L. I., Jáky, M.; Freeman, F.; Fuselier, C. O.; Karchefski, E. M. Inorg. Chim. Acta (1978), 31, L457.

(13)   (a) Watanabe, W.; Westheimer, F. W. J. Chem.Phys. (1949), 17, 61. (b) Hampton, J.; Leo, A.; Westheimer, F. W. J. Am. Chem. Soc. (1956), 78, 306. (c) Roček, J.; Radkowsky, A. E. Ibid. (1968), 90, 2986. (d) Wiberg, K. B.; Schäfer, H. Ibid. (1969), 91, 927. (e) Rahman, M.; Roček, J. Ibid. (1971), 93, 5455, 5462. (f) Wiberg, K. B.; Mukherjee, S. K. Ibid. (1974), 96, 1884. (g) Wiberg, K. B. "Oxidation in Organic

Chemistry, Part A"; Academic Press, Inc.: New York, 1965, pp. 69-184.

(14)   (a) Gunstone, F. D. "Hydroxylation Methods," in "Advances in Organic Chemistry," Raphael, R. A.; Taylor, E. C.; Wynberg, H., Eds.; Interscience: New York, 1960, Vol. 1, pp. 133-135. (b) Sam, D. J.; Simmons, H. E. J. Am. Chem. Soc. (1972), 94, 4024. (c) Sala, T.; Sargent, M. V. J. Chem. Soc., Chem. Commun. (1978), 253. (d) Schmidt, H. J.; Schafer, H. J. Angew. Chem. Int. Ed. (1979), 18, 68, 69.

(15)   (a) Snatzke, G. Chem. Ber. (1961), 94, 729. (b) Collins, J. C.; Hess, W. W.; Frank, F. J. Tetrahedron Lett. (1968), 3363. (c) Corey, E. J.; Suggs, J. W. Ibid. (1975), 2647. (d) Poos, G. I.; Guth, G. E.; Beyler, R. E.; Sarett, L. H. J. Am. Chem. Soc. (1953), 75, 422. (e) Sharpless, K. B.; Kageyasu, A. Ibid. (1975), 97, 5927.

(16)   Cotton, F. A.; Wilkinson, G. "Advanced Inorganic Chemistry," 4th ed.; John Wiley and Sons: New York, 1980, pp. 736-749.

(17)   Levason, W.; McAuliffe, C. A. Coord. Chem. Rev. (1972), 7, 353.

(18)   Briggs, T. S. J. Inorg. Nucl. Chem. (1968), 30, 2866.

(19)   Hill, C. L.; Hollander, F. J. J. Am. Chem. Soc. (1982), 104, 7318.

(20)   The Mn(V) compound Cl(TPP)Mn = O has been claimed but its structure has not yet been established. Groves, J. T.; Kruper, Jr., W. J.; Haushalter, R. C. J. Am. Chem. Soc. (1980), 102, 6375.

(21)   Synthesis of the unsubstituted ligand, 1,2-bis(2-hydroxybenzamido) ethane (H_4HBA-Et), and a Cu(II) complex of it have been reported. Ojima, H. Nippon Kaguku Zusshi (1967), 88, 329. Chem. Abstr. (1967), 67, 7589r.

(22)   Jones, R. D.; Summerville, D. A.; Basolo, F. Chem. Rev. (1979), 79, 139.

(23)   Sigel, H.; Martin, R. B. Chem. Rev. (1982), 82, 385.

(24)   (a) Margerum, D.W.; Wong, L. F.; Bossu, F. P.; Chellapa, K. L.; Czarnecki, J. J.; Kirksey, Jr., S. T.; Neubecker, T. A. Adv. Chem. Ser. (1977), 162, 281. (b) Margerum, D. W. Pure & Appl. Chem. (1983), 55, 23.

(25)   (a) Bour,J. J.; Birker, P. J. M. W. L.; Steggerda, J. J. Inorg. Chem. (1971), 10, 1202. (b) Birker, P. J. M. W. L. Ibid. (1977), 16, 2478. (c) Kimura, E.; Sakonaka, A.; Machida, R. J. Am. Chem. Soc. (1982), 104, 4255. (d) Fabbrizzi, L.; Perotti, A.; Poggi, A. Inorg. Chem. (1983), 22, 1411. (e) Oliver, K. J.; Waters, T. N. J. Chem. Soc., Chem. Commun. (1982), 1111.

(26)   Kirschenbaum, L. J.; Rush, J. D. J. Am. Chem. Soc. (1984), 106, 1003.

(27)   Rybka, J. S.; Margerum, D. W. Inorg. Chem. (1981), 20, 1453.

(28)   Kirksey, Jr., S. T.; Neubecker, T. A.; Margerum, D. W. J. Am. Chem. Soc. (1979), 101, 1631.

(29)   Spies, G.H. Ph.D. Thesis, California Institute of Technology, October, 1984.

(30)   Barner-Thorsen, C. J.; Keech, J. T.; Lee, S. C.; Peake, G. T.; Richmond, T. G.; Spies, G. H.; York, J. B. Unpublished results.

(31)   (a) Baral, S.; Cotton, F. A.; Ilsley, W. H. Inorg. Chem. (1981), 20, 2696. (b) Cotton, F. A.; Ilsley, W.H.; Kaim, W. J. Am. Chem. Soc. (1980), 102, 3464, 3475.

(32)   Krafft, T. E. Unpublished results.

(33) Smith, K. M., Ed. "Porphyrins and Metalloporphyrins"; Elsevier: New York, 1975.

(34) Groves, J. T.; Kruper, Jr., W. J.; Haushalter, R. C.; Butler, W. M. Inorg. Chem. (1982), 21, 1363.

(35) Groves, J. T.; Kruper, Jr., W. J. J. Am. Chem. Soc. (1979), 101, 7613.

(36) (a) Breslow, R.; Gellman, S. H. J. Chem. Soc., Chem. Commun. (1982), 1400. (b) Hill, C. L.; Schardt, B. C. J. Am. Chem. Soc. (1980), 102, 6374. (c) Groves, J. T.; Kruper, Jr., W. J.; Haushalter, R. C. Ibid. (1980), 102, 6375.

(37) (a) Groves, J. T.; Nemo, T. E. J. Am. Chem. Soc. (1983), 105, 5786, 6243. (b) Groves, J. T.; Myers, R. S. Ibid. (1983), 105, 5791.

(38) Traylor, P. S.; Dolphin, D.; Traylor, T. G. J. Chem. Soc., Chem. Commun. (1984), 279.

(39) Murakami, Y.; Matsuda, Y.; Yamada, S. J. Chem. Soc., Dalton Trans. (1981), 855.

(40) Siddall, T. L.; Migaura, N.; Huffman, J. C.; Kochi, J. K. J. Chem. Soc., Chem. Commun. (1983), 1185.

(41) (a) Stromberg, R.; Ainalem, I. B. Acta Chem. Scand. (1968), 22, 1439. (b) Stromberg, R.; Brosset, C. Ibid. (1960), 14, 441.

(42) Topich, J.; Halpern, J. Inorg. Chem. (1979), 18, 1339.

(43) Krumpolc, M.; Rocek, J. J. Am. Chem. Soc. (1979), 101, 3206.

(44) (a) Barefield, E. K.; Mocella, M. T. Inorg. Chem. (1973), 12, 2829. (b) Lovecchio, F. V.; Gore, E. S.; Busch, D. H. J. Am. Chem. Soc. (1974), 96, 3109.

(45) (a) Gersten, S. W.; Samuels, G. J.; Meyer, T. J. J. Am. Chem. Soc.

(1982), <u>104</u>, 4029. (b) Moyer, B. A.; Thompson, M. S.; Meyer, T. J. <u>Ibid.</u> (1980), <u>102</u>, 2310. (c) Gaudiello, J. G.; Bradley, P. G.; Norton, K. A.; Woodruff, W. H.; Bard, A. J. <u>Inorg. Chem.</u> (1984), <u>23</u>, 3.

CHAPTER 2

Ligand Syntheses and Coordination of the Tetradentate Tetraanionic

Ligand, 1,2-bis(3,5-dichloro-2-hydroxybenzamido)ethane,

H_4CHBA-Et, to Osmium

Introduction

The first goal of this project was to find simple and economic syntheses for the HBA ligands. Several approaches to the problem were pursued. A general and facile synthetic route, which was first developed by Dr. George Spies,[1] is reported in this chapter. A broad range of substituted compounds can now be produced from readily available starting materials.

Initial studies on the coordination chemistry of the HBA ligands focused on chromium,[1,2] manganese[3] and iron.[1] Although this work produced some interesting complexes, particularly with chromium, the chemistry proved to be more difficult than anticipated. In an effort to develop a more productive exploratory system we turned our attention to osmium chemistry.[4] The work in this and subsequent chapters deals with osmium complexes derived from the ligand H_4CHBA-Et.

H_4CHBA-Et and H_4HBA-Et were largely employed in the initial studies with chromium, manganese, iron and osmium. Both ligands contain methylene units on the bridge. These were recognized as potential sites of decomposition[5] (see Chapter 1, page 10 and Chapter 3), but the ligands were deemed suitable for initial studies of HBA coordination chemistry since the starting metal complexes were generally not very oxidizing.

A straightforward method for coordinating H_4CHBA-Et to osmium as a tetradentate, tetraanion was discovered. The initial complex, $K_2[Os(\eta^4\text{-}CHBA\text{-}Et)(O)_2]$, can be converted into other osmium chelate compounds in various oxidation states. Two of these have been characterized by X-ray crystal structure determinations. Unique structural features and properties of these $\eta^4\text{-}CHBA\text{-}Et^{4-}$ osmium complexes are discussed.

Results and Discussion

Ligand Syntheses

Two general synthetic routes to the HBA ligands were initially pursued. The first method, **A** (developed by Dr. George Spies),[1] involves reaction between an acid chloride and a diamine (Scheme 2.1). Smooth conversion of the desired 2-acetylsalicyclic acid to the acid chloride is effected by treatment with oxalyl chloride. Prior acetylation of the phenol is necessary to prevent its reaction with the acid chloride. Reaction of the acid chloride with half an equivalent of the appropriate diamine yields the acetylated ligand. Strong base

Scheme 2.1. HBA ligand synthesis - method **A**.[1]
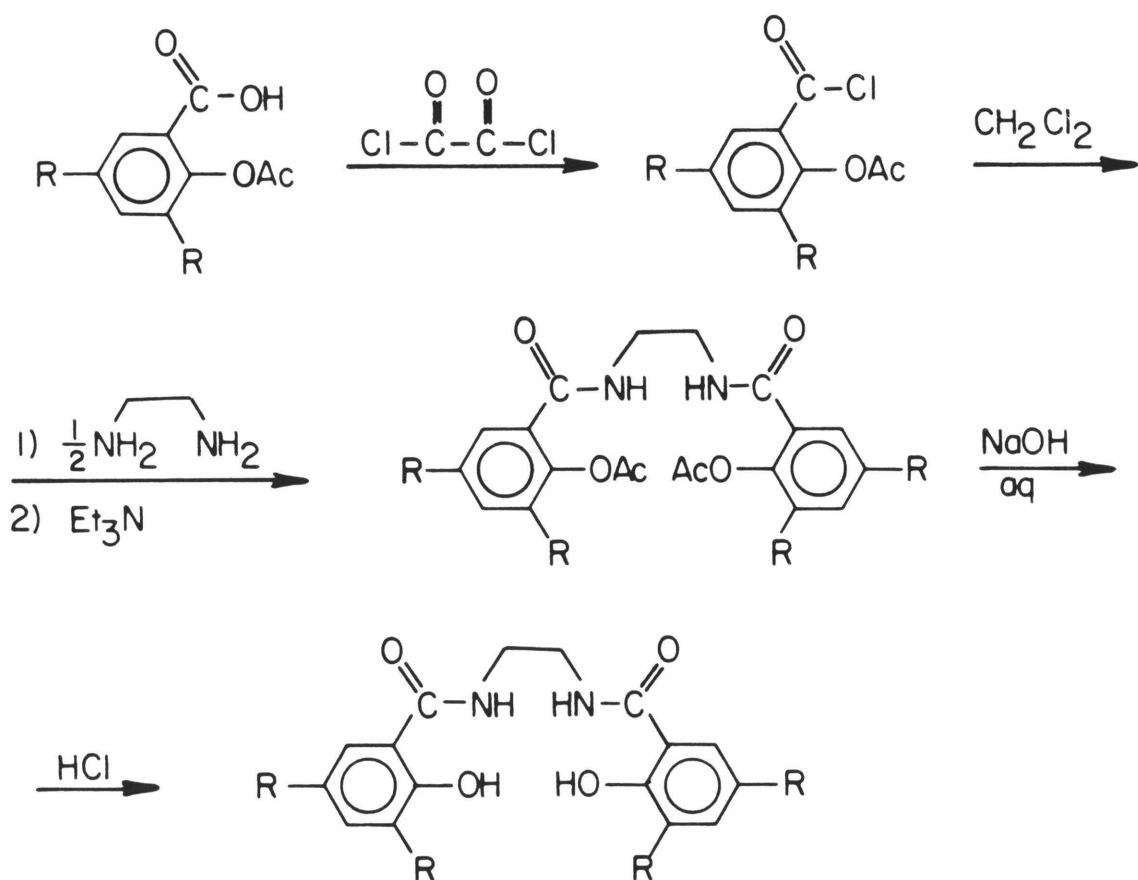
cleaves the acetyl groups and reacidification produces the neutral product.

The second method, **B**, employs phosgene in the formation of a
salicyclic acid carbonate cyclic anhydride (Scheme 2.2). This reaction both
protects the phenol and converts the carboxylic acid to the more reactive

Scheme 2.2. HBA ligand synthesis - method **B**.
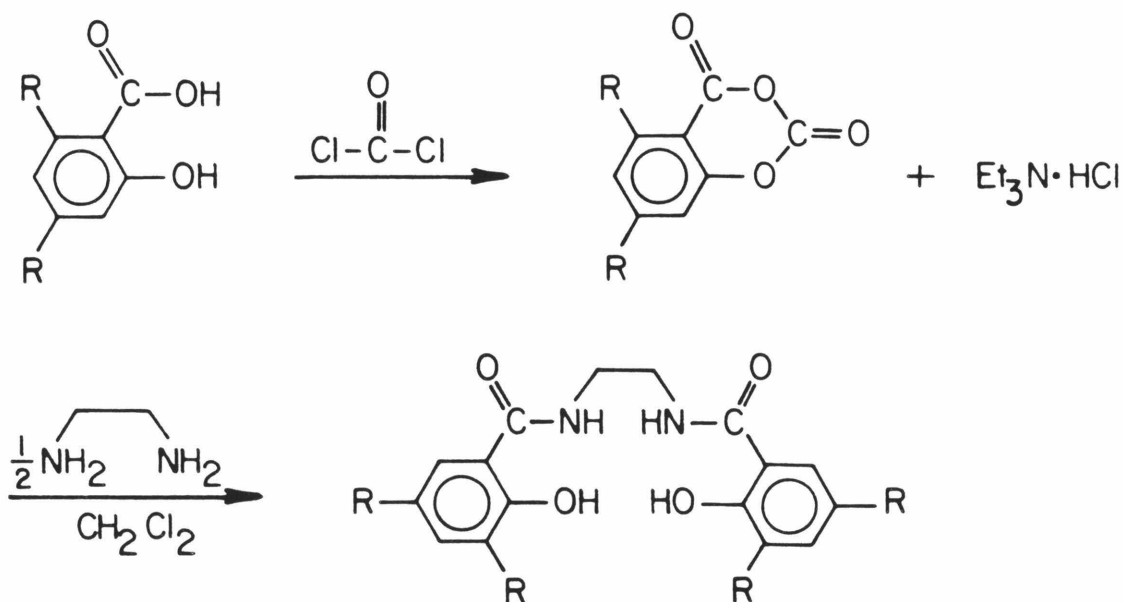
anhydride. Subsequent reaction of the intermediate with half an equivalent
of the diamine forms the ligand with loss of CO_2.

These methods have been used to synthesize numerous HBA ligands
including H_4HBA-Et,[1] H_4CHBA-Et, H_4CHBA-DMBu, H_4t-BuHBA-DMBu,
H_4HBA-oBz[1] and H_4CHBA-DCB[4a] (see Table 1.2, page 11). Although
H_4CHBA-Et and H_4CHBA-DMBu were successfully produced using the
phosgene reaction, route **A** appears to be the method of choice. It is a

general method which typically gives good yields, is experimentally simpler than the phosgene route and does not require elaborate safety procedures.

The pure HBA ligands are white microcrystalline solids. They have relatively high melting points (e.g., H_4CHBA-Et m.p. = 255°C), are nonhydroscopic and are stable indefinitely. Their solubility properties vary somewhat, but they are generally soluble in polar organic solvents such as CH_2Cl_2, acetone, THF and pyridine, and are insoluble in water and nonpolar hydrocarbons. Each of the new ligands has been characterized by IR, ^{1}H NMR and elemental analysis. The IR spectrum of H_4CHBA-Et (Fig. 2.1) is representative of these compounds. It shows overlapping N-H and O-H stretching signals between 3100 and 3500 cm^{-1}, typical amide I and amide II bands at 1632 and 1548 cm^{-1}, respectively, and arene ring stretching at 1585 cm^{-1}.[6]

Osmium Complexes of H_4CHBA-Et

$K_2[Os(\eta^4$-CHBA-Et)(O)$_2]$, 2. A number of unsuccessful attempts to coordinate HBA ligands to osmium were pursued with various osmium complexes including $OsCl_3$, $(NH_4)_2OsCl_6$ and OsO_4.[7] The proper choice of starting material and reaction conditions proved to be critical factors. Dr. Judy Christie obtained promising preliminary results with potassium osmate, $K_2[Os(OH)_4(O)_2]$. Two η^4-CHBA-Et^{4-} osmium complexes, 2 and 5 (vide infra), were obtained and partially characterized.[7] Unfortunately, the yield was variable and quite low. Closer investigation showed that under appropriate conditions $K_2[Os(OH)_4(O)_2]$ is an ideal complex in which the tetradentate tetraanion can easily undergo metathetical exchange with the four hydroxyl groups (Scheme 2.3).
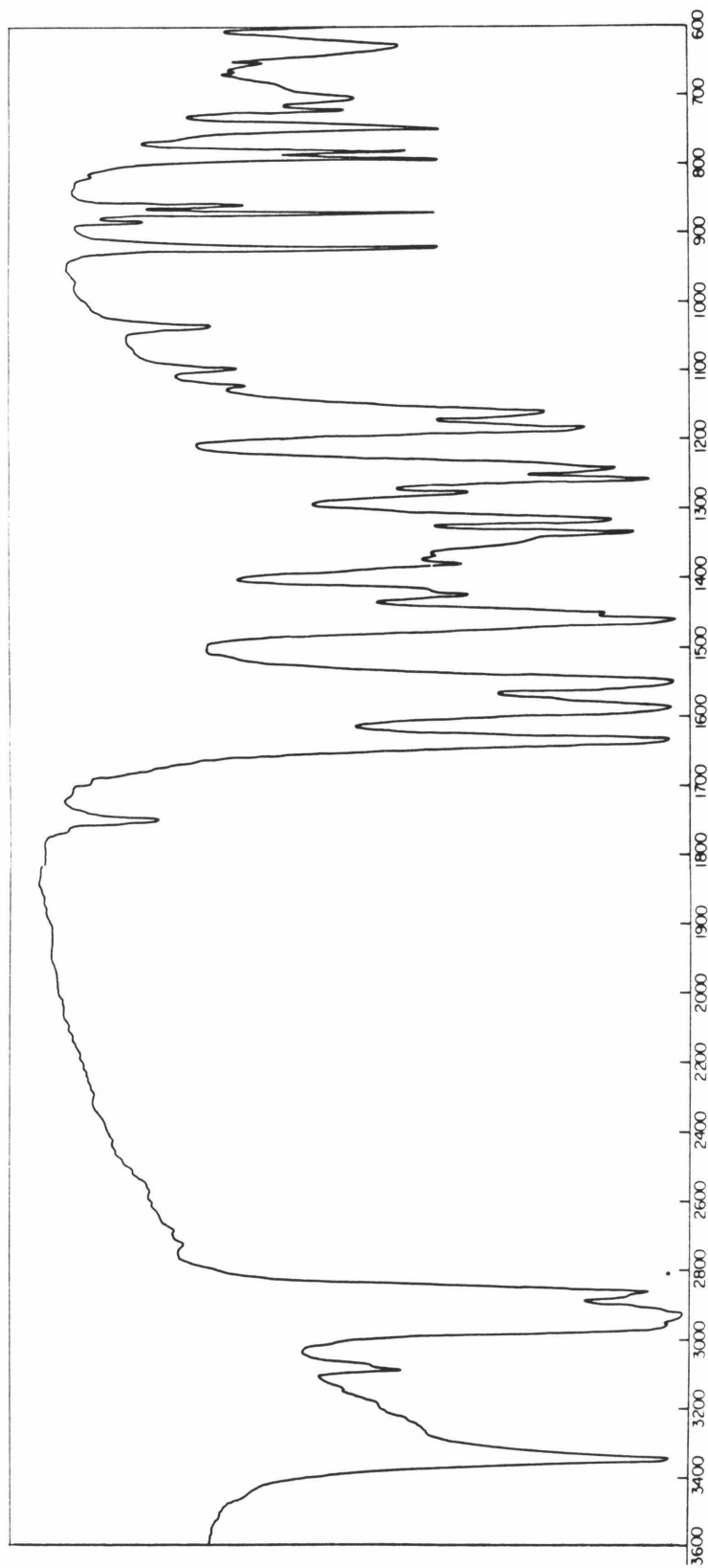
Figure 2.1. IR spectrum of H_4CHBA-Et, **1** (nujol mull).

Treatment of a colorless acetone solution of the ligand H_4CHBA-Et, **1**, with a blue methanol solution of $K_2[Os(OH)_4(O)_2]$ produces an immediate color change to the deep orange of the product, $K_2[Os(\eta^4\text{-CHBA-Et})(O)_2]$, **2**. The reaction is stoichiometric and proceeds quantitatively at room

Scheme 2.3. Coordination of H_4CHBA-Et, **1**, to osmium.
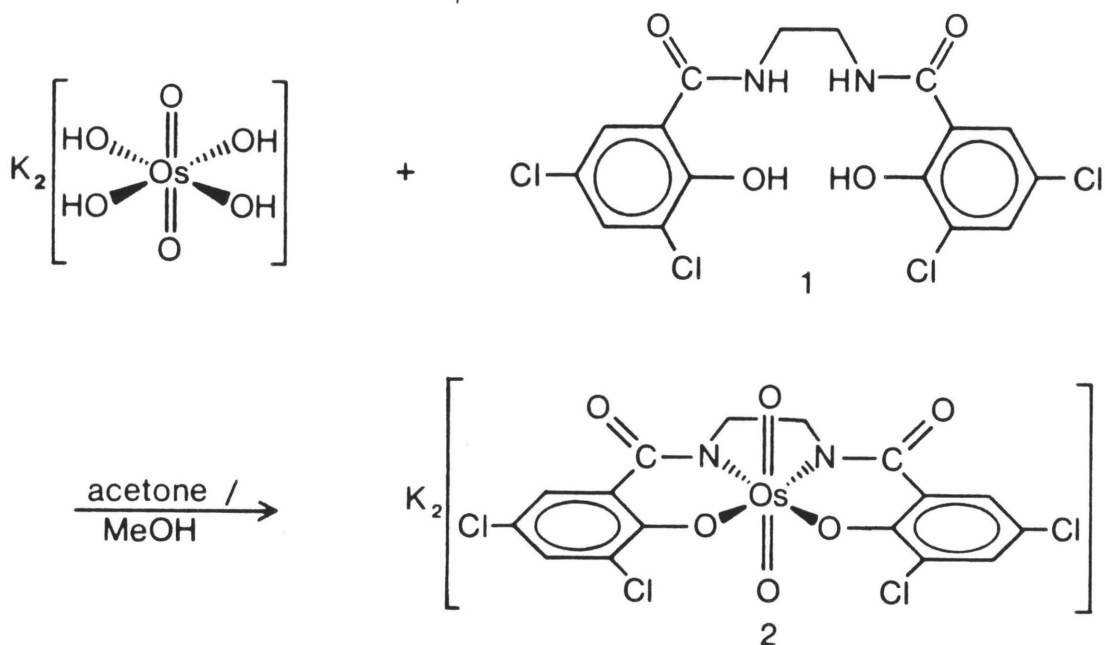
temperature. Recrystallization affords a 90% yield of the osmium(VI) salt as an orange microcrystalline solid which is stable indefinitely.

The complex **2** has been characterized by IR, NMR and Raman[7] spectroscopy and by elemental analysis. Suitable crystals for X-ray analysis could not be obtained. A variety of cations were employed in these attempts. The IR spectrum of **2** is shown in Figure 2.2. The features of particular interest are the bands in the carbonyl region, which have moved to lower frequency on coordination of the ligand, and the strong band at 820 cm^{-1}. ^{18}O labeling has
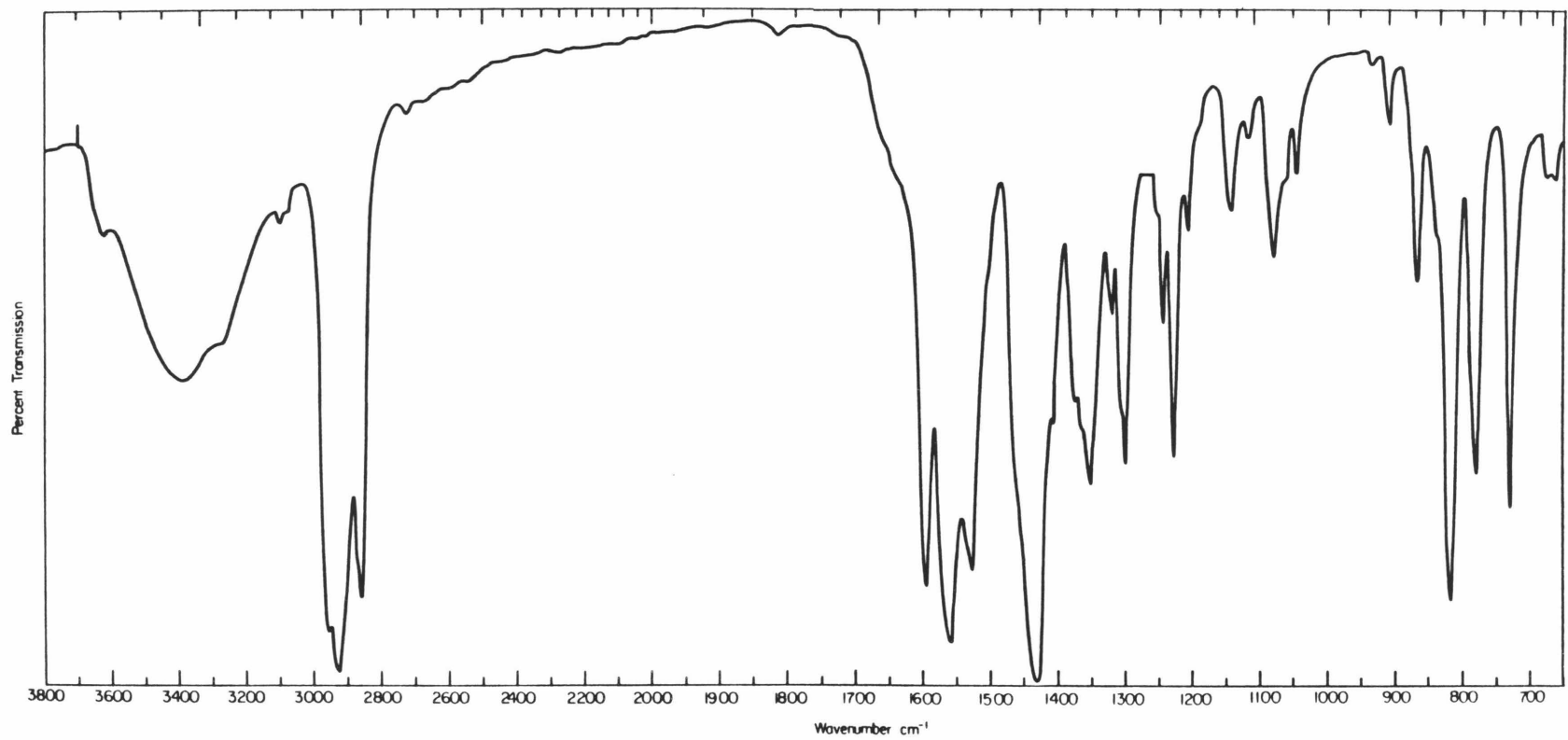
Figure 2.2. IR spectrum of $K_2[Os(\eta^4\text{-CHBA-Et})(O)_2]$, **2** (nujol mull).

identified the 820 cm^{-1} band as an asymmetric trans-dioxo stretch. Like other octahedral trans-dioxo osmium(VI) complexes, this material is diamagnetic[8] and exhibits a simple NMR spectrum. Together, the IR and ^{1}H NMR data require equatorial coordination of the ligand 1 as a tetradentate tetraanion. Once bound in this fashion the ligand remains coordinated through a variety of chemical transformations. The complexes described in this and subsequent chapters show no sensitivity to ligand hydrolysis or other displacement reactions.

The synthetic route to 2 is a general method for preparation of analogous compounds with other HBA ligands.[4a,9] The osmium(VI) trans oxo anions have been prepared with H_4HBA-Et, H_4HBA-oBz, H_4CHBA-DCB, H_4CHBA-iPr, and with the bidentate ligand 3,5-dichloro-2-hydroxybenzamide. Coordination of the ligands H_4HBA-DMBu and H_4CHBA-DMBu, in which the bridging ethane unit is substituted with four methyl groups, has not yet been successful. This is apparently a steric consequence, although molecular models suggest that the constraints should not be severe. Salen ligands with the same tetramethylethane bridge have been successfully coordinated to cobalt.[10]

A variety of reactions with 2 have been attempted. Non-aqueous solutions of 2 in air slowly precipitate a very dark green solid whose IR spectrum is almost identical with 2 except for lack of the trans oxo band at 820 cm^{-1}. Further characterization of this material was unsuccessful. Attempts to oxidize 2 chemically or electrochemically were not productive. Complex 2 reacts with acids, perhaps according to equation 2.1. Although these reactions appear tractable, the products were not fully characterized.

$$K_2 \left[\underset{O}{\overset{O}{\underset{\|}{\underset{Os}{\overset{\|}{\overset{VI}{\|}}}}}} \right] \xrightarrow{\text{HX}} \underset{X}{\overset{X}{\underset{\|}{\underset{Os}{\overset{\|}{\overset{VI}{\|}}}}}} + \text{KOH} \qquad (2.1)$$
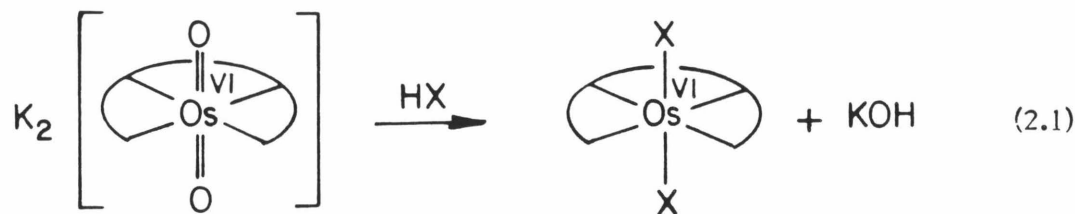
Complex **2** is not a strong oxidant and is unreactive with substrates such as alcohols and olefins. It does, however, oxidize phosphine to phosphine oxide and is reduced by other chemical reductants (vide infra).

K$_2$({Os(η^4-CHBA-Et)(OPPh$_3$)}-μ-O), **3**. Reactions of **2** with phosphines generally lead to multiple products. On one occasion reduction with triphenylphosphine in air resulted in the slow deposition of very dark crystals of the μ-oxo bridged osmium(IV) dimer, K$_2$({Os(η^4-CHBA-Et)- (OPPh$_3$)}$_2$-μ-O), **3** (Scheme 2.4). An X-ray crystal structure determination was performed on **3**.[4b,11] The structure shows two pseudooctahedral osmium centers, each bearing a CHBA-Et^{4-} ligand coordinated in the equatorial plane. The two osmiums are joined by a linear μ-oxo bridge with the chelating ligands rigorously eclipsed as illustrated in Scheme 2.4.

This was the first structurally characterized example of an HBA ligand bound as a tetradentate, tetraanion to a single metal center.[12] The structure exhibits the first examples of bonds between osmium(IV) and an N-coordinated organic amido ligand, a phenoxide ligand, and a phosphine oxide ligand. It also features unusual coordination environments for the potassium ions (Fig. 2.3). One potassium ion lies at the center of a square pyramid in which the basal plane consists of the four CHBA-Et phenolic oxygens and the apex is an oxygen atom from an acetone solvate molecule. This potassium is further

Scheme 2.4. Synthesis of $K_2\{ \{Os(\eta^4\text{-CHBA-Et})(OPPh_3)\} \text{-}\mu\text{-O}\}$.
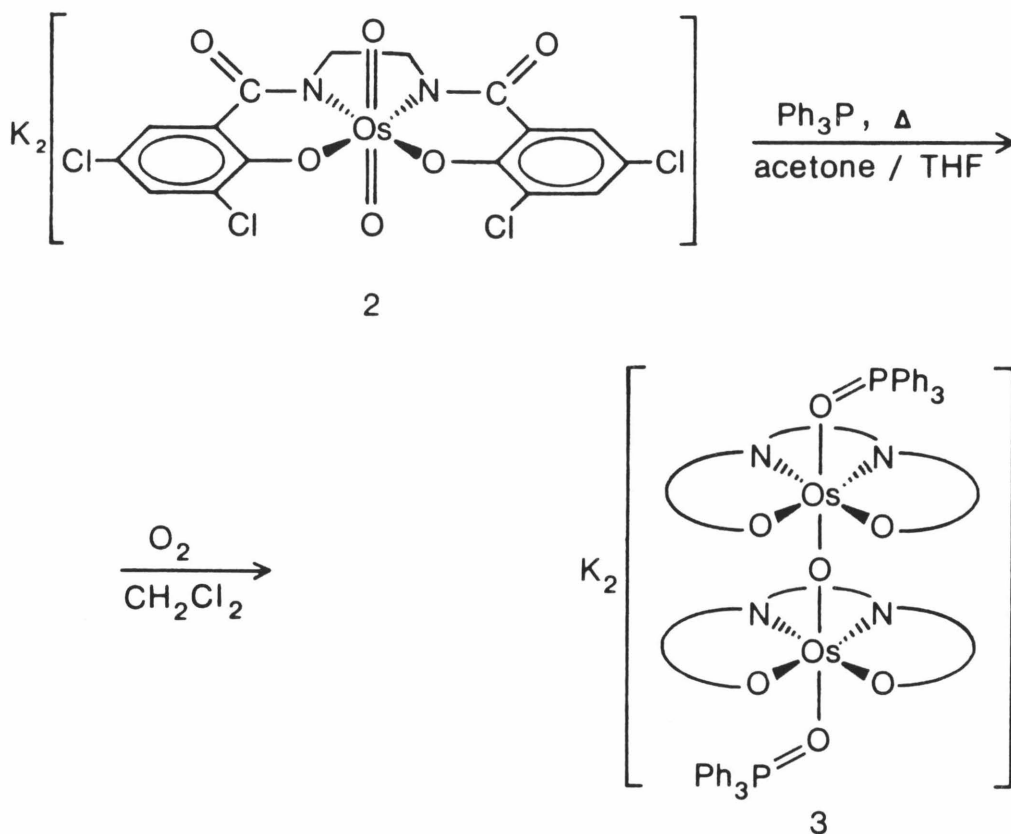
coordinated to the μ-oxo ligand. The second potassium bridges two of the dinuclear anions by coordination to two eclipsed carbonyl oxygens on each dimer. These four oxygens form a distorted tetrahedron around the four-coordinate potassium ion. Such low coordination numbers for potassium are quite rare. Only one other four coordinate example has been structurally characterized.[13]

Bond lengths and angles throughout the molecule are normal (Fig. 2.4). The free ligand H_4CHBA-Et has been structurally characterized.[1] Only small changes in bond lengths are found in the coordinated ligand. It should be
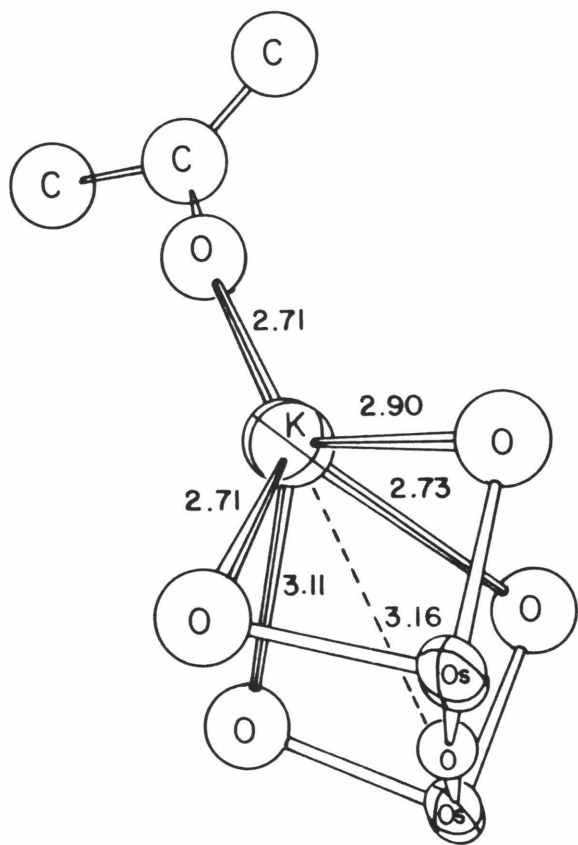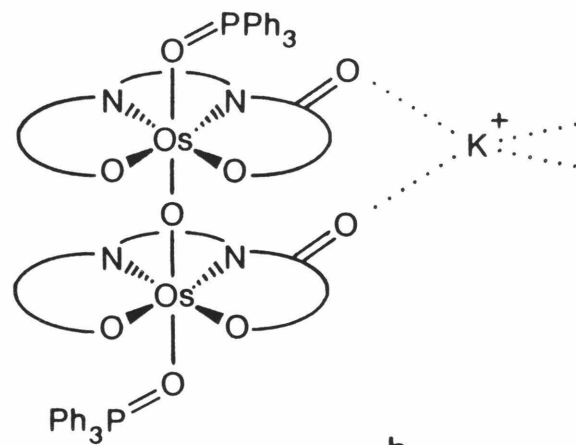
Figure 2.3. Unusual potassium ion coordination environments in $K_2[\{Os(\eta^4\text{-}CHBA\text{-}Et)(OPPh_3)\}\text{-}\mu\text{-}O]$, 3. (a) Potassium ion coordinated to four phenolic oxygens and one acetone solvate molecule. (b) Bridging four-coordinate potassium ion.

Figure 2.4. Schematic representation of K_2 [{ Os(η ^{4}-CHBA-Et)(OPPh$_3$) } $_2$-μ-O] , **3**, with averaged bond lengths (Å) and angles (^{o}). Average O(3)-P(1)-C angle = 110°. Average C-P(1)-C angle = 108°.

noted that the carbonyl carbon-oxygen bonds in both **3** and the free ligand are somewhat longer than those found in other structures of CHBA complexes (see Chapter 3). This is apparently due to coordination of potassium ion in complex **3** and to hydrogen bonding in the free ligand. The eclipsed conformation of the ligands in **3** causes quite close Cl····Cl contacts which range from 3.6 to 3.9 Å (sum of van der Waal's radii $\simeq$ 3.6 Å). The potassium ion coordination is presumably an important factor in holding the molecule in this configuration. μ-Oxo bridged octahedral osmium(IV) centers have been previously observed.[14]

$\underline{Os(\eta^4\text{-CHBA-Et})(py)_2}$. Reduction of **2** with triphenylphosphine in the presence of pyridine produces the red-orange paramagnetic osmium(III) complex $K\left(Os(\eta^4\text{-CHBA-Et})(py)_2\right)$, **4**, in high yield (ca. 90%) (Scheme 2.5). H_2O_2 cleanly oxidizes **4** to the deep royal blue osmium(IV) compound $Os(\eta^4\text{-CHBA-Et}(py)_2$, **5**. The transformation also occurs much more slowly by aerial oxidation. The neutral complex **5** can readily be obtained as a highly crystalline solid which is stable indefinitely. This material has been characterized by IR, ^{1}H NMR, elemental analysis, magnetic susceptibility and an X-ray crystal structure determination.[15]

The structure of **5** (Fig. 2.5) is the first of an osmium(IV) pyridine complex. The ligand **1** is coordinated as a tetradentate tetraanion to the equatorial positions of a distorted octahedron. The bond lengths (Table 2.1) and angles (Table 2.2) in the chelate are all normal and vary only slightly from those found in the free ligand.[1] The ethane bridge of the ligand is skewed so that the metallacyclopentane ring in **5** is nonplanar. The two pyridine ligands occupy the axial positions with a relative dihedral angle of

Scheme 2.5. Synthesis of Os(η^4-CHBA-Et)(py)$_2$, **5**.

Figure 2.5. Molecular structure of Os(η^4CHBA-Et)(py)$_2$, 5.
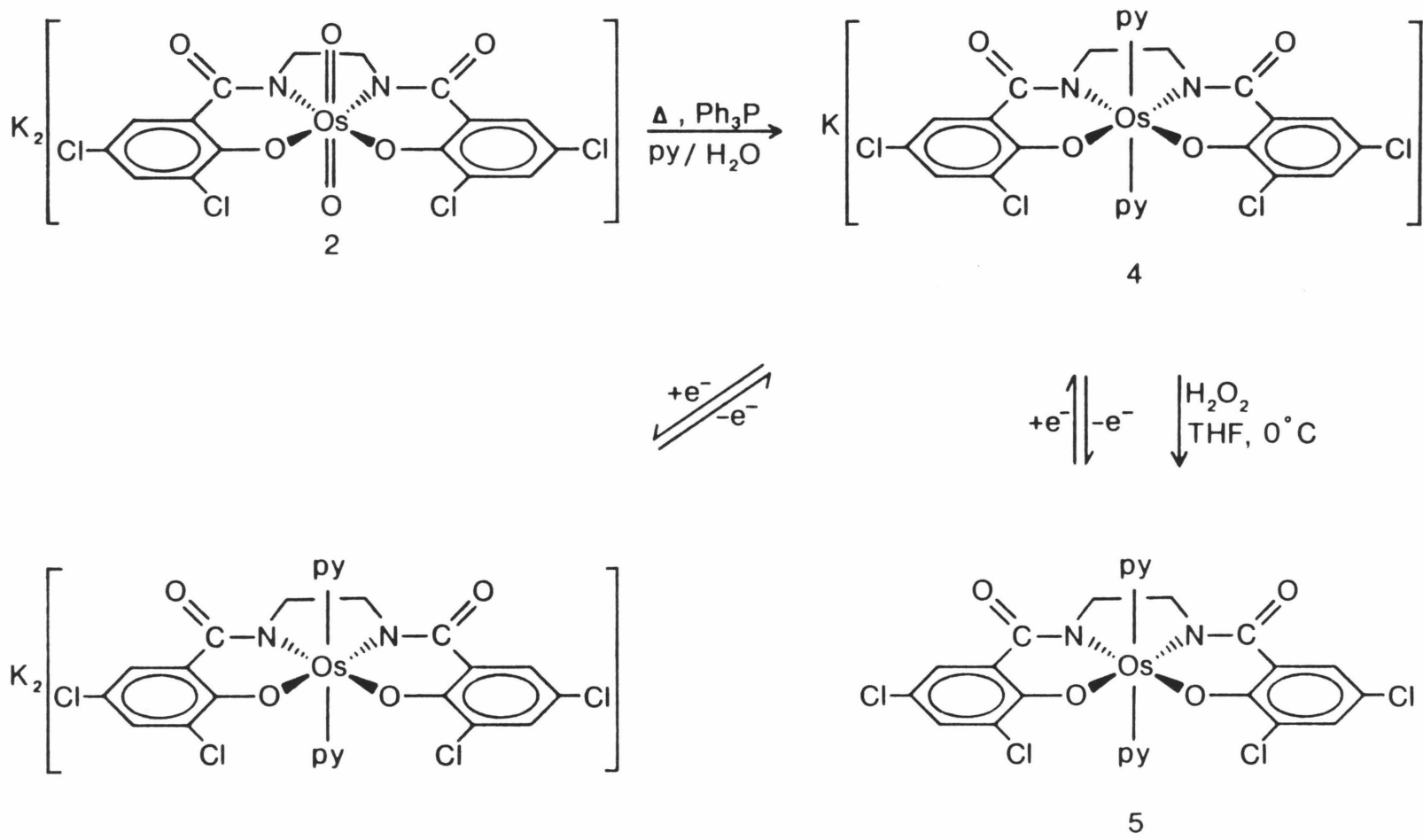
Table 2.1. Bond distances for Os(η^4-CHBA-Et)(py)$_2$, 5 (Å).

Atoms	Distance	Atoms	Distance
Os – N(1A)	1.980(3)	C(6A) – C(7A)	1.376(8)
Os – O(1A)	1.997(3)	C(7A) – Cl(2A)	1.740(5)
Os – N(1B)	1.960(4)	C(7A) – C(8A)	1.418(6)
Os – O(1B)	2.003(3)	C(3B) – C(4B)	1.399(7)
Os – N(3A)	2.099(3)	C(4B) – C(5B)	1.367(7)
N(1A) – C(1A)	1.473(6)	C(5B) – Cl(1B)	1.747(5)
C(1A) – C(1B)	1.520(7)	C(5B) – C(6B)	1.372(7)
N(1B) – C(1B)	1.477(6)	C(6B) – C(7B)	1.384(7)
N(1A) – C(2A)	1.351(6)	C(7B) – Cl(2B)	1.724(5)
C(2A) – O(2A)	1.231(6)	C(7B) – C(8B)	1.408(6)
C(2A) – C(3A)	1.513(6)	N(3A) – C(10A)	1.349(6)
C(3A) – C(8A)	1.414(6)	C(10A) – C(11A)	1.370(7)
O(1A) – C(8A)	1.327(5)	C(11A) – C(12A)	1.374(8)
N(1B) – C(2B)	1.361(6)	C(12A) – C(13A)	1.372(8)
C(2B) – O(2B)	1.228(6)	C(13S) – C(14A)	1.368(8)
C(2B) – C(3B)	1.508(6)	N(3A) – C(14A)	1.351(6)
C(3B) – C(8B)	1.413(6)	N(3B) – C(10B)	1.351(6)
O(1B) – C(8B)	1.337(5)	C(10B) – C(11B)	1.373(8)
C(3A) – C(4A)	1.402(7)	C(11B) – C(12B)	1.376(8)
C(4A) – C(5A)	1.368(8)	C(12B) – C(13B)	1.374(8)
C(5A) – Cl(1A)	1.744(7)	C(13B) – C(14B)	1.371(7)
C(5A) – C(6A)	1.370(9)	N(3B) – C(14B)	1.351(6)

Table 2.2. Bond angles for Os(η^4-CHBA-Et)(py)$_2$, 5 (deg).

Atoms			Angle	Atoms			Angle
O(1A)	– Os	– N(1A)	92.4(1)	C(1A)	– C(1B)	– N(1B)	108.5(4)
N(1B)	– Os	– N(1A)	83.9(1)	C(1B)	– N(1B)	– Os	113.2(3)
O(1B)	– Os	– N(1A)	176.7(1)	C(2B)	– N(1B)	– Os	129.0(3)
N(3A)	– Os	– N(1A)	94.0(1)	C(2B)	– N(1B)	– C(1B)	117.7(4)
N(3B)	– Os	– N(1A)	91.0(1)	C(8A)	– O(1A)	– Os	125.6(3)
N(1B)	– Os	– O(1A)	175.5(1)	C(8B)	– O(1B)	– Os	121.5(2)
O(1B)	– Os	– O(1A)	90.9(1)	O(2A)	– C(2A)	– N(1A)	123.1(4)
N(3A)	– Os	– O(1A)	86.2(1)	C(3A)	– C(2A)	– N(1A)	118.1(4)
N(3B)	– Os	– O(1A)	91.6(1)	C(3A)	– C(2A)	– O(2A)	118.8(4)
O(1B)	– Os	– N(1B)	92.8(1)	C(4A)	– C(3A)	– C(2A)	114.9(4)
N(3A)	– Os	– N(1B)	91.5(1)	C(8A)	– C(3A)	– C(2A)	126.3(4)
N(3B)	– Os	– N(1B)	91.0(1)	C(8A)	– C(3A)	– C(4A)	118.7(4)
N(3A)	– Os	– O(1B)	85.5(1)	C(3A)	– C(8A)	– O(1A)	126.0(4)
N(3B)	– Os	– O(1B)	89.8(1)	C(7A)	– C(8A)	– O(1A)	116.8(4)
N(3B)	– Os	– N(3A)	174.7(1)	C(7A)	– C(8A)	– C(3A)	117.2(4)
C(1A)	– N(1A)	– Os	113.2(3)	O(2B)	– C(2B)	– N(1B)	122.6(4)
C(2A)	– N(1A)	– Os	130.5(3)	C(3B)	– C(2B)	– N(1B)	118.1(4)
C(2A)	– N(1A)	– C(1A)	116.1(4)	C(3B)	– C(2B)	– O(2B)	119.4(4)
C(1B)	– C(1A)	– N(1A)	109.8(4)				

Table 2.2. Continued.

Atoms	Angle	Atoms	Angle
C(4B) - C(3B) - C(2B)	115.0(4)	C(6B) - C(7B) - C(8B)	122.5(4)
C(8B) - C(3B) - C(2B)	126.1(4)	Cl(2B) - C(7B) - C(6B)	118.9(4)
C(8B) - C(3B) - C(4B)	118.9(4)	Cl(2B) - C(7B) - C(8B)	118.6(3)
C(3B) - C(8B) - O(1B)	125.7(4)	C(10A) - N(3A) - Os	123.2(3)
C(7B) - C(8B) - O(1B)	116.5(4)	C(14A) - N(3A) - Os	119.0(3)
C(7B) - C(8B) - C(3B)	117.7(4)	C(10A) - N(3A) - C(14A)	117.7(4)
C(5A) - C(4A) - C(3A)	121.3(5)	N(3A) - C(10A) - C(11A)	122.3(4)
C(6A) - C(5A) - C(4A)	121.2(6)	C(10A) - C(11A) - C(12A)	119.8(5)
Cl(1A) - C(5A) - C(4A)	119.5(5)	C(11A) - C(12A) - C(13A)	118.1(5)
Cl(1A) - C(5A) - C(6A)	119.3(5)	C(12A) - C(13A) - C(14A)	120.3(5)
C(5A) - C(6A) - C(7A)	118.6(6)	C(13A) - C(14A) - N(3A)	121.9(5)
C(6A) - C(7A) - C(8A)	122.5(5)	C(10B) - N(3B) - Os	119.4(3)
Cl(2A) - C(7A) - C(6A)	118.9(4)	C(14B) - N(3B) - Os	123.7(3)
Cl(2A) - C(7A) - C(8A)	118.6(4)	C(10B) - N(3B) - C(14B)	116.9(4)
C(5B) - C(4B) - C(3B)	121.1(4)	N(3B) - C(10B) - C(11B)	122.9(5)
C(6B) - C(5B) - C(4B)	121.8(5)	C(10B) - C(11B) - C(12B)	119.7(5)
Cl(1B) - C(5B) - C(4B)	119.2(4)	C(11B) - C(12B) - C(13B)	117.8(5)
Cl(1B) - C(5B) - C(6B)	119.1(4)	C(12B) - C(13B) - C(14B)	120.3(5)
C(5B) - C(6B) - C(7B)	118.1(5)	C(13) - C(14B) - N(3B)	122.4(5)

73°. This staggered configuration may be principally due to crystal packing forces. The relative orientation of <u>trans</u>-pyridine ligands in $Co(acac)_2(py)_2$ and $Ni(acac)_2(py)_2$, staggered and eclipsed respectively, has been attributed to crystal packing.[16]

Complex 5 is paramagnetic with a room temperature magnetic moment of 1.23 Bohr magnetons. This is far below the spin-only value of 2.83 BM expected for an octahedral or pseudooctahedral d^4 configuration. Low room temperature magnetic moments (1.2-1.7 BM) are typical of octahedral osmium (IV) compounds due to a large spin-orbit coupling constant.[17] The complex exhibits a well-resolved, paramagnetically shifted ^1H NMR spectrum as shown in Figure 2.6. Spectra of this type have been previously observed for osmium (IV) complexes.[18] The signal for the ethylene bridge protons is a singlet at 68.55 ppm. This is shifted much more dramatically than signals in previously reported osmium(IV) spectra. The aromatic protons of the chelate are found at 14.92 (d, 2) and 10.54 ppm (d, 2). Note that the signals for the pyridine ortho and para protons are significantly shifted upfield from the normal diamagnetic range (H_o, -6.29, d, 4; H_p, -1.39, t, 2), whereas the signal for the meta protons is not affected (H_m, 7.72, t, 4). The shift of the pyridine ortho and para signals may be a paramagnetic contact shift induced by inter- action of the unpaired d electrons with the second LUMO of pyridine. This orbital, $3B_1$, has lobes on nitrogen and at the ortho and para positions, but not the meta positions.[19] The first LUMO, $2A_1$, cannot interact with the metal, since it has no component on nitrogen. A significant mixing of the osmium $d\pi$ orbitals with the pyridine $3B_1$ orbital would give rise to a π-backbonding interaction.
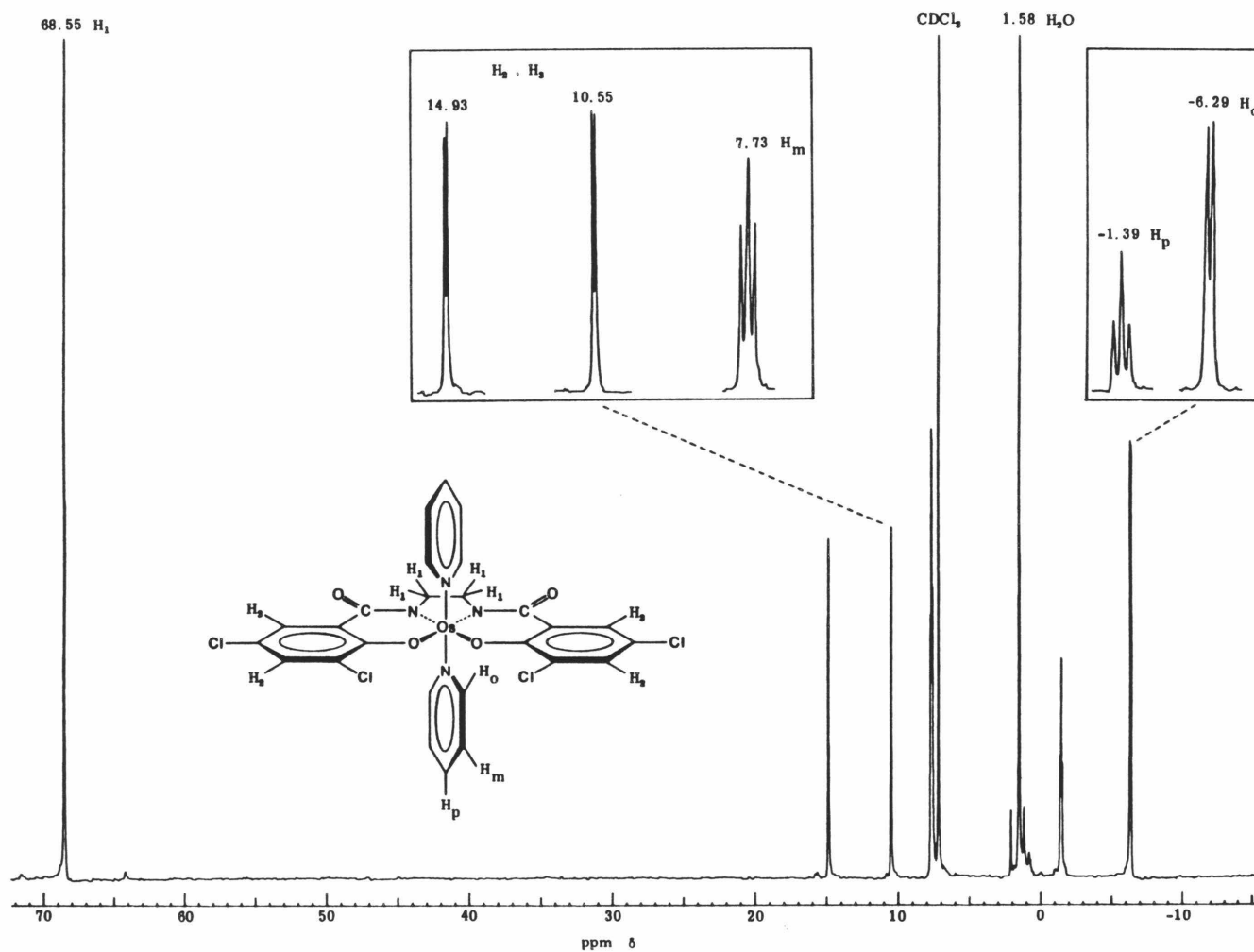
Figure 2.6. 90-MHz ^{1}H NMR spectrum of **5** (CDCl₃).

Taube and others[20] have concluded that π-backbonding to nitrogen bases such as pyridine is important in certain ruthenium(II) complexes, but much less important in corresponding ruthenium(III) compounds. Even though such back-bonding is much more important for osmium than for ruthenium,[21] its operation in the osmium(IV) oxidation state would be most unusual. Nevertheless, the NMR data suggest that some interaction may be present. In this particular system it may be quite reasonable to find π-backbonding, since electrochemical results indicate that the metal is extremely electron-rich for an osmium(IV) center (vide infra). The orientation of the pyridine ligands is consistent with a metal -π* interaction, but this could also be due to crystal packing effects[16] (see Chapter 3, page 77). The osmium-nitrogen (py) bond length (2.099 (3) Å) does not appear to be significantly short and therefore does not signal the presence of significant multiple bonding between osmium and pyridine. However, good comparisons are not available. Only a small decrease in the metal-nitrogen distance is found in ruthenium systems when π-backbonding is operative.[22]

Cyclic voltammetry was used to probe the redox chemistry of complex 5 and to test the oxidative stability of the η^4-CHBA-Et^{4-} ligand. All electrochemistry reported here was performed by Stephen Gipson. A typical cyclic voltammogram of 5 (1 mM in CH_2Cl_2, 0.1 M TBAP) at a BPG electrode is shown in Figure 2.7. Potentials were measured against the ferrocinium/ferrocene (Fc$^+$/Fc) couple, which was consistently measured at ca. +0.48 V versus SCE in the medium used. Two reversible diffusion-controlled one-electron responses are found with formal potentials of -0.65 V for the osmium(IV/III) couple and -1.88 V for the osmium(III/II) couple. In
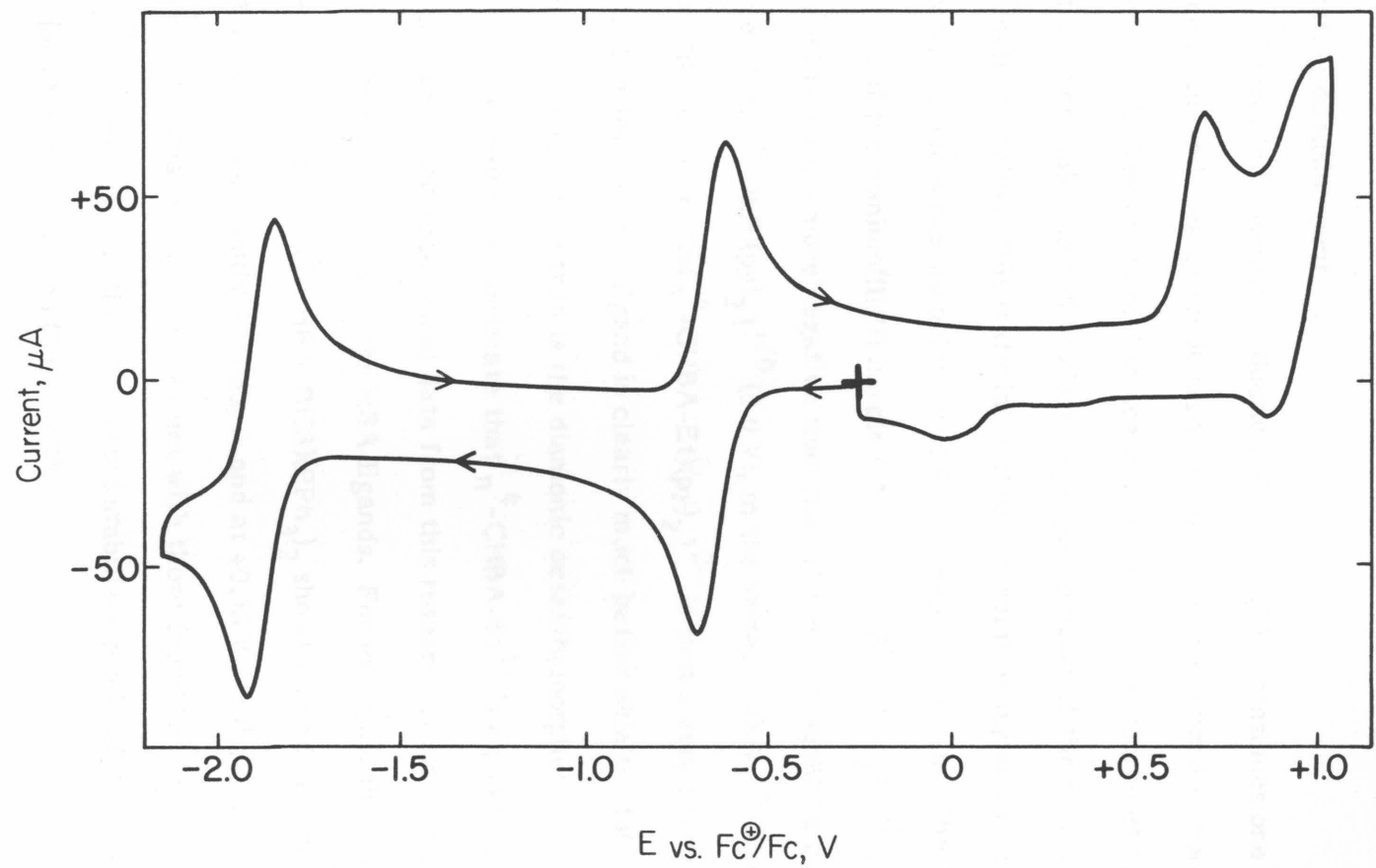
Figure 2.7. Cyclic voltammogram of 1 mM 5 in CHCl$_2$, 0.1 M TBAP at 0.174 cm^2 BPG electrode. Scan rate = 200 mV s^{-1}.

addition, two irreversible responses appear at E_p = +0.70 V and ca. +1.00 V. Plots of peak currents versus the square root of scan rate over the range 20-500 mV s^{-1} are linear for the two reversible couples and the first oxidation, indicating diffusion control.

Controlled potential reduction of 5 at -0.90 V consumes one electron per molecule and cleanly produces 4 which can be reoxidized to pure 5 (Scheme 2.5, page 35). Reduction of 5 in acetonitrile at -2.10 V consumes two electrons per molecule and produces a purple solution of the corresponding osmium(II) complex. This material is stable in solution under an inert atmosphere, but is rapidly oxidized to 4 upon exposure to air. The formal potential of the osmium(III/II) couple $\left(Os(\eta^4\text{-CHBA-Et})(py)_2\right)^{-/2-}$, -1.88 V, is almost two volts more negative than that of the corresponding porphyrin complex $\left(Os(\eta^4\text{-OEP})(py)_2\right)^{+/0}$ (0.0 V), in the same medium.[23] The osmium(II) complex $\left(Os(\eta^4\text{-CHBA-Et})(py)_2\right)^{2-}$ is thus a very powerful reducing agent. The tetraanionic ligand is clearly much better able to stabilize the higher oxidation state than is the dianionic octaethylporphyrinato ligand.

These results demonstrate that $\eta^4\text{-CHBA-Et}^{4-}$ is a powerful donor ligand. Other electrochemical data from this research group indicate that this is a general property of the HBA ligands. For example, the cyclic voltammogram of $Os(\eta^4\text{-CHBA-DCB})(PPh_3)_2$ shows reversible responses at -0.47 V for the osmium(IV/III) couple and at +0.58 V for the osmium(V/IV) couple.[4a] Comparison of these values with those found for $OsCl_4(PPh_3)_2$[24] and $OsCl_6^{2-}$[25] reveals that the HBA ligand stabilizes osmium(V) more strongly than does the chloro ligand (Table 2.3).

In spite of this strong donation by the HBA ligands, and the significant

Table 2.3. Comparison of some formal potentials for Os compounds.[a]

Compound	IV/III[b]	V/IV[b]
$Os(\eta^4\text{-CHBA-DCB})(PPh_3)_2$	-0.47	+0.58
$OsCl_4(PPh_3)_2$	-0.12	(+1.34)[c]
$OsCl_6{}^{2-}$	-1.19	+0.74

[a]References 24 and 25. [b]Potentials are reported against the Fc+/Fc couple which was measured at ca. +0.48 V vs. SCE. [c]Peak potential for an irreversible oxidation.

lowering of the osmium redox potentials, the oxidative sensitivity of the ethane bridge in the prototype ligand, H_4CHBA-Et, causes the oxidation of complex **5** to be irreversible (see Chapter 3 for a discussion of this ligand oxidation). In the room temperature cyclic voltammogram of **5** (Fig. 2.7), the oxidation at +0.70 V remains irreversible, even at fast scan rates. This can, however, be converted to a reversible osmium(IV/V) couple at +0.86 V if the cyclic voltammogram is run at low temperature in liquid SO_2 (Fig. 2.8). Here we see an additional reversible oxidation at +1.37 V and an irreversible wave at +2.01 V.

Complex **5** is generally unreactive. The chelate ligand is inert to substitution even in strongly acidic environments. Attempts to exchange the pyridines for other ligands such as phosphines or isocyanides were unsuccessful. This could be a kinetic problem, since the analogous complexes $Os(\eta^4\text{-CHBA-DCB})L_2$ and $Os(\eta^4\text{-HBA-}\underline{o}\text{Bz})L_2$ can be made by substitution procedures with a variety of ligands.[4a,2b] Efforts to synthesize complexes of this type directly from $K_2\{Os(\eta^4\text{-CHBA-Et})(O)_2\}$, **2**, were also unsuccessful. It is interesting
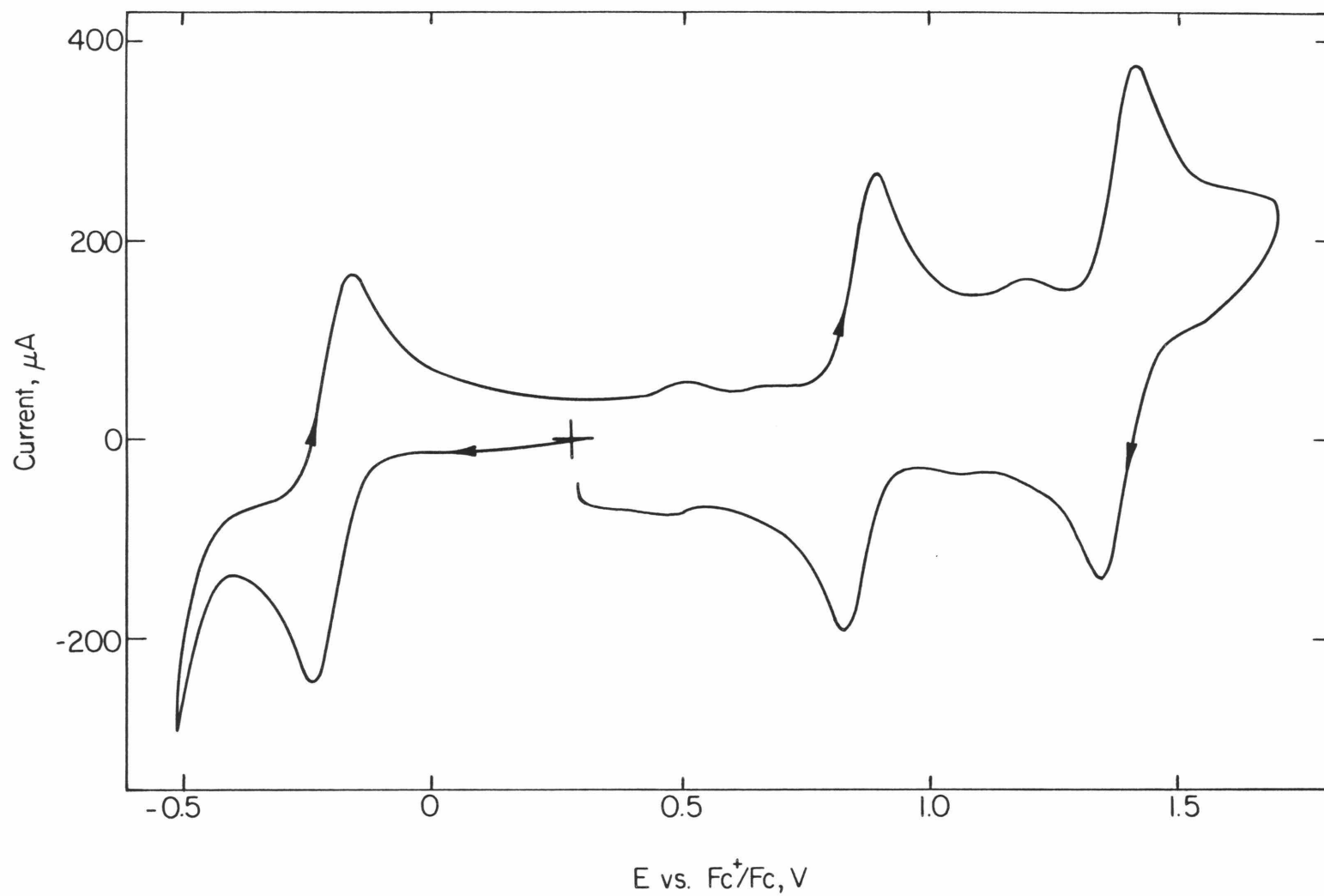
Figure 2.8. Cyclic voltammogram of 2 mM **5** at -40°C in liquid SO_2, 0.1 M ($\underline{n}$-Bu$_4$N)BF$_4$ at a glassy carbon electrode. Scan rate = 200 mV s^{-1}.

to note that **5** reacts with an excess of hydroxide to generate the reduced osmium compound $[Os(\eta^4\text{-CHBA-Et})(py)_2]^-$, **4**. The reaction proceeds in a variety of solvents with either aqueous or nonaqueous hydroxide. Nitrogen bases such as ethylene diamine, triethylamine and <u>tert</u>-butylamine also effect the reaction. Similar reactivity with base is seen with other osmium(IV) HBA complexes.[2b]

Conclusions

We have developed a straightforward synthetic route to the HBA ligands. The method is sufficiently general to allow extension to more elaborate systems if needed. The ligands readily coordinate to osmium(VI) as tetradentate, tetraanions and remain coordinated in this fashion under all conditions examined. The crystal structures of $K_2(\{Os(\eta^4\text{-CHBA-Et})\text{-}(OPPh_3)\}\text{-}\mu\text{-O})$, **3**, and $Os(\eta^4\text{-CHBA-Et})(py)$, **5**, reveal several unique structural features including an unusual four-coordinate potassium, and the first examples of bonds between osmium(IV) and an N-coordinated organic amido ligand, a phenoxide ligand, a phosphine oxide ligand and a pyridine ligand. The paramagnetic complex **5** exhibits an interesting ^1H NMR spectrum with strongly shifted, but very well-resolved signals. The possibility of π-backbonding to the pyridine ligands in **5** has been considered. Although available data are inconclusive about the importance of such an interaction, the problem is sufficiently interesting to warrant further attention. Electrochemical studies of **5** demonstrate that $CHBA\text{-}Et^{4-}$ is a powerful donor ligand which reduces the osmium redox couples by as much as two volts when compared to a porphyrin ligand.

Experimental

General Considerations

Materials. All solvents were reagent grade (Aldrich, Baker, Mallinckrodt, M.C.B. or U.S.I.) and were used as received unless otherwise noted. Acetic anhydride (reagent, Mallinckrodt), 2-acetylsalicyclic acid (Aldrich), Cl_2 (Matheson), 3,5-dichlorosalicyclic acid (Pfaltz and Bauer), 2,3-dimethyl-2,3-dinitrobutane (98%, Aldrich), glacial acetic acid (Aldrich), HCl (37.5% Mallinckrodt), H_2O_2 (30% Superoxol, Baker), isobutyl alcohol (M.C.B.), KOH (reagent, Baker), NaOH (reagent, Baker), OsO_4 (99.8%, Alfa), phosgene (Linde), pyridine (reagent, Mallinckrodt), Sn (Baker), salicyclic acid (reagent, Baker), triethylamine (reagent, M.C.B.), and triphenylphosphine (99%, Aldrich) were all used as received. The oxalyl chloride and ethylenediamine (Aldrich) used in the ligand syntheses were both freshly distilled.

Physical Measurements. ^{1}H NMR spectra were measured at 90 MHz on a Varian EM 390 or a JEOL FX 90Q spectrometer unless otherwise noted. [1]H chemical shifts are reported in ppm δ vs. Me_4Si with the solvent (CDCl$_3$ δ = 7.25, $\underline{d}_6$-acetone δ = 2.05) as internal standard. Infrared spectra were taken as Nujol mulls on KBr windows and were recorded on a Beckman IR 4240 spectrophotometer. Raman data were recorded on a SPEX spectrometer. Magnetic susceptibilities were measured on a Cahn Electrobalance DTL by the Faraday method and are reported in Bohr magnetons. Elemental analyses were obtained at the Caltech Analytical Facility. All electrochemical experiments were carried out by S. L. Gipson at Caltech. Details of these procedures can be found in reference 4a or will appear in the near future.

X-ray Crystallography. The X-ray structure of **3** was performed by

Dr. George Spies. Details on the data collection and structure determination of **3** can be found in references 1 and 4b.

Data Collection and Structure Determination of **5**. A suitable crystal was obtained by slow crystallization from THF/water. Oscillation and Weissenberg photographs showed symmetry no higher than $\overline{1}$. The intensity data were collected on a locally modified Syntex $P2_1$ diffractometer with graphite monochromator and $MoK\overline{\alpha}$ radiation (λ = 0.7107 Å). Unit cell parameters (Table 2.4) from least-squares refinement of $\sin^2\theta$ based on fifteen 2θ values, each 2θ an average of four values ($\pm2\theta$, $\pm\omega$, ϕ, χ; $\pm2\theta$, $\pm\omega$, $\pi+\phi$, $\pi-\chi$). The three check reflections indicated no decomposition and the data were reduced to F_o^2; the variances of the intensities were obtained from counting statistics with an additional term (0.02 x scan counts)^2. The form factors were taken from reference 27.

The osmium atom coordinates were derived from a Patterson map, and successive electron density maps revealed the remaining atoms. Hydrogen atoms were introduced into the model at idealized positions with fixed U = 0.063 Å^2. Several cycles of least-squares refinement, minimizing $\Sigma w\Delta^2$, with with $w = \sigma^{-2}(F_o^2)$ and $\Delta = F_o^2 - (F_c/k)^2$, resulted in S = 1.92 and R_F = 0.034.[28] The final value for the isotopic extinction coefficient was 0.396(36) x 10^{-6}. The calculations were carried out on a Vax 11/780 using the CRYM system of programs.[29]

Ligand Syntheses

2,3-Diamino-2,3-dimethylbutane. The method of Bewad[30] was modified for the tin reduction of the dinitro compound. 2,3-Dimethyl-2,3-dinitrobutane

Table 2.4. Data collection and refinement information for **5**.

formula	$C_{26}H_{18}OsN_4O_4Cl_4$
formula weight	782.47
space group	$P\bar{1}$
a, Å	10.083 (4)
b, Å	12.310 (5)
c, Å	12.241 (4)
σ, deg	97.38 (3)
β, deg	96.49 (4)
γ, deg	113.0 (3)
v, Å³	1364.7 (9)
Z	2
D_{calcd}, gcm⁻³	1.90
crystal size, mm	0.14 x 0.19 x 0.92
λ, Å	0.7107
μ, mm⁻¹	5.11
scan type	θ-2θ
2θ limits	$3 < 2\theta < 60°$
scan rate, deg/min	2
scan width, deg	2.4
total collected refl	12429
final refl	6630
refinement on	F^2
sec. extinction	$3.9\ (4) \times 10^{-7}$
final no. of parameters	353
final cycle[a]	
R_F	0.034 (6435)
R'_F	0.029 (5805)
S	1.92 (6630)

[a]The number of contributing reflections are given in parentheses; see reference 28 for definitions.

(17.6 g, 0.1 mol) in concentrated HCl (200 mL) was stirred vigorously at 50-60°C during the gradual addition of 20 mesh Sn (85 g). The solution was stirred until most of the tin dissolved and then refluxed for 30 min. Concentrated NaOH was added until the solution was strongly basic and the contents were steam distilled. Approximately 400 mL of distillate were collected and made slightly acidic by addition of HCl. The mixture was evaporated to dryness with heating. The ammonium salt (18.0 g, 95%) was obtained as a white crystalline solid. NMR showed the product to be free of organic impurities.

5-t-Butylacetylsalicyclic acid. The method of Meyer and Bernhauer[31] was modified for the alkylation of salicyclic acid. Isobutyl alcohol (240 mL) was added dropwise to a slurry of salicyclic acid (174 g) in 80% H_2SO_4 (3 L). The mixture was stirred for 2 h at 65°C, cooled and the product collected by filtration. The solid was extracted into CH_2Cl_2. The organic layer was separated, dried over $CaCl_2$, filtered and evaporated to dryness. The substituted salicyclic acid was acetylated as described in the literature.[32]

H_4t-BuHBA-DMBu. 5-t-Butylacetylsalicyclic acid (6.5 g, 0.027 mol) and freshly distilled oxalyl chloride (12 mL) were heated under reflux for 5 h after which the excess oxalyl chloride was distilled off under vacuum. The residual solid was dissolved in 50 mL of CH_2Cl_2 and then evaporated to dryness. This was repeated twice to ensure complete removal of all oxalyl chloride. 2,3-Diamino-2,3-dimethylbutane hydrochloride (2.613 g, 0.014 mol) was dissolved in water and the solution made basic with NaOH. The amine was extracted into CH_2Cl_2 and this solution was added dropwise to a solution of the acid chloride in CH_2Cl_2 (50 mL). After stirring the solution for 0.5 h, Et_3N (3.8 mL) was added and the mixture was stirred for an additional 1 h.

The mixture was heated under vacuum to remove the volatile organics. Acetone was added to the resulting inhomogeneous aqueous layer to dissolve the solids. Removal of the acetone followed by neutralization of the aqueous layer with HCl caused precipitation of the product. The solid was collected, washed with water and recrystallized from acetone/water: yield 3.5 g (55%); IR (Nujol) 3360 (m, ν(NH)), 3155 (s broad, ν(OH)), 1665 (s, amide I, ν(C=O)), 1588 (m, ν(arene)), 1565 (s, amide II) cm^{-1}; ^{1}H NMR (acetone-d$_6$) δ 8.12 (d, 2, Ph), 7.47 (dd, 2, Ph), 6.87 (d, 2, Ph), 1.63 (s, 12, -CH$_3$), 1.37 (s, 18, t-Bu). Anal. calcd. for $C_{28}H_{40}N_2O_4$: C, 71.76; H, 8.60; N, 5.98. Found: C, 71.79; H, 8.47; N, 6.12.

H$_4$CHBA-Et, 1. Method A. This method (developed by Dr. George Spies)[1] was found to be superior to method B. 2-Acetylsalicyclic acid (50.0 g, 0.277 mol) and of neat oxalyl chloride (50-60 mL) were added to a 250-mL round-bottom flask and stirred at 30°C for 4 h. The remaining oxalyl chloride was distilled off under vacuum. The residue was dissolved in CH$_2$Cl$_2$ (30 mL) and then evaporated to dryness. This step was repeated several times. Ethylenediamine (9.28 mL, 0.138 mol) in CH$_2$Cl$_2$ (100 mL) was added to a 500-mL round-bottom flask and cooled to 0°C. The acid chloride residue was dissolved in CH$_2$Cl$_2$ (100 mL) , transferred to a dripping funnel and slowly added to the ethylenediamine solution while stirring rapidly. The resulting slurry was stirred for 1 h. An excess of triethylamine was added and the mixture was stirred for an additional 0.5 h. This mixture was treated with 6 M NaOH (ca. 100 mL) and heated under vacuum to remove the volatile organics. The remaining aqueous solution was decanted from the undissolved organic residues which were then dissolved in a minimal amount of acetone

and retreated with 6 M NaOH solution. All aqueous portions were combined
and cautiously acidified with concentrated HCl. The precipitate was collected,
washed with water, and recrystallized from acetone/water: yield 33.3 g (80%).
Characterization of the unchlorinated intermediate, H_4HBA-Et, appears
elsewhere.[1] Chlorination proceeded as follows: The unchlorinated product
(5.0 g) was dissolved in glacial acetic acid (80-100 mL) in a 500-mL filtration
flask. Chlorine gas was bubbled through the stirred solution for 0.5 h. The
precipitated product was collected, washed with water, and recrystallized
from acetone/water: yield 6.6 g (90%); m.p. = 254-256°C; IR (Nujol) 3343
(s, ν(NH)), 3280 (s broad, ν (OH)), 1632 (s, amide I, ν(C=O)), 1585 (s, ν(arene)),
1548 (s, amide II) (also see Fig. 2.1) cm^{-1}; ^{1}H NMR (acetone-d_6) δ 7.74 (d,
2, Ph), 7.54 (d, 2, Ph), 3.70 (s, 4, -CH_2-). Anal. calcd. for $C_{16}H_{12}Cl_4N_2O_4$:
C, 43.87; H, 2.76; Cl, 32.37; N, 6.39. Found: C, 44.01; H, 2.81; Cl, 32.59;
N, 6.36.

Method B. 3,5-Dichlorosalicyclic acid (2.07 g, 0.01 mol) and Et_3N (3.06
mL, 0.022 mol) were dissolved in dry THF (100 mL) in a 250-mL 3-neck flask.
Phosgene[33] was passed through a back-up trap, bubbled through the reaction
mixture and passed out through two successive traps filled with solid KOH.
Phosgene indicator paper[33] was used to check for leaks in the system and to
check efficiency of the traps. Addition of phosgene to the clear colorless
solution caused formation of a white precipitate. After 10 min the mixture
developed a slight pink color. The addition was continued for an additional 5
min and the solvent and excess $COCl_2$ were then pumped off through the KOH
traps. The residue was twice dissolved in CH_2Cl_2 and evaporated to dryness
to remove the last traces of phosgene. The resulting solid was redissolved

in CH_2Cl_2 (200 mL) and Et_3N (3.06 mL). Addition of ethylenediamine

(0.334 mL, 0.005 mol) in CH_2Cl_2 (50 mL) produced a white precipitate. The

mixture was heated under reflux for 4 h and evaporated to dryness. The

product was extracted into acetone and a small quantity of HCl was added to

precipitate any remaining Et_3N as the ammonium salt. The acetone solution

was concentrated and the product precipitated by the addition of water.

Recrystallization from acetone/water yielded the product as a white

microcrystalline solid (1.31 g, 60%).

H_4CHBA-DMBu. 3,5-Dichlorosalicyclic acid (2.07 g, 0.01 mol) was

converted to the carbonate-cyclic anhydride with phosgene as described in

the synthesis of H_4CHBA-Et, 1 (Method B). The intermediate was dissolved

in CH_2Cl_2 (250 mL) containing Et_3N (1.53 mL, 0.011 mol). 2,2,3,3-

Tetramethylethylenediamine hydrochloride (0.945 g, 0.005 mol) was added but

did not appear to dissolve appreciably. The solution was refluxed for 5 h

after which there remained undissolved solid. An aliquot was removed from

the reaction and worked up as in the synthesis of H_4CHBA-Et (Method B). IR

indicated that no ligand had been formed. It was assumed that the insolubility

of the ammonium salt had resulted in the failure to produce free amine in

solution. Na_2CO_3 and H_2O were added and the resulting two-phase system

was heated under reflux for 12 h. The reaction mixture was worked up in the

usual way to produce very light yellow crystals of the product.

Recrystallization from CH_2Cl_2/EtOH yielded white crystals of the product

(0.5 g). NMR indicates the presence of solvated ethanol (0.8 EtOH per

molecule of ligand): IR (Nujol) 3380 (m, ν(NH)), 3295 (m broad, ν(OH)), 1645

(s, amide I, ν(C=O)), 1587 (s, ν(arene)), 1550 (s, amide II) cm^{-1}; ^{1}H NMR

(CDCl$_3$) δ 7.57 (d, 2, Ph), 7.43 (d, 2, Ph), 1.60 (s, 12, -CH$_3$). Anal. calcd. for C$_{20}$H$_{20}$Cl$_4$N$_2$O$_4$·0.8 (C$_2$H$_6$O): C, 48.85; H, 4.71; N, 5.27. Found: C, 48.81; H, 4.80; N, 4.97.

Osmium Complex Syntheses

All reactions were carried out in air.[34] K$_2$[Os(OH)$_4$(O)$_2$] was prepared as described in the literature.[35]

__K$_2$[Os(η^4-CHBA-Et)(O)$_2$]·H$_2$O, 2.__ Addition of a blue methanol solution of K$_2$[Os(OH)$_4$(O)$_2$] (0.500 g in 100 mL) to a colorless acetone solution containing 1 equiv of pure H$_4$CHBA-Et (0.595 g in 80 mL) produced an immediate color change to deep orange. The solution was stirred at room temperature for 10 min, then evaporated to dryness to give a quantitative yield of the product. Recrystallization of 200 mg from acetone/CH$_2$Cl$_2$ yielded the orange microcrystalline product (179 mg, 90%). After heating the sample at 80°C for 12 h under vacuum, NMR showed the presence of one H$_2$O per molecule of complex. On standing in air the compound reabsorbs ca. 3 additional molecules of H$_2$O per molecule of complex: Raman (aqueous) 870 (ν_s(OsO$_2$)) cm^{-1}; IR (Nujol) 820 (vs, ν_{as}(OsO$_2$)) (also see Fig. 2.2) cm^{-1}; ^{1}H NMR (acetone-d$_6$) δ 8.21 (d, 2, Ph, $J_{H,H}$ = 3 Hz), 7.27 (d, 2, Ph, $J_{H,H}$ = 3 Hz), 3.88 (s, 4, -CH$_2$-), 3.77 (s, 2, H$_2$O). Anal. calcd. for C$_{16}$H$_8$Cl$_4$K$_2$N$_2$O$_6$Os·(H$_2$O): C, 25.54; H, 1.34; N, 3.72. Found: C, 25.44; H, 1.50; N, 3.61. Incorporation of ^{18}O was effected by allowing the compound to stand with H$_2$^{18}O for 24 h; IR (Nujol) 788 (vs, ν_{as} (Os^{18}O$_2$)) cm^{-1}.

__Os(η^4-CHBA-Et)(py)$_2$, 5.__ K$_2$[Os(η^4-CHBA-Et)(O)$_2$]·(H$_2$O)$_4$, 2 (0.540 g), was dissolved in pyridine (20 mL) and H$_2$O (15 mL). Two equivalents of

triphenylphosphine (0.356 g) in pyridine (15 mL) were added and the mixture was heated with stirring at 60°C for 0.5 h. The reaction was accompanied by a color change to deep red-orange. The solution was evaporated to dryness and the residue was then warmed under vacuum for an additional 12 h to insure complete removal of the solvents. The dry residue was washed with CH_2Cl_2 (20 mL) to remove the phosphines. The reduced intermediate, **4**, was collected as a red-brown solid which was then redissolved in THF (50 mL) and H_2O (10 mL). To this solution was added 30% H_2O_2 (ca. 20 mL) in THF (20 mL) while cooling in a 0°C bath. The solution was stirred at room temperature for ca. 15 min or until the color change to deep royal blue was complete. Addition of methanol (20 mL) followed by slow removal of the THF yielded the deep blue crystalline product (0.405 g, 77% based on **2**). An analytical sample was obtained by slow crystallization from THF/hexane: IR (nujol) 1611 (m, py), 1599 (s), 1587 (sh), 1564 (vs), 1535 (s), 1291 (vs), 1212 (m), 1065 (m, py), 1043 (m, py), 1016 (m, py), 866 (m), 772 (s), 728 (s) cm^{-1}; ^1H NMR ($CDCl_3$) δ 68.55 (s, 4, $-CH_2-$), 14.93 (d, 2, Ph, $J_{H,H}$ = 3 Hz), 10.55 (d, 2, Ph, $J_{H,H}$ = 3 Hz), 7.73 (dd, 4, H_m, $J_{m,o}$ = $J_{m,p}$ = 8 Hz), -1.39 (t, 2, H_p, $J_{p,m}$ = 8 Hz), -6.29 (d, 4, H_o, $J_{o,m}$ = 8 Hz) (also see Fig. 2.6). Anal. calcd. for $C_{26}H_{18}Cl_4N_4O_4Os$: C, 39.91; H, 2.32; N, 7.16. Found: C, 39.93; H, 2.42; N, 7.14.

References and Notes

(1) Spies, G. H. Ph.D. Thesis, California Institute of Technology, October, 1984.

(2) Collins, T. J.; Santarsiero, B. D.; Spies, G. H. J. Chem. Soc., Chem. Commun. **1983**, 681.

(3) Krafft, T. E. Unpublished results.

(4) (a) Anson, F. C.; Christie, J. A.; Collins, T. J.; Coots, R. J.; Furutani, T. T.; Gipson, S. L.; Keech, J. T.; Krafft, T. E.; Santarsiero, B. D.; Spies, G. H. J. Am. Chem. Soc. **1984**, 106, 4460. (b) Collins, T. J.; Krafft, T. E.; Santarsiero, B. D.; Spies, G. H. J. Chem. Soc., Chem. Commun. **1984**, 198.

(5) Rybka, J. S.; Margerum, D. W. Inorg. Chem. **1981**, 20, 1453.

(6) Silverstein, R. M.; Bassler, G. C.; Morrill, T. C. "Spectrometric Identification of Organic Compounds"; John Wiley and Sons: New York, 1974, pp. 104-107.

(7) Christie, J. A. Unpublished results.

(8) Schroeder, M. Chem. Rev. **1980**, 80, 187.

(9) Krafft, T. E.; Lee, S. C.; Peake, G. T. Unpublished results.

(10) (a) Avdeef, A.; Schaefer, W. P. J. Am. Chem. Soc. **1976**, 98, 5133. (b) Gall, R. S.; Rogers, J. F.; Schaefer, W. P.; Christoph, G. G. Ibid. **1976**, 98, 5135. (c) Huie, B. T.; Leyden, R. M.; Schaefer, W. P. Inorg. Chem. **1979**, 18, 125.

(11) The X-ray structure determination of **3** was carried out by G. H. Spies at Caltech. See references 1 and 4b.

(12) A chromium(III) dimer has been structurally characterized in which the

ligand CHBA-Et bridges two metal centers and is coordinated by both deprotonated N-bound and protonated O-bound amides. Collins, T. J.; Santarsiero, B. D.; Spies, G. H. <u>J. Chem. Soc., Chem. Commun.</u> **1983,** 681.

(13)   Zintl, E.; Harder, A.; Dauth, B. <u>Z. Electrochem.</u> **1934,** <u>40</u>, 588.

(14)   Tebbe, K. F.; Von Schnering, H. G. <u>Z. Anorg. Allg. Chem.</u> **1973,** <u>396</u>, 66.

(15)   The X-ray structure determination of **5** was carried out at Caltech with much assistance from G. H. Spies and B. D. Santarsiero. See reference 4a.

(16)   Elder, R. C. <u>Inorg. Chem.</u> **1968,** <u>7</u>, 1117; **1968,** <u>7</u>, 2316.

(17)   Cotton, F. A.; Wilkinson, G. "Advanced Inorganic Chemistry"; 4th ed.; John Wiley and Sons: New York, 1980, pp. 644-652 and 912-417.

(18)   (a) Pawson, D.; Griffith, W. P. <u>J. Chem. Soc., Dalton Trans.</u> **1975,** 417. (b) Randall, E. W.; Shaw, D. <u>J. Chem. Soc. A</u> **1969,** 2867. (c) Chatt, J.; Leigh, G. J.; Mingos, D. M. P.; Paske, R. J. <u>Ibid.</u> **1968,** 2636. (d) Chatt, J.; Leigh, G. J.; Mingos, D. M. P.; Randall, E. W.; Shaw, D. <u>Chem. Commun.</u> **1968,** 419.

(19)   Jorgensen, W. L.; Salem, L. "The Organic Chemist's Book of Orbitals"; Academic Press: New York, 1973, p. 265.

(20)   (a) Richardson, D. E.; Taube, H. <u>J. Am. Chem. Soc.</u> **1983,** <u>105</u>, 40. (b) Ford, P.; Rudd, De F. P.; Gaunder, R.; Taube, H. <u>Ibid.</u> **1968,** <u>90</u>, 1187. (c) Zwickel, A. M.; Creutz, C. <u>Inorg. Chem.</u> **1971,** <u>10</u>, 2395. (d) Gaunder, R. G.; Taube, H. <u>Ibid.</u> **1970,** <u>9</u>, 2627.

(21)   Magnuson, R. H.; Taube, H. <u>J. Am. Chem. Soc.</u> **1975,** <u>97</u>, 5129.

(22)   Richardson, D. E.; Walker, D. D.; Sutton, J. E.; Hodgson, K. O.;

Taube, H. Inorg. Chem. **1979**, <u>18</u>, 2216.

(23) Brown, G. M.; Hopf, F. R.; Meyer, T. J.; Whitten, D. G. J. Am. Chem. Soc. **1975**, <u>97</u>, 5385.

(24) Gipson, S. L.; Treco, B. G. R. T. Unpublished results.

(25) Magnuson, R. H. Inorg. Chem. **1984**, <u>23</u>, 387.

(26) Peake, G. T.; Keech, J. T. Unpublished results.

(27) Atomic scattering factors were taken from: "International Tables for X-ray Crystallography"; Witton: Birmingham, 1974, Vol. IV, pp. 72-97.

(28) The goodness-of-fit $S = \left(\Sigma w\Delta^2/(n-v) \right)^{1/2}$, n = number of reflections, v = number of parameters; $R_F = \Sigma |\Delta F| / \Sigma |F_o|$ (based on reflections with I > 0), $\Delta F = |F_o| - |F_c|$, $R'_F = F_F$ (based on reflections with I > $3\sigma_I$).

(29) The CRYM computing system was used (Duchamp, D. J., California Institute of Technology).

(30) Bewad, J. Chem. Ber. **1906**, <u>39</u>, 1232.

(31) Meyer, H.; Bernhauer, K. Monatshefte für Chemie **1929**, <u>53/54</u>, 738.

(32) Durst, H. D.; Gokel, G. W. "Experimental Organic Chemistry"; McGraw Hill: New York, 1980, pp. 256.

(33) Appropriate precautions should be taken when working with phosgene gas which is highly toxic. "The Merck Index"; 9th ed.; Merck and Company: Rahway, New Jersey, 1976, pp. 955.

(34) Although the complexes reported here are all stable species, appropriate precautions should be taken when working with osmium complexes, since evolution of toxic OsO_4 is possible.[35]

(35) Malin, J. M. Inorg. Synth. **1980**, <u>20</u>, 61.

CHAPTER 3

Selective Oxidative Transformations of the Metallacyclopentane

and Metallacyclopentene Ring Components in the

Complex Os(η^4-CHBA-Et)(py)$_2$

and Derivative Complexes

Introduction

The osmium(IV) complex $Os(\eta^4\text{-CHBA-Et})(py)_2$, **5**, was found to exhibit irreversible oxidative electrochemistry (see Chapter 2). Oxidation to the corresponding osmium(V) complex is only possible on the cyclic voltammetry time scale at low temperature. Controlled potential oxidation of **5** instead leads to a complex series of irreversible changes. We became interested in pursuing this chemistry for two reasons. First, because of ligand design considerations, we wished to determine whether the irreversibility was due to ligand decomposition, and, if so, to establish the nature of the process. Second, electrochemical evidence suggested that some product of the osmium oxidation was able to catalyze the electrochemical oxidation of alcohols (see Chapter 4). Studies on the oxidation of **5** are reported in this chapter.

Controlled potential oxidation of **5** in the presence of alcohol or water was found to trigger a series of chemical and electrochemical transformations in which the ethane backbone of the ligand is oxidized in a selective and stepwise fashion.[1] Several key intermediates have been isolated, independently synthesized and characterized. X-ray crystal structures of four compounds in the series are reported. Significant structural and chemical features of the isolated intermediates are discussed and mechanistic aspects of the ligand oxidation process are addressed.

Results and Discussion

Electrochemical Oxidation of $Os(\eta^4\text{-CHBA-Et})(py)_2$, 5

The oxidative sensitivity of the ethane unit bridging the two amide nitrogens causes the oxidation of the complex $Os(\eta^4\text{-CHBA-Et})(py)_2$, 5, to be irreversible. Electrochemical oxidation of 5 by cyclic voltammetry is irreversible at room temperature (see Chapter 2, page 43), even in the presence of an added oxidizable substrate such as an alcohol. All electrochemistry reported here was performed by Stephen Gipson. Controlled potential oxidation of 5 (1-2 mM) at +0.87 V vs. Fc^+/Fc in CH_2Cl_2 containing ROH (R = alkyl, H) (0.5-1 M) consumes at least six electrons per osmium atom and gives a quantitative conversion of 5 to one of the two new complexes, 9 and 9', or a mixture of both.[1] The distribution between 9 and 9' depends on the nature of R (vide infra).

The electrolysis of 5 was monitored by thin layer chromatography (TLC) of the anolyte solution.[2] These results suggested that the conversion from 5 to 9 or 9' proceeds through three distinct intermediates, 6, 7, and 8, which appear as a mixture of transient species in solution (Scheme 3.1). Comparison of TLC results when different alcohols are employed indicates that 6 and 8 contain the alcohol group while 7, 9, and 9' do not. Intermediates 9 and 9' can each be converted to active catalysts for the electrochemical oxidation of alcohols (see Chapter 4). Isolation of the various intermediates from the electro-chemical media is inconvenient, since they are present as a complex mixture. The large quantity of supporting electrolyte also complicates separation. We therefore sought independent chemical syntheses of these compounds.

Scheme 3.1. Controlled potential oxidation of $Os(\eta^4\text{-CHBA-Et})(py)_2$, **5** (1-2 mM), in the presence of ROH (0.5 M) in CH_2Cl_2 at +0.87 V vs. Fc^+/Fc.
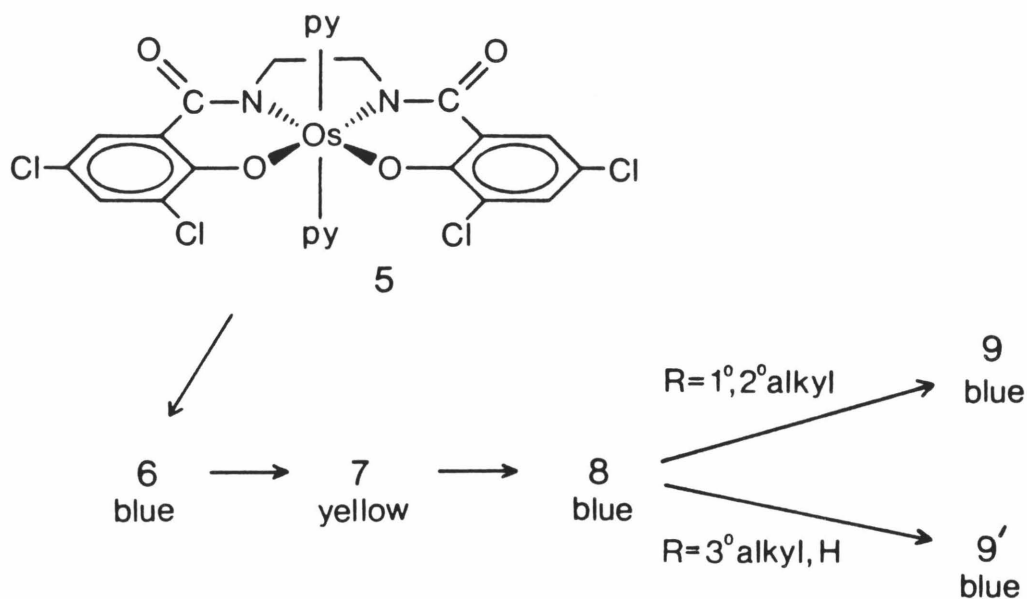
Synthesis and Characterization of Oxidation Intermediates

$\underline{Os(\eta^4\text{-CHBA-ethylene})(py)_2}$, **7**.[3] Purification of complex **5** on silica gel columns often produces a very minor yellow impurity. The color and TLC properties of this material were found to match those of the intermediate complex **7**, which is formed in the electrochemical oxidation of **5** (Scheme 3.1). The cyclic voltammogram of the isolated impurity also showed signals which matched some of the peaks seen in the cyclic voltammogram of the electrochemical reaction mixture. Controlled potential electrolysis of the compound was used to identify it as complex **7**. Oxidation of **7** at +0.87 V in the presence of alcohol or water produces **8** and then **9** and/or **9'**.

Attempts to produce **7** chemically focused on the fact that it appears only when **5** has been in contact with silica gel. It was discovered that

absorption of **5** onto silica gel, followed by heating in air, produces a substantial quantity of the yellow complex **7** (Scheme 3.2). Removal of **7** from the silica leaves a mixture of $(Os(\eta^4\text{-CHBA- Et})(py)_2)^-$, **4**, and the starting material, **5**. By our cycling the silica gel several times, more than 90% of **5** can be converted to **7**. A lower yield of **7** can be obtained by heating solid **5**

Scheme 3.2
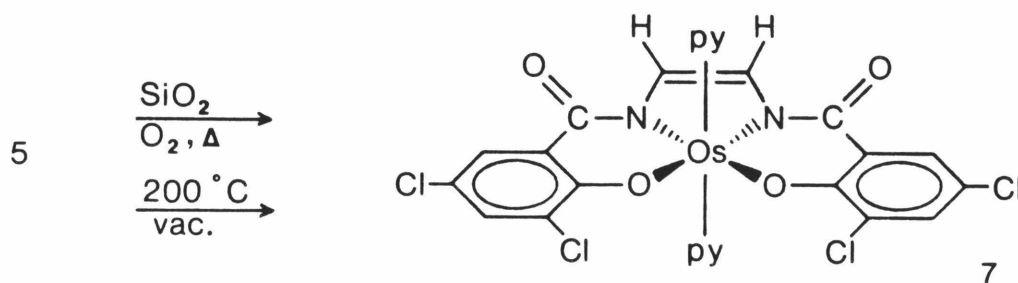
to ca. 200°C under vacuum. Complex **7** has been characterized by IR, ^{1}H and ^{13}C NMR, magnetic susceptibility and elemental analysis. The derivative complex which bears axial tert-butyl pyridine (t-Bupy) ligands has also been characterized by an X-ray crystal structure determination. These results confirm the structure depicted in Scheme 3.2 and demonstrate that conversion from **5** to **7** involves oxidative dehydrogenation of the ligand backbone to form the ethylene bridge found in **7**.

The ^{1}H NMR spectrum of the neutral paramagnetic complex **7** is shown in Figure 3.1 (also see Table 3.11, page 101). The spectrum is well resolved, like that of complex **5** (see Chapter 2, page 41), and displays significant paramagnetic shifts in some signals.[4] As with **5**, the signals for the pyridine ortho and para protons are significantly shifted upfield, while the meta proton
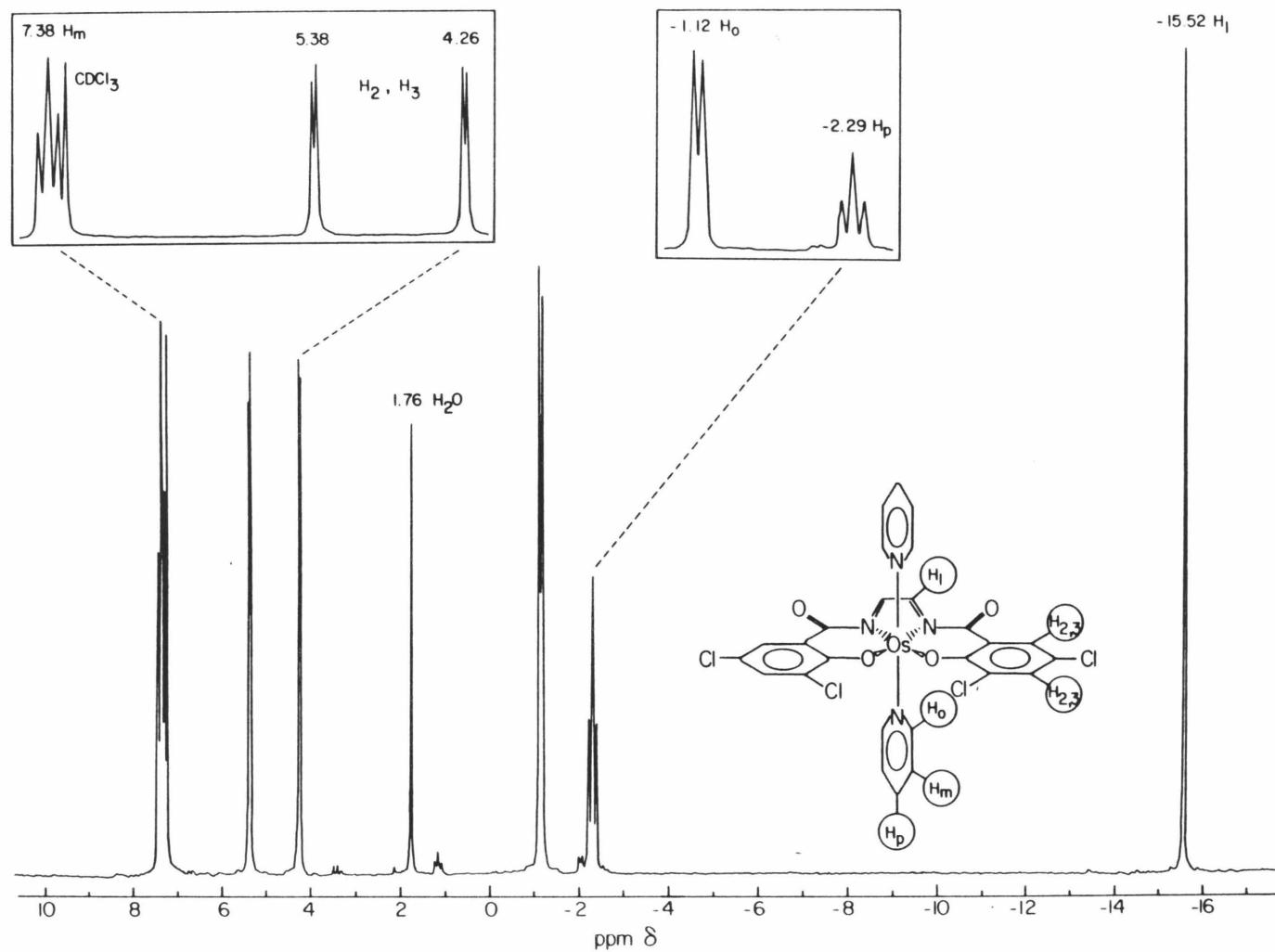
Figure 3.1. 90-MHz ^{1}H NMR spectrum of 7 (CDCl₃).

is not affected. This may again be an indication of π-backbonding from osmium to the pyridine π^* orbital, $3B_1$.[5] The same effect is seen for all of the osmium(IV) pyridine complexes discussed in this thesis.[6] It should be noted that the t-Bupy complexes exhibit almost identical chemical shifts for the ortho and meta protons as those found for the corresponding pyridine complexes (Table 3.11). The signal for the methine protons of the metallacyclopentene ring in 7 is found at -15.52 ppm. This is 84 ppm upfield from the position of the methylene protons of the metallacyclopentane ring in 5 (+68.55 ppm). The ^{13}C NMR data (Table 3.12, page 105) for 7 show each methine carbon on the bridge coupled to a single proton.

The unsaturated five-membered metallacycle of 7 can be represented by two resonance structures in which the formal oxidation state of the metal is different (Fig. 3.2). The electrochemical and structural data suggest a variable
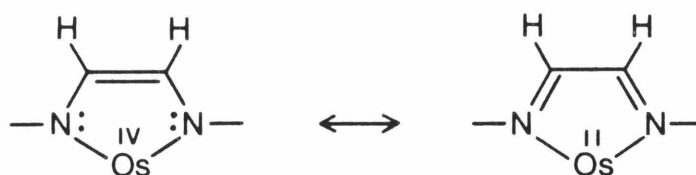
Figure 3.2. Resonance structures in 7.

contribution from the diimine structure depending on the oxidation level. In the neutral osmium(IV) state there is little if any resonance stabilization, but upon oxidation to osmium(V) there is a significant contribution from the diimine structure.

The cyclic voltammogram of 7 in CH_2Cl_2 in the absence of alcohol or water is shown in Figure 3.3. Two reversible diffusion-controlled one-electron
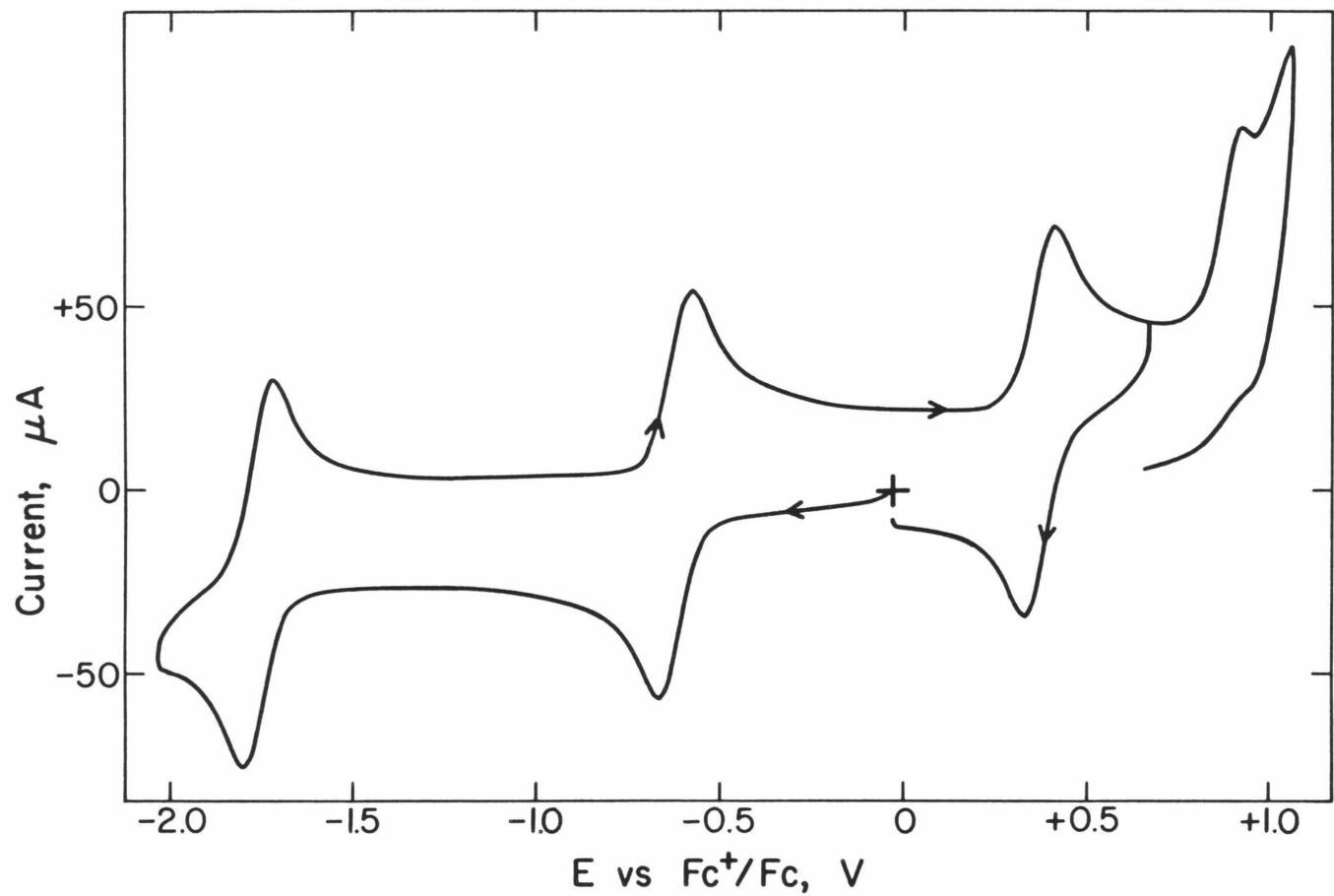
Figure 3.3. Cyclic voltammogram of 1 mM **7** in CH_2Cl_2, 0.1 M TBAP at 0.174 cm^2 BPG electrode. Scan rate = 200 mV s^{-1}.

waves are found at E^f = -0.62 and -1.76 V. A reversible oxidation appears at E^f = +0.37 V and an irreversible oxidation is found at E_p = +0.92 V. The potentials for the two reductions are very similar to those exhibited by complex **5**. The reversible oxidation at +0.37 V, however, is 330 mV lower than the corresponding irreversible oxidation in **5**. The potentials measured in SO_2 at low temperature provide a better comparison, since the oxidative waves are reversible for both complexes (Table 3.1, Fig. 3.4). Here the first oxidation for **7** is 380 mV lower than for **5**. This first oxidation in osmium(IV)

Table 3.1 Formal potentials for **5** and **7** at -40°C in SO_2.

Compound	IV/III[a]	V/IV[a]	2nd Oxid.[a]	3rd Oxid.[a]	4th Oxid.[a]
5	-0.19	+0.86	+1.37	(+2.01)[b]	--
7	-0.13	+0.48	+1.11	+1.89	(+2.17)[b]

[a]Potentials are reported against the Fc^+/Fc couple which was measured at ca. +0.48 V vs. SCE. [b]Peak potential for an irreversible oxidation.

complexes of the type $Os(HBA)L_2$ is believed to be metal centered, since the potentials vary in a rational way with different ligands L.[1,7] The above results then suggest that some resonance stabilization is operative when **7** is oxidized to osmium(V).

The crystal structure[8] of the osmium(IV) complex $Os(\eta^4\text{-CHBA-}$ ethylene)(t-Bupy)$_2$, **7**, shows the osmium in a pseudo-octahedral environment with the chelate ligand bound in the equatorial plane and t-Bupy ligands in the axial positions (Fig. 3.5, Tables 3.2 and 3.3). Bond lengths in the amide groups
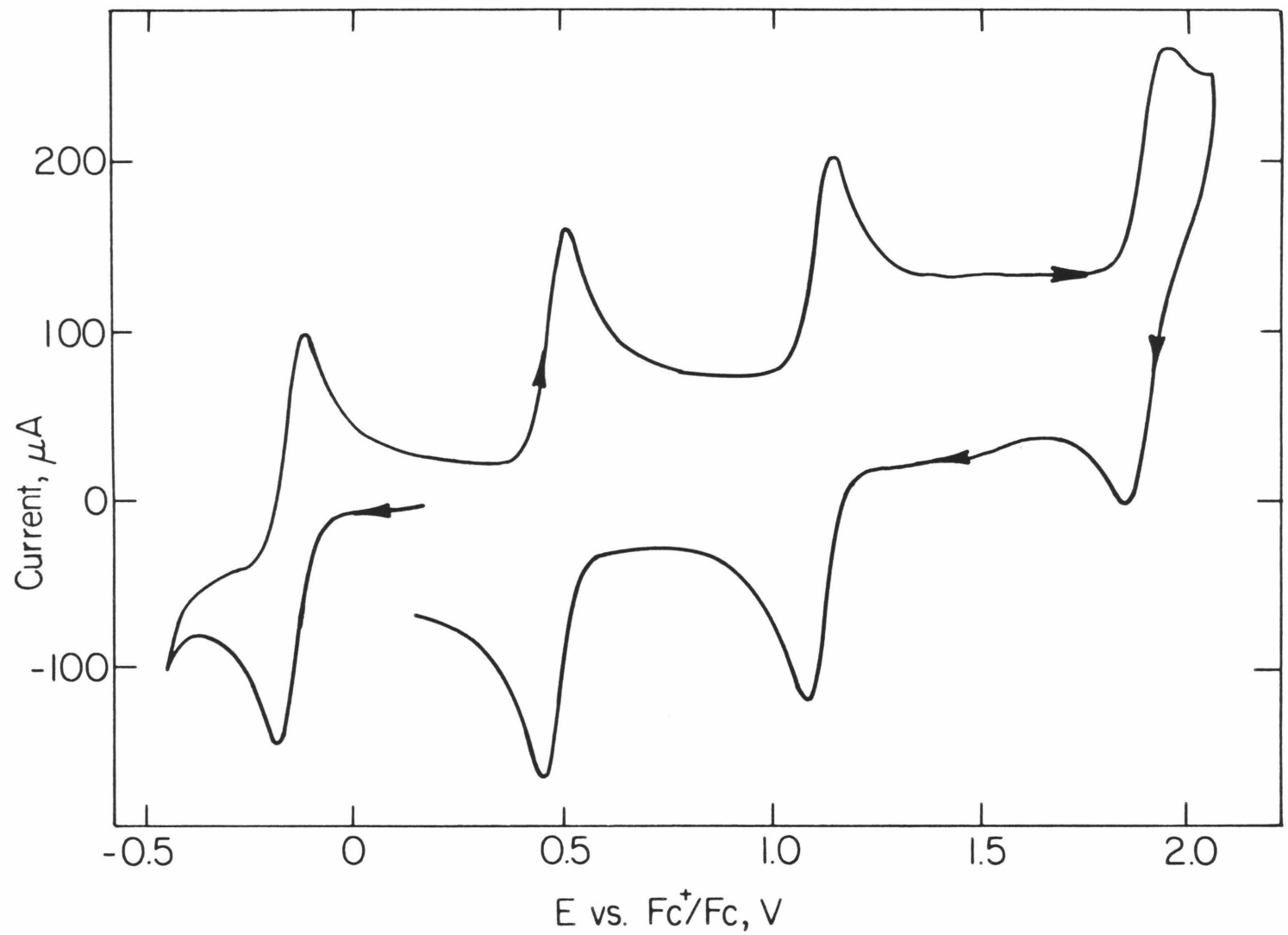
Figure 3.4. Cyclic voltammogram of 2 mM **7** at -40°C in liquid SO_2, 0.1 M ($\underline{n}$-Bu$_4$N)BF$_4$ at a glassy carbon electrode. Scan rate = 200 mV s^{-1}.
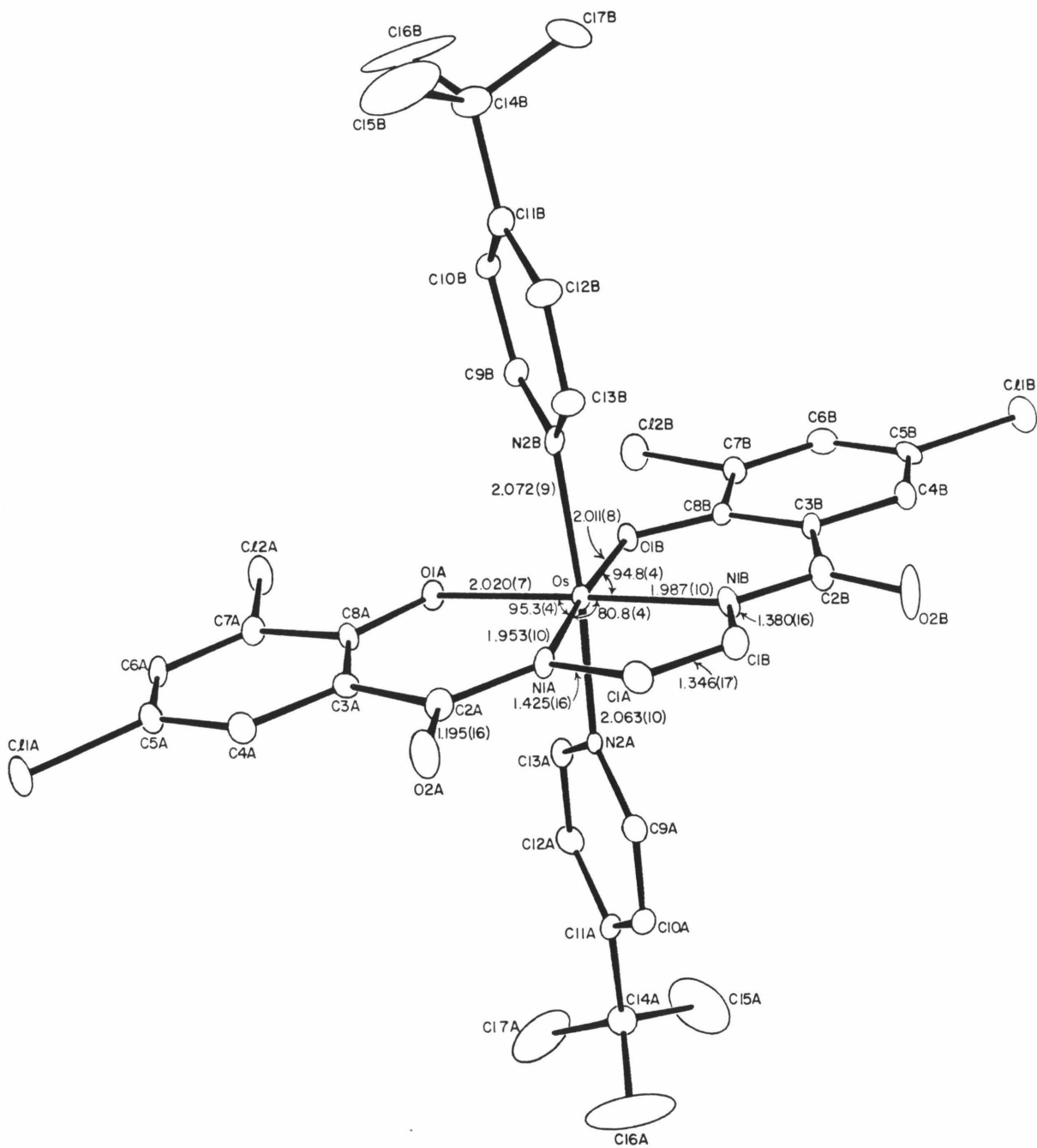
Figure 3.5. Molecular structure of Os(η^4-CHBA-ethylene)(t-Bupy)$_2$, 7.

Table 3.2. Bond distances for Os(η^4-CHBA-ethylene)(t-Bupy)$_2$, 7 (Å).

Atoms	Distance	Atoms	Distance
Os-O(1A)	2.020(7)	Os-O(1B)	2.011(8)
Os-N(1A)	1.953(10)	Os-N(1B)	1.987(10)
Os-N(2A)	2.072(9)	Os-N(2B)	2.063(10)
Cl(1A)-C(5A)	1.762(14)	Cl(1B)-C(5B)	1.753(15)
Cl(2A)-C(7A)	1.703(13)	Cl(2B)-C(7B)	1.718(13)
Cl(3)-C(18)	1.655(23)	Cl(4)-C(18)	1.628(23)
O(1A)-C(8A)	1.340(14)	O(1B)-C(8B)	1.311(14)
O(2A)-C(2A)	1.195(16)	O(2B)-C(2B)	1.211(17)
N(1A)-C(1A)	1.425(16)	N(1B)-C(1B)	1.380(16)
N(1A)-C(2A)	1.415(16)	N(1B)-C(2B)	1.393(17)
N(2A)-C(9A)	1.333(16)	N(2B)-C(9B)	1.308(15)
N(2A)-C(13A)	1.371(15)	N(2B)-C(13B)	1.363(16)
C(1A)-C(1B)	1.346(17)		
C(2A)-C(3A)	1.496(17)	C(2B)-C(3B)	1.519(18)
C(3A)-C(4A)	1.429(17)	C(3B)-C(4B)	1.405(18)
C(3A)-C(8A)	1.425(17)	C(3B)-C(8B)	1.384(17)
C(4A)-C(5A)	1.383(18)	C(4B)-C(5B)	1.320(19)
C(5A)-C(6A)	1.364(18)	C(5B)-C(6B)	1.415(20)
C(6A)-C(7A)	1.373(18)	C(6B)-C(7B)	1.356(19)
C(7A)-C(8A)	1.432(17)	C(7B)-C(8B)	1.426(17)
C(9A)-C(10A)	1.379(18)	C(9B)-C(10B)	1.400(17)
C(10A)-C(11A)	1.409(17)	C(10B)-C(11B)	1.404(18)
C(11A)-C(12A)	1.363(18)	C(11B)-C(12B)	1.363(18)
C(11A)-C(14A)	1.502(19)	C(11B)-C(14B)	1.491(21)
C(12A)-C(13A)	1.364(17)	C(12B)-C(13B)	1.373(19)
C(14A)-C(15A)	1.425(35)	C(14B)-C(15B)	1.436(32)
C(14A)-C(16A)	1.383(31)	C(14B)-C(16B)	1.401(32)
C(14A)-C(17A)	1.399(31)	C(14B)-C(17B)	1.420(35)

Table 3.3. Bond angles for Os(η ^{4}-CHBA-ethylene)($\underline{t}$-Bupy)$_2$, 7 (deg).

Atoms	Angle	Atoms	Angle
O(1A)-Os-O(1B)	89.1(3)		
O(1A)-Os-N(1A)	95.3(4)	O(1A)-Os-N(1B)	176.1(4)
O(1A)-Os-N(2A)	86.7(3)	O(1A)-Os-N(2B)	86.8(3)
O(1B)-Os-N(1A)	175.5(4)	O(1B)-Os-N(1B)	94.8(4)
O(1B)-Os-N(2A)	87.9(3)	O(1B)-Os-N(2B)	87.2(3)
N(1A)-Os-N(1B)	80.8(4)	N(2A)-Os-N(2B)	171.9(4)
N(1A)-Os-N(2A)	91.4(4)	N(1A)-Os-N(2B)	94.0(4)
N(1B)-Os-N(2A)	93.6(4)	N(1B)-Os-N(2B)	93.2(4)
Os-O(1A)-C(8A)	122.5(7)	Os-O(1B)-C(8B)	123.4(7)
Os-N(1A)-C(1A)	114.6(8)	Os-N(1B)-C(1B)	113.6(8)
Os-N(1A)-C(2A)	129.7(8)	Os-N(1B)-C(2B)	126.7(8)
Os-N(2A)-C(9A)	123.2(8)	Os-N(2B)-C(9B)	121.2(8)
Os-N(2A)-C(13A)	119.8(7)	Os-N(2B)-C(13B)	122.6(8)
C(2A)-N(1A)-C(1A)	115.7(10)	C(2B)-N(1B)-C(1B)	119.8(10)
C(13A)-N(2A)-C(9A)	117.0(10)	C(13B)-N(2B)-C(9B)	116.0(10)
C(1B)-C(1A)-N(1A)	114.0(11)	C(1A)-C(1B)-N(1B)	117.0(11)
N(1A)-C(2A)-O(2A)	122.9(12)	N(1B)-C(2B)-O(2B)	119.3(12)
C(3A)-C(2A)-O(2A)	121.3(11)	C(3B)-C(2B)-O(2B)	120.9(12)
C(3A)-C(2A)-N(1A)	115.8(10)	C(3B)-C(2B)-N(1B)	119.7(11)
C(4A)-C(3A)-C(2A)	111.2(10)	C(4B)-C(3B)-C(2B)	113.0(11)
C(8A)-C(3A)-C(2A)	130.0(11)	C(8B)-C(3B)-C(2B)	126.3(11)
C(8A)-C(3A)-C(4A)	118.8(11)	C(8B)-C(3B)-C(4B)	120.7(11)
C(5A)-C(4A)-C(3A)	118.7(11)	C(5B)-C(4B)-C(3B)	121.9(12)

Table 3.3. Continued.

Atoms	Angle	Atoms	Angle
C(4A)-C(5A)-Cl(1A)	118.6(10)	C(4B)-C(5B)-Cl(1B)	120.3(11)
C(6A)-C(5)-Cl(1A)	118.0(10)	C(6B)-C(5B)-Cl(1B)	119.5(11)
C(6A)-C(5A)-C(4A)	123.4(12)	C(6B)-C(5B)-C(4B)	120.2(13)
C(7A)-C(6A)-C(5A)	119.5(12)	C(7B)-C(6B)-C(5B)	118.0(12)
C(6A)-C(7A)-Cl(2A)	121.1(10)	C(6B)-C(7B)-Cl(2B)	118.0(10)
C(8A)-C(7A)-Cl(2A)	118.1(9)	C(8B)-C(7B)-Cl(2B)	118.5(9)
C(8A)-C(7A)-C(6A)	120.9(11)	C(8B)-C(7B)-C(6B)	123.6(12)
C(3A)-C(8A)-O(1A)	126.4(10)	C(3B)-C(8B)-O(1B)	129.1(11)
C(7A)-C(8A)-O(1A)	114.9(10)	C(7B)-C(8B)-O(1B)	115.4(10)
C(7A)-C(8A)-C(3A)	118.7(11)	C(7B)-C(8B)-C(3B)	115.6(11)
C(10A)-C(9A)-N(2A)	121.9(12)	C(10B)-C(9B)-N(2B)	124.1(11)
C(11A)-C(10A)-C(9A)	121.9(12)	C(11B)-C(10B)-C(9B)	119.6(11)
C(12A)-C(11A)-C(10A)	114.5(11)	C(12B)-C(11B)-C(10B)	115.6(12)
C(14A)-C(11A)-C(10A)	122.0(11)	C(14B)-C(11B)-C(10B)	121.6(12)
C(14A)-C(11A)-C(12A)	123.5(12)	C(14B)-C(11B)-C(12B)	122.8(12)
C(13A)-C(12A)-C(11A)	122.5(12)	C(13B)-C(12B)-C(11B)	121.6(12)
C(12A)-C(13A)-N(2A)	122.2(11)	C(12B)-C(13B)-N(2B)	123.0(12)
C(15A)-C(14A)-C(11A)	109.3(16)	C(15B)-C(14B)-C(11B)	113.8(16)
C(16A)-C(14A)-C(11)	115.7(16)	C(16B)-C(14B)-C(11B)	111.8(16)
C(17A)-C(14A)-C(11A)	112.3(15)	C(17B)-C(14B)-C(11B)	112.0(17)
C(16A)-C(14A)-C(15A)	112.7(20)	C(16B)-C(14B)-C(15B)	102.7(19)
C(17A)-C(14A)-C(15A)	103.6(19)	C(17B)-C(14B)-C(15B)	104.4(20)
C(17A)-C(14A)-C(16A)	102.5(19)	C(17B)-C(14B)-C(16B)	111.6(20)

Table 3.4. Comparison of averaged bond lengths in **7** to other CHBA complexes.
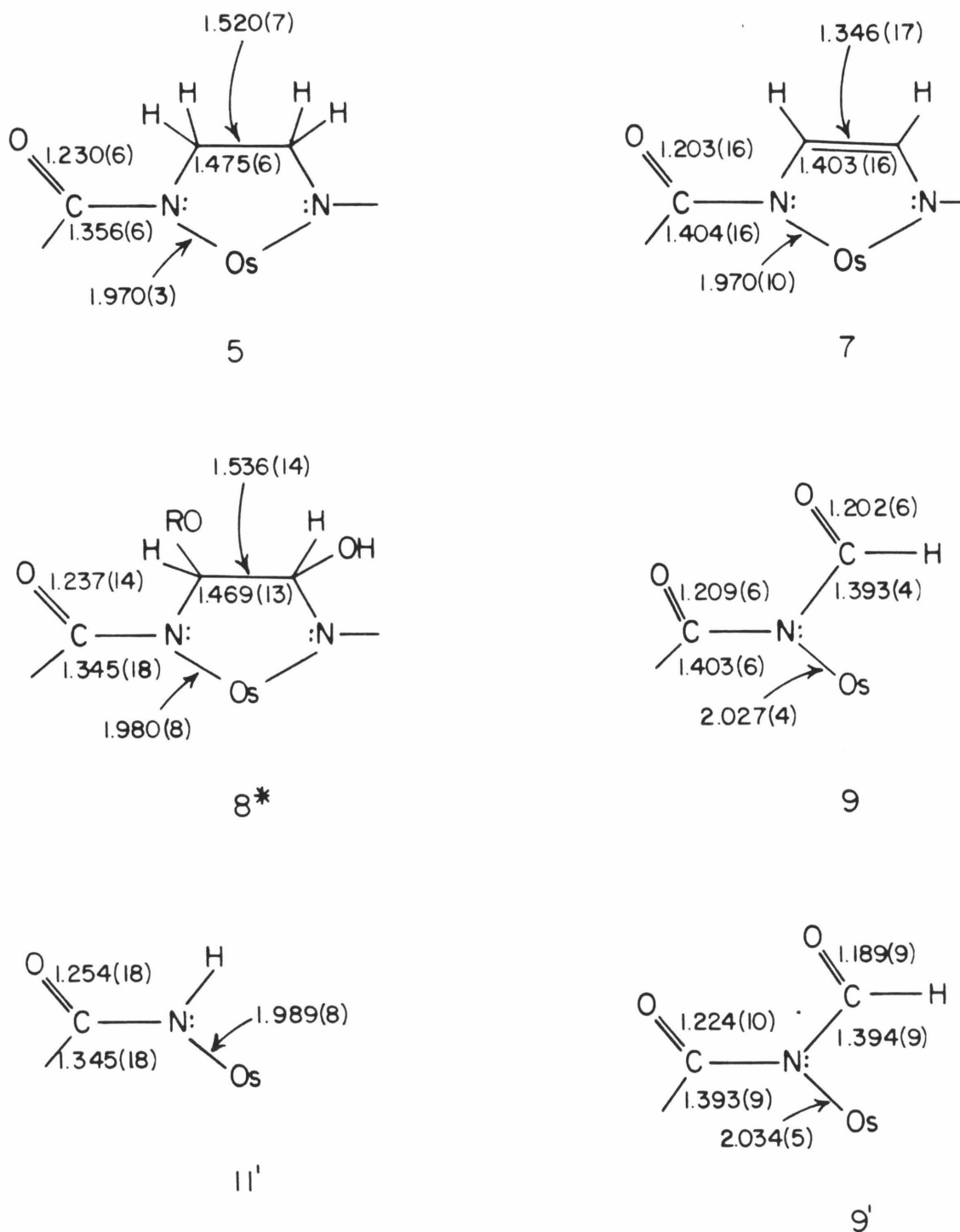
and the metallacyclopentene ring of 7 imply that at most a small contribution from the diimine is present. Table 3.4 compares some relevant bond lengths for several structurally characterized complexes in the ligand oxidation series. Compounds 5, 8* and 11' exhibit somewhat shorter amide carbon-nitrogen bonds and slightly longer carbon-oxygen bonds than do compounds 7, 9 and 9'. This difference can be attributed to a greater delocalization of the nitrogen lone pair onto the carbonyl group in 5, 8* and 11'. Competition for the nitrogen

lone pair in compounds 7, 9 and 9' would decrease this delocalization onto the carbonyl group. In 9 and 9' the competition is from the second carbonyl group and in 7 the competition arises from the diimine resonance structure (Scheme 3.2).

The structure of 7 shows considerable asymmetry in the metallacyclo-pentene ring, so bond length comparisons here may be somewhat dubious. Nevertheless, the averaged carbon-nitrogen distanced in the five-membered ring is about the same length as the carbon-nitrogen bonds in 9 and 9' where resonance delocalization certainly provides some double bond character. However, the carbon-carbon bond in the ring is not significantly longer than expected for a full carbon-carbon double bond. Overall, the structural results suggest that the osmium(IV) formulation is the most appropriate for neutral 7, but some small contribution from the diimine resonance structure may be present. The osmium(IV) formulation is also consistent with the magnetic

data. Complex **7** exhibits a room temperature magnetic moment of 1.24 Bohr magnetons vs. 1.23 BM for complex **5**. These are both in the normal range for octahedral osmium(IV) compounds (1.2-1.7 BM).[9]

The t-Bupy ligands in **7** are eclipsed rather than staggered as found in complex **5**. This relative orientation of the axial pyridine ligands appears to be determined principally by crystal packing effects. Comparison of five structurally characterized osmium(IV) CHBA complexes with axial pyridine ligands reveals no apparent electronic control over the orientation. If electronic control were important, one would expect those complexes which are most electron-rich to have staggered rings in order to maximize the π-back-bonding interaction. The results show that **5** (Fig. 2.5), **8*** (Fig. 3.10) and **9'** (Fig. 3.13) bear staggered pyridines while in **7** and **11'** (Fig. 4.2) the rings are eclipsed. Based on electronic considerations one would have expected **7**, which is arguably the most electron-rich complex, to have staggered rings. Complex **9'**, which is the least electron-rich, would have the least reason to bear staggered rings. These results do not rule out π-backbonding in these compounds, but they do suggest that crystal packing is the dominant affect for determining ring conformation in the solid state.

Compound **7** displays a particularly unusual feature in its infrared spectra (Figs. 3.6 and 3.7). A very strong and broad signal is seen between 3300 and 4000 cm^{-1}. This is by far the most intense band below 4000 cm^{-1} and it is present in both the solid sate and solution spectra. No functional groups are present in the molecule which would account for a vibrational mode in this region and no combination bands of such intensity are expected to appear in this position. The X-ray structure, NMR, and elemental analysis data
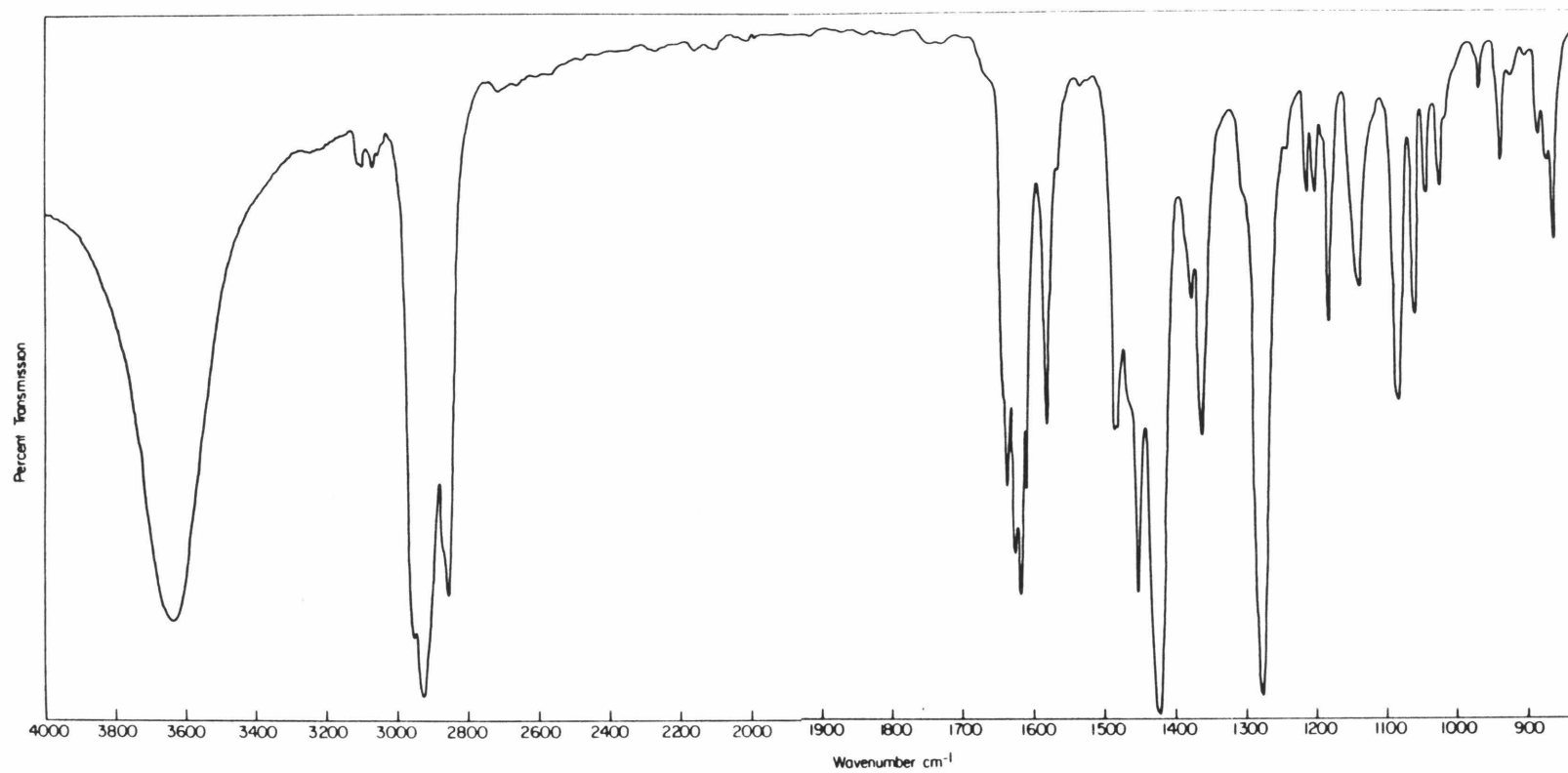
Figure 3.6. IR spectrum of Os(η^4-CHBA-ethylene)(py)$_2$, 7 (nujol mull).
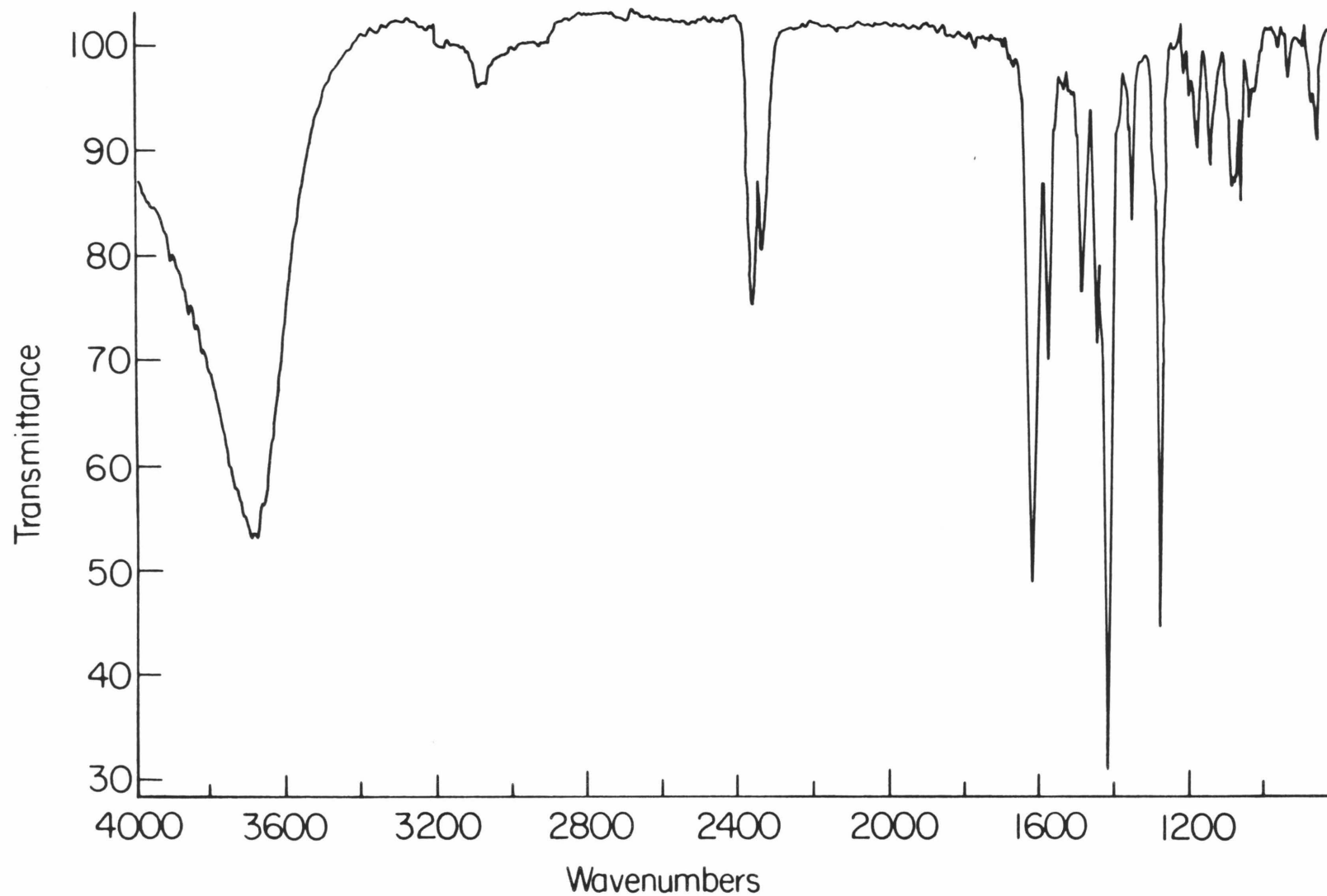
Figure 3.7. IR spectrum of Os(η^4-CHBA-ethylene)(py)$_2$, **7** (CH$_2$Cl$_2$).[12]

rule out the presence of any hydroxyl groups. The band is also somewhat higher than the normal range for O-H stretching activity.[10] The band could be a low-energy electronic transition (λ_{max} = 2750 nm, $\varepsilon \simeq 5 \times 10^2$). Although electronic transitions have been previously observed in the IR region, most of these involve mixed valence dimers and few have been seen at such low energy.[11]

The reactivity of **7** is similar to **5** with the exception that it is more easily oxidized. It is inert toward replacement of the chelate ligand, being stable in the presence of strong acid. Attempts to exchange the pyridines for other ligands either produced no reaction or led to decomposition at elevated temperatures (>100°C). The compound is reduced to osmium(III) by strong base as was found for **5**.

$\underline{Os(\eta^4\text{-CHBA-t-1,2-di-RO-Et})(py)_2}$, **8**.[3] Complex **8** is another intermediate formed during the electrochemical oxidation of **5** in the presence of alcohol or water. TLC results showed that **8** contains the alcohol or some part of it.[2] Chemical conversion of **7** to **8** was therefore pursued with alcohol or water present. It was discovered that **8** can be produced in high yield by oxidation of **7** with dichlorodicyanobenzoquinone (DDQ) in CH_2Cl_2 in the presence of alcohol (Scheme 3.3). The five-membered metallacycle in **8** is symmetrically substituted by <u>trans</u>-alkoxide groups. If the oxidation is performed in the presence of both alcohol and a small quantity of water, the unsymmetrically substituted complex **8***, which bears <u>trans</u>-alkoxide and hydroxide groups, is formed as the major product. In addition, two symmetrical complexes, **8** (R = H or alkyl) are formed as minor products. These compounds have been identified as intermediates **8** by their TLC properties, their cyclic

Scheme 3.3
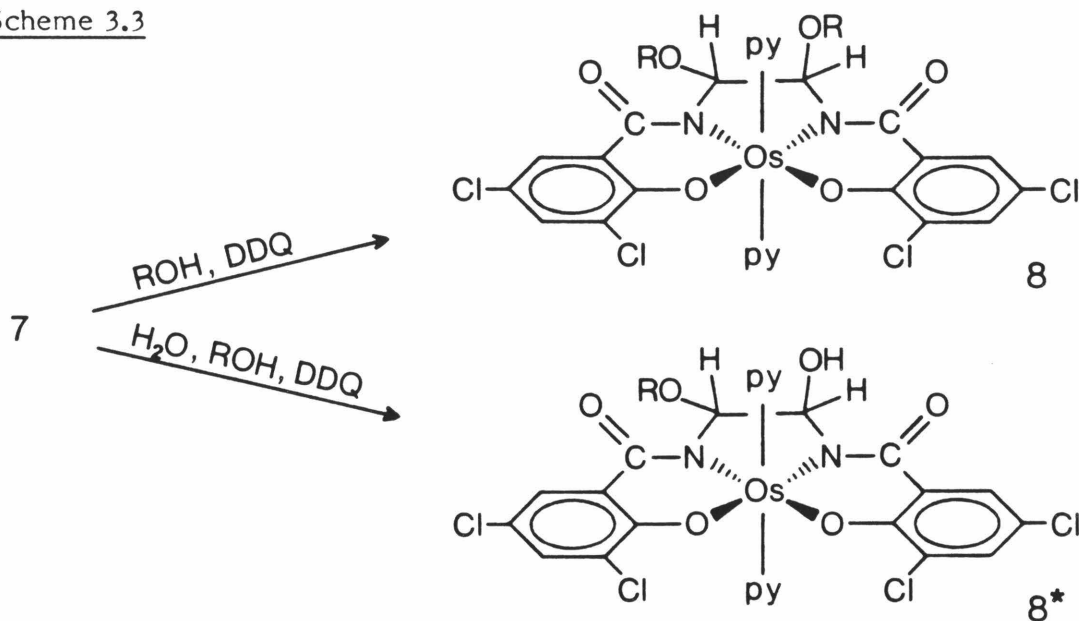
voltammograms and by the demonstration that controlled potential electrolysis converts them to **9** or **9'** as expected.

The structures of the complexes have been confirmed by ^{1}H and ^{13}C NMR (Tables 3.11 and 3.12) and each has been characterized by IR and elemental analysis. The asymmetric compound **8b*** (R = Me) has also been characterized by an X-ray crystal structure determination. The ^{1}H NMR spectrum of **8a** (R = Et) (Figure 3.8) illustrates the quality of resolution which can be observed for these paramagnetic complexes. Once again, the pyridine ortho and para protons are shifted upfield while the meta is not. The four-bond coupling $^4J_{o,p}$ (1.5 Hz) is clearly visible. The methylene protons of the ethoxide groups are diastereotopic and, under the paramagnetic influence of the osmium(IV) center, appear at quite different chemical shifts (7.54 and 6.08 ppm). Each is a doublet of quartets by virtue of coupling to the methyl group and to each other. The ^{13}C NMR data show the bridge to be
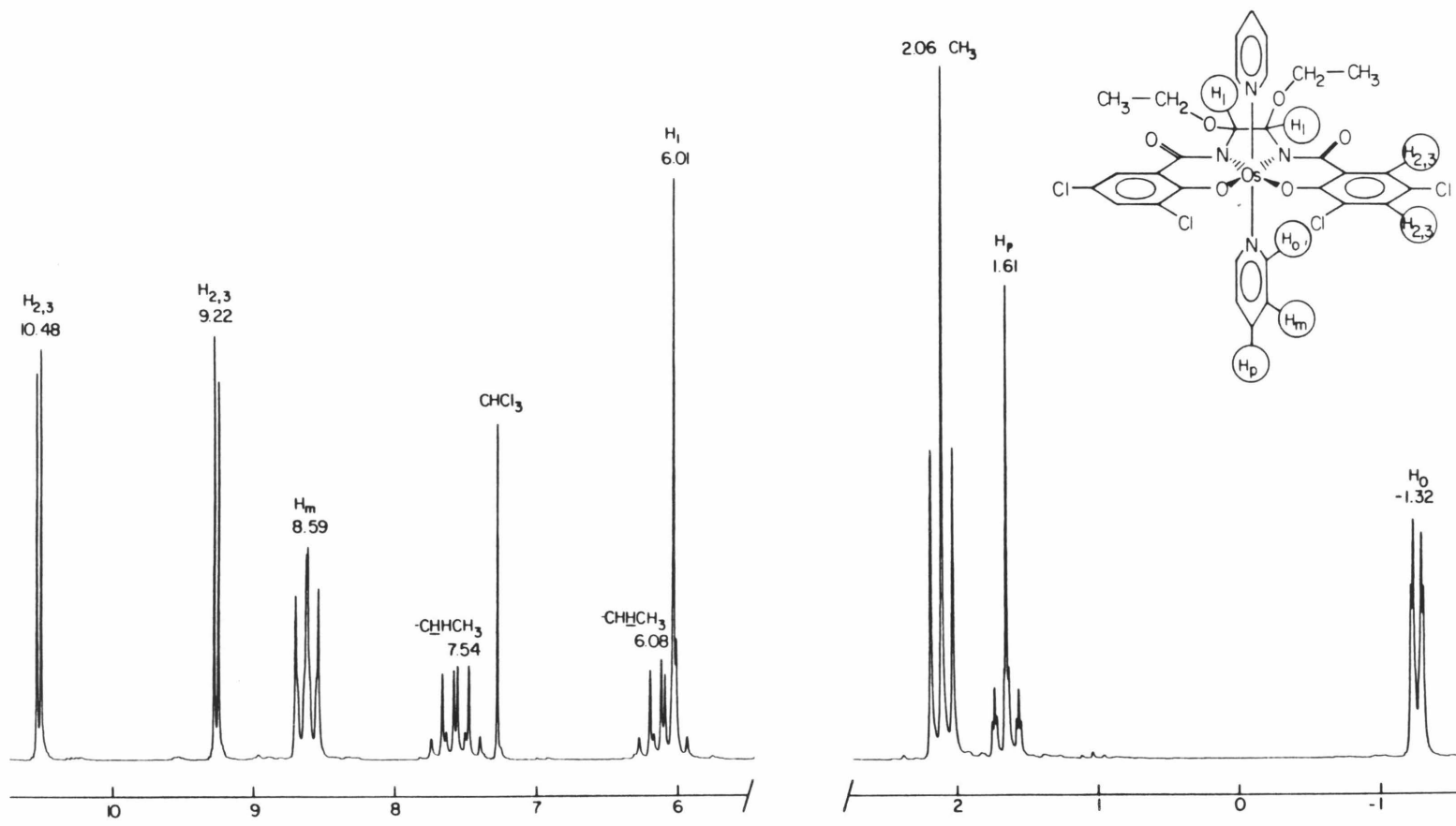
Figure 3.8. 90-MHz ^{1}H NMR spectrum of **8a** (CDCl$_3$).

symmetrically substituted with one ethoxide on each carbon. The equivalence

of the two pyridine rings implies trans substitution of the alkoxides. The cis

substituted product would be inequivalent above and below the plane of the

chelate ligand and would be expected to exhibit different signals for the two

pyridine rings (vide infra). None of the cis substituted product is observed.

Two different coordination geometries at the metal center are consis-

tent with the spectral data. One is the trans-pyridine arrangement with an

equatorial chelate. The second is the cis-α isomer (Fig. 3.9) in which the

phenolic oxygens occupy the axial positions and the pyridines are mutually cis

in the equatorial plane. In the cis-β isomer the two pyridines would be

inequivalent, as would the two halves of the chelate. The trans and cis-α

trans   cis-α cis-β
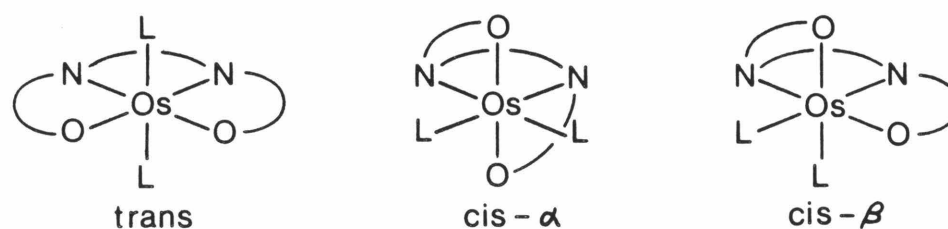
Figure 3.9

isomers have the same symmetry and are therefore indistinguishable by ^{1}H or

^{13}C NMR. The trans arrangement found in the previous X-ray structures

suggests that 8 is also trans. A more compelling reason for making this

assignment is that the asymmetric compound 8b* also displays the trans

configuration in its crystal structure.

The structure of 8b* (R = Me)[13] (Fig. 3.10, Tables 3.5 and 3.6) shows

the chelate ligand coordinated to the equatorial positions of a distorted octa-
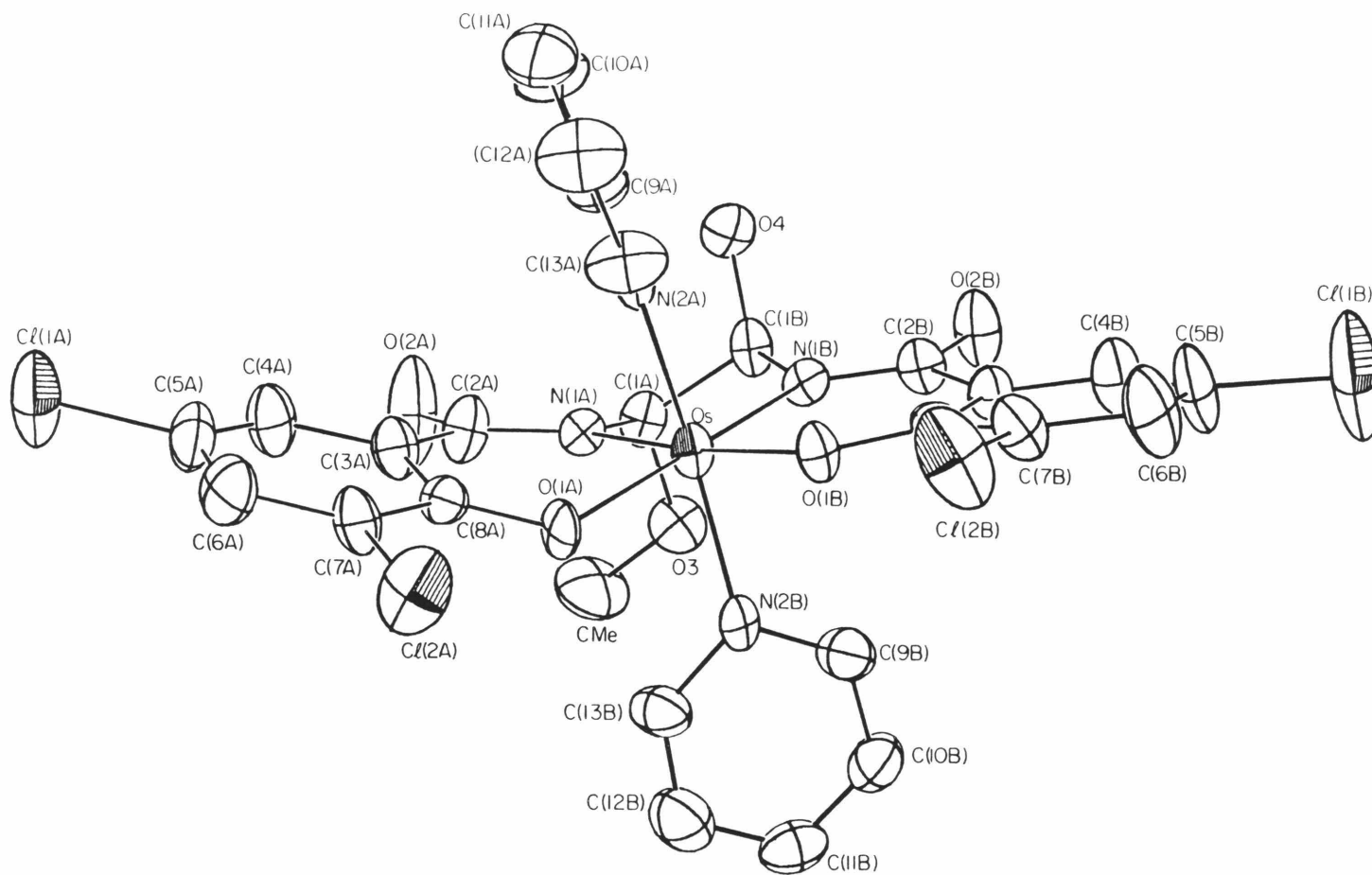
Figure 3.10.   Molecular structure of Os(η^4-CHBA-t-1-OH-2-MeO-Et)(py)$_2$, **8b***.

Table 3.5. Bond distances for **8b*** (Å).

Atoms	Distance	Atoms	Distance
Os–O(1A)	1.991(7)	Os–O(1B)	1.973(7)
Os–N(1A)	1.976(8)	Os–N(1B)	1.983(8)
Os–N(2A)	2.084(8)	Os–N(2B)	2.072(8)
Cl(1A)–C(5A)	1.742(12)	Cl(1B)–C(5B)	1.733(14)
Cl(2A)–C(7A)	1.747(11)	Cl(2B)–C(7B)	1.722(12)
O(1A)–C(8A)	1.305(12)	O(1B)–C(8B)	1.310(12)
O(2A)–C(2A)	1.210(15)	O(2B)–C(2B)	1.264(13)
O(3)–C(1A)	1.422(13)	O(4)–C(1B)	1.389(12)
O(3)–C(Me)	1.401(17)		
N(1A)–C(1A)	1.460(13)	N(1B)–C(1B)	1.477(13)
N(1A)–C(2A)	1.349(14)	N(1B)–C(2B)	1.340(13)
N(2A)–C(9A)	1.340(14)	N(2B)–C(9B)	1.333(14)
N(2A)–C(13A)	1.363(14)	N(2B)–C(13B)	1.323(14)
C(1A)–C(1B)	1.536(14)		
C(2A)–C(3A)	1.502(15)	C(2B)–C(3B)	1.484(14)
C(3A)–C(4A)	1.409(16)	C(3B)–C(4B)	1.398(16)
C(3A)–C(8A)	1.443(15)	C(3B)–C(8B)	1.450(14)
C(4A)–C(5A)	1.344(17)	C(4B)–C(5B)	1.377(18)
C(5A)–C(6A)	1.366(17)	C(5B)–C(6B)	1.358(18)
C(6A)–C(7A)	1.377(16)	C(6B)–C(7B)	1.392(17)
C(7A)–C(8A)	1.394(15)	C(7B)–C(8B)	1.393(15)
C(9A)–C(10A)	1.367(18)	C(9B)–C(10B)	1.383(17)
C(10A)–C(11A)	1.398(19)	C(10B)–C(11B)	1.343(18)
C(11A)–C(12A)	1.340(20)	C(11B)–C(12B)	1.392(19)
C(12A)–(13A)	1.310(19)	C(12B)–C(13B)	1.346(18)

Table 3.6. Bond angles for **8b*** (deg).

Atoms	Angle	Atoms	Angle
O(1A)-Os-O(1B)	93.1(3)		
O(1A)-Os-N(1A)	91.6(3)	O(1A)-Os-N(1B)	174.3(3)
O(1A)-Os-N(2A)	83.4(3)	O(1A)-Os-N(2B)	88.3(3)
O(1B)-Os-N(1A)	173.6(3)	O(1B)-Os-N(1B)	92.3(3)
O(1B)-Os-N(2A)	84.9(3)	O(1B)-Os-N(2B)	92.5(3)
N(1A)-Os-N(1B)	83.1(3)	N(2A)-Os-N(2B)	173.1(3)
N(1A)-Os-N(2A)	92.1(3)	N(1A)-Os-N(2B)	92.0(3)
N(1B)-Os-N(2A)	96.8(3)	N(1B)-Os-N(2B)	89.7(3)
Os-O(1A)-O(8A)	122.9(6)	Os-O(1B)-C(8B)	126.9(6)
Os-N(1A)-C(1A)	112.3(6)	Os-N(1B)-C(1B)	114.3(6)
Os-N(1A)-C(2A)	128.0(7)	Os-N(1B)-C(2B)	129.2(7)
Os-N(2A)-C(9A)	125.8(7)	Os-N(2B)-C(9B)	125.2(7)
Os-N(2A)-C(13A)	119.3(7)	Os-N(2B)-C(13B)	121.1(7)
C(Me)-O(3)-C(1A)	114.2(9)	O(4)-C(1B)-N(1B)	119.5(8)
O(3)-C(1A)-N(1A)	112.2(8)	O(4)-C(1B)-C(1A)	111.3(8)
O(3)-C(1A)-C(1B)	106.3(8)		
C(2A)-N(1A)-C(1A)	119.5(8)	C(2B)-N(1B)-C(1B)	116.3(8)
C(13A)-N(2A)-C(9A)	114.8(9)	C(13B)-N(2B)-C(9B)	113.6(9)
C(1B)-C(1A)-N(1A)	108.9(8)	C(1A)-C(1B)-N(1B)	107.9(8)
N(1A)-C(2A)-O(2A)	123.1(10)	N(1B)-C(2B)-O(2B)	122.4(9)
C(3A)-C(2A)-O(2A)	118.2(10)	C(3B)-C(2B)-O(2B)	117.2(9)

Table 3.6. Continued.

Atoms	Angle	Atoms	Angle
C(3A)-C(2A)-N(1A)	118.7(9)	C(3B)-C(2B)-N(1B)	120.4(9)
C(4A)-C(3A)-C(2A)	116.4(10)	C(4B)-C(3B)-C(2B)	115.9(9)
C(8A)-C(3A)-C(2A)	125.2(9)	C(8B)-C(3B)-C(2B)	124.8(9)
C(8A)-C(3A)-C(4A)	118.3(9)	C(8B)-C(3B)-C(4B)	119.1(9)
C(5A)-C(4A)-C(3A)	121.7(11)	C(5B)-C(4B)-C(3B)	120.7(11)
C(4A)-C(5A)-Cl(1A)	120.0(9)	C(4B)-C(5B)-Cl(1B)	119.6(10)
C(6A)-C(5A)-Cl(1A)	118.3(9)	C(6B)-C(5B)-Cl(1B)	118.9(10)
C(6A)-C(5A)-C(4A)	121.6(11)	C(6B)-C(5B)-C(4B)	121.4(12)
C(7A)-C(6A)-C(5A)	118.4(11)	C(7B)-C(6B)-C(5B)	119.0(12)
C(6A)-C(7A)-Cl(2A)	118.8(9)	C(6B)-C(7B)-Cl(2B)	118.8(9)
C(8A)-C(7A)-Cl(2A)	117.4(8)	C(8B)-C(7B)-Cl(2B)	118.2(8)
C(8A)-C(7A)-C(6A)	123.7(10)	C(8B)-C(7B)-C(6B)	122.9(11)
C(3A)-C(8A)-O(1A)	124.7(9)	C(3B)-C(8B)-O(1B)	125.3(9)
C(7A)-C(8A)-O(1A)	119.0(9)	C(7B)-C(8B)-O(1B)	118.3(9)
C(7A)-C(8A)-C(3A)	116.2(9)	C(7B)-C(8B)-C(3B)	116.4(9)
C(10A)-C(9A)-N(2A)	122.3(11)	C(10B)-C(9B)-N(2B)	125.7(11)
C(11A)-C(10A)-C(9A)	120.2(12)	C(11B)-C(10B)-C(9B)	118.5(12)
C(12A)-C(11A)-C(10A)	116.6(13)	C(12B)-C(11B)-C(10B)	117.2(12)
C(13A)-C(12A)-C(11A)	121.0(13)	C(13B)-C(12B)-C(11B)	119.6(12)
C(12A)-C(13A)-N(2A)	125.1(12)	C(12B)-C(13B)-N(2B)	125.3(11)

hedron with staggered axial pyridine ligands. The general features of the structure are very similar to that of complex 5 (see Chapter 2). One of the carbonyl carbon-oxygen bonds in **8b*** is considerably longer than the other (1.21 vs. 1.26 Å). This could be due to intramolecular hydrogen bonding with the hydroxyl proton. The ortep in Figure 3.10 shows the ethane bridge behind the osmium with the methoxide group below the plane of the ligand and the hydroxyl oxygen above. The metallacyclopentane ring is nonplanar with the ethane bridge skewed so that the methoxide and hydroxide groups occupy axial positions on the ring. The molecule has no symmetry so the pyridine rings above and below the plane of the chelate are inequivalent as are the two halves of the chelate ligand itself.

The asymmetry in **8b*** is clearly evident in its ^{1}H NMR spectrum (Fig. 3.11, Table 3.11). The aromatic protons of the chelate appear as four doublets at 14.43, 12.79, 10.67 and 10.29 ppm ($J_{H,H}$ = 3 Hz). Each integrates for a single proton. Two distinct sets of pyridine signals are seen with the meta protons at 8.94 and 7.83 ppm, the para protons at -0.57 and -1.00 ppm, and the ortho at -2.59 and -6.85 ppm. The remaining signals are associated with the ligand bridge. The methoxide methyl appears as a singlet at 4.87 ppm (3H). The two methylene protons are found at 16.87 (d, H_b, $J_{b,c}$ = 3 Hz) and 8.59 ppm (s, H_a) with the hydroxyl proton at 7.57 ppm (d, H_c, $J_{c,b}$ = 3 Hz).
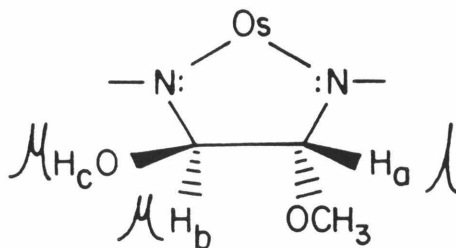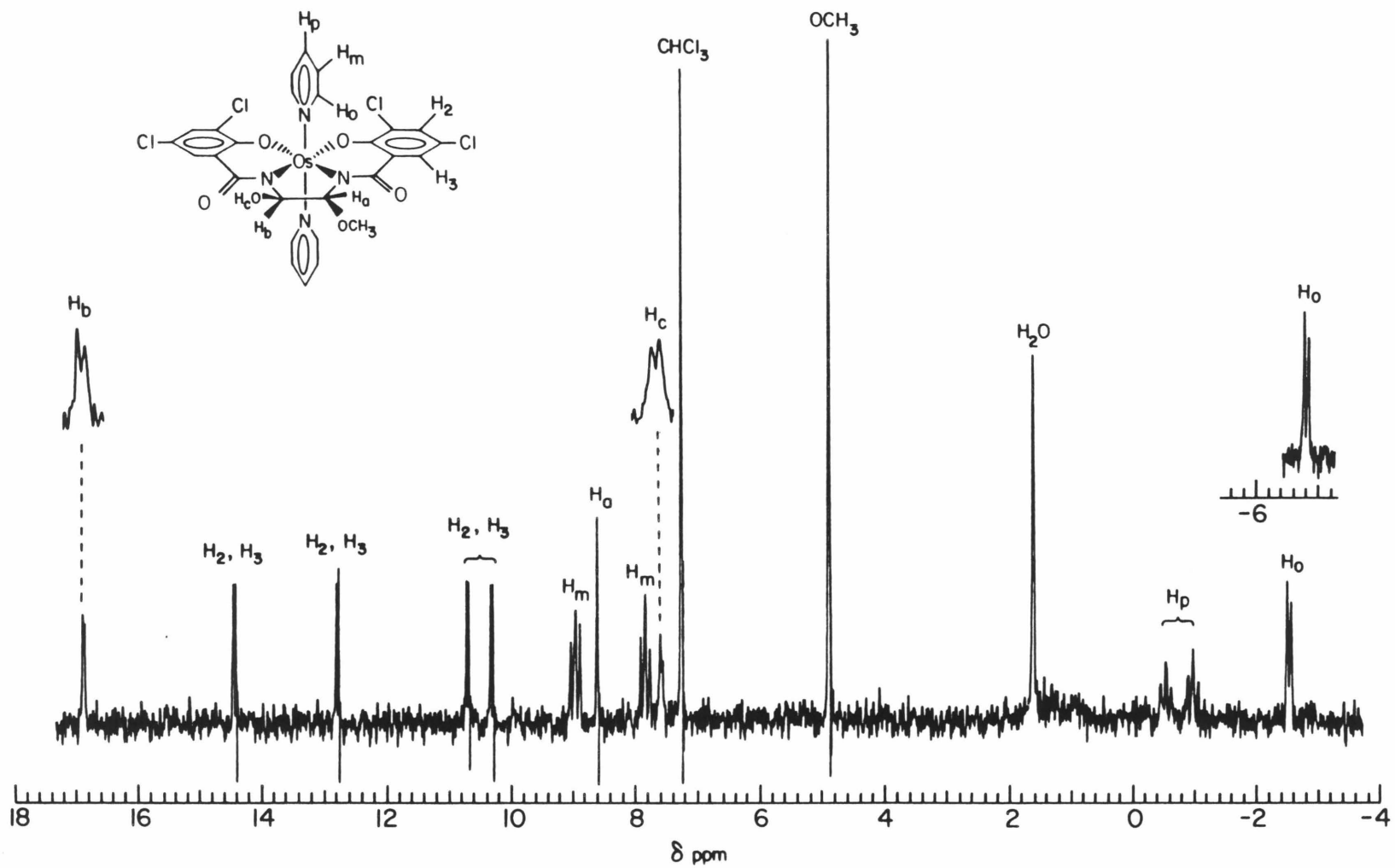
Figure 3.11. 90-MHz ^{1}H NMR spectrum of **8b*** (R = Me) (CDCl$_3$).

H_c exchanges with D_2O, causing collapse of the H_b doublet.

Coupling between H_b and H_c indicates that the exchange rate for H_c is slow which is unexpected for a hydroxyl proton in a nonpolar medium.[14] The lack of observed coupling between H_b and H_a is also somewhat unusual. Vicinal coupling constants in saturated systems are highly dependent on the dihedral angle, θ, between the nuclei with the largest values observed for $\theta = 0^\circ$ or 180° and the smallest values observed when $\theta = 90^\circ$.[15] In the crystal structure of **8b*** H_a and H_b are both equatorial with a dihedral angle close to 90°. It seems unlikely, however, that the five-membered ring is held in this configuration in solution. Substituent effects can also lower coupling constants[14] and could be important in this case.

Compound **8** is stable with acid and shows no tendency toward displacement of the chelate or pyridine ligands. It reacts with strong base, as do **5** and **7**, to yield the osmium(III) compound. The compounds are fairly stable, both in the solid state and in solution, but they sometimes undergo hydrolysis of the alkoxy groups on the ligand bridge to yield **8*** or the bis hydroxy compound.

$\underline{Os(\eta^2\text{-Fo-CHBA})_2(\text{t-Bupy})_2, \text{ 9 and 9'}}$. Electrochemical oxidation of **5** at +0.87 V in the presence of alcohol or water proceeds through intermediates **7** and **8** and finally to the complexes **9** and/or **9'** (Scheme 3.4). Intermediate **6**, which is detected by TLC, is produced in very small concentration during the electrooxidation of **5**, but not **7**.[2] We have not yet been able to isolate and characterize this material. The compound is no longer thought to be involved in the major reaction pathway (vide infra).

Initial attempts to produce **9** and **9'** by chemical oxidation of **8** were not successful; however, both complexes were isolated from the electrochemical

Scheme 3.4. Chemical and electrochemical oxidation of 5.

L = py, t-Bupy
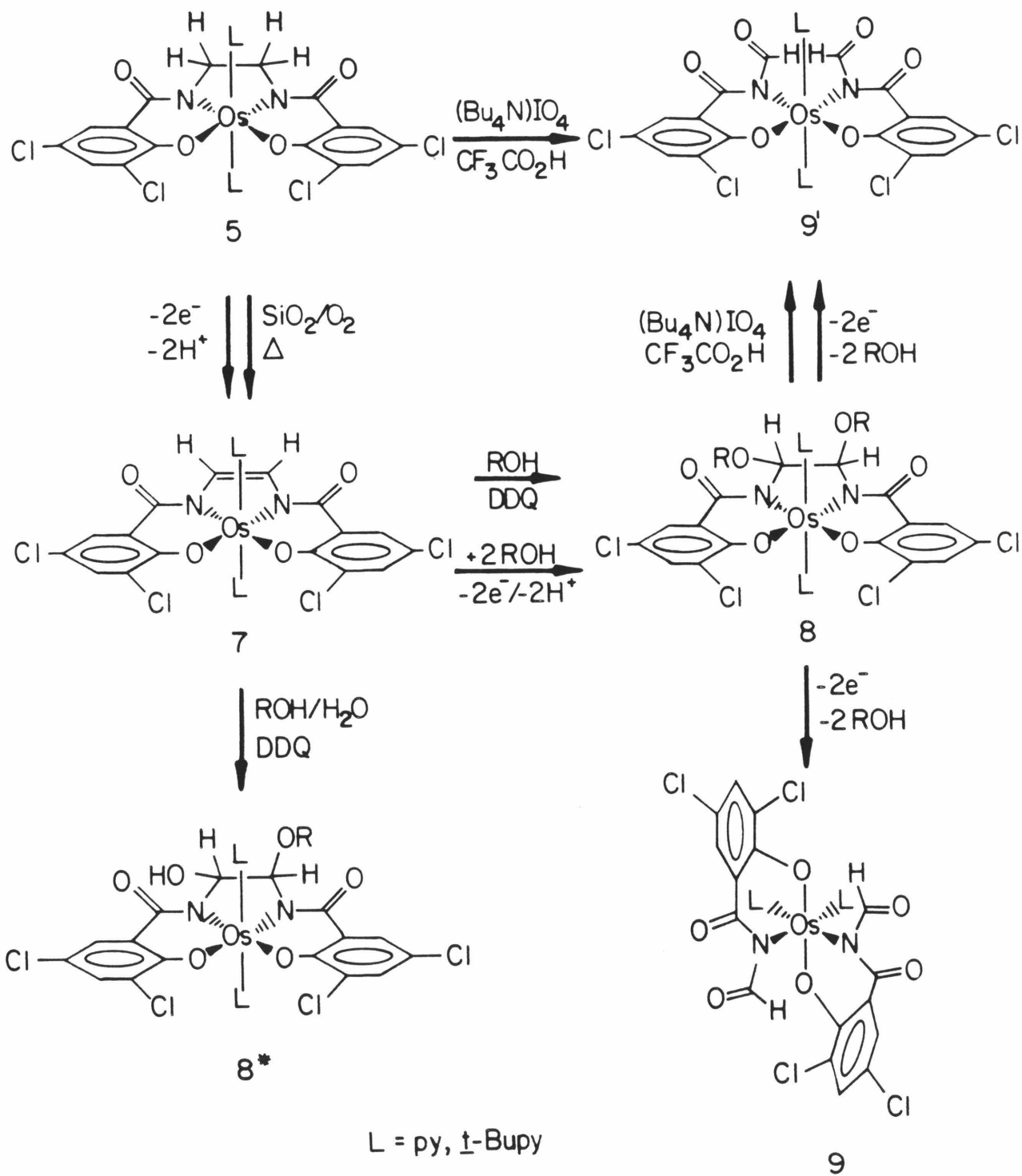
media.[2] Both have been characterized by IR, ^{1}H NMR, elemental analysis and by X-ray crystal structure determinations. Poor solubility of complex **9** (L = py) prompted the synthesis of the entire series, **5** through **9/9'**, with L = t-Bupy. The enhanced solubility of the t-Bupy derivative facilitated the ^{1}H and ^{13}C NMR characterization of **9** and allowed the formation of crystals which were suitable for structural analysis of both **9** and **9'**.

The NMR data (Tables 3.11 and 3.12) suggested that **9** and **9'** were different isomers of the same compound and pointed to the structural formulation depicted in Scheme 3.4. Each metal bears two identical bidentate ligands which coordinate through a phenolic oxygen and a deprotonated organic imido nitrogen. The X-ray crystal structures confirmed the formulation and defined the coordination geometry as trans for **9'** and cis-α for **9**. Conversion of **8** to **9** or **9'** therefore involves cleavage of the carbon-carbon bond of the five-membered metallacycle with destruction of the ether and/or hydoxyl linkages. The distribution between the two diastereomers **9** and **9'** is primarily a function of the alcohol employed in the electrolysis (Scheme 3.4). This point is addressed in the next section on the mechanism of the ligand oxidation.

The compounds **9** and **9'** are the first structurally characterized N-coordinated organic imido complexes of osmium. The structure of the cis-α isomer, **9**,[16] is shown in Figure 3.12 with bond lengths and angles in Tables 3.7 and 3.8. The view in Figure 3.12 shows one of the bidentate ligands in the lower foreground with the other in the lower background. The osmium is in a slightly distorted octahedral environment with two imido nitrogens and two t-Bupy ligands in the equatorial plane and the phenolic oxygens in the axial
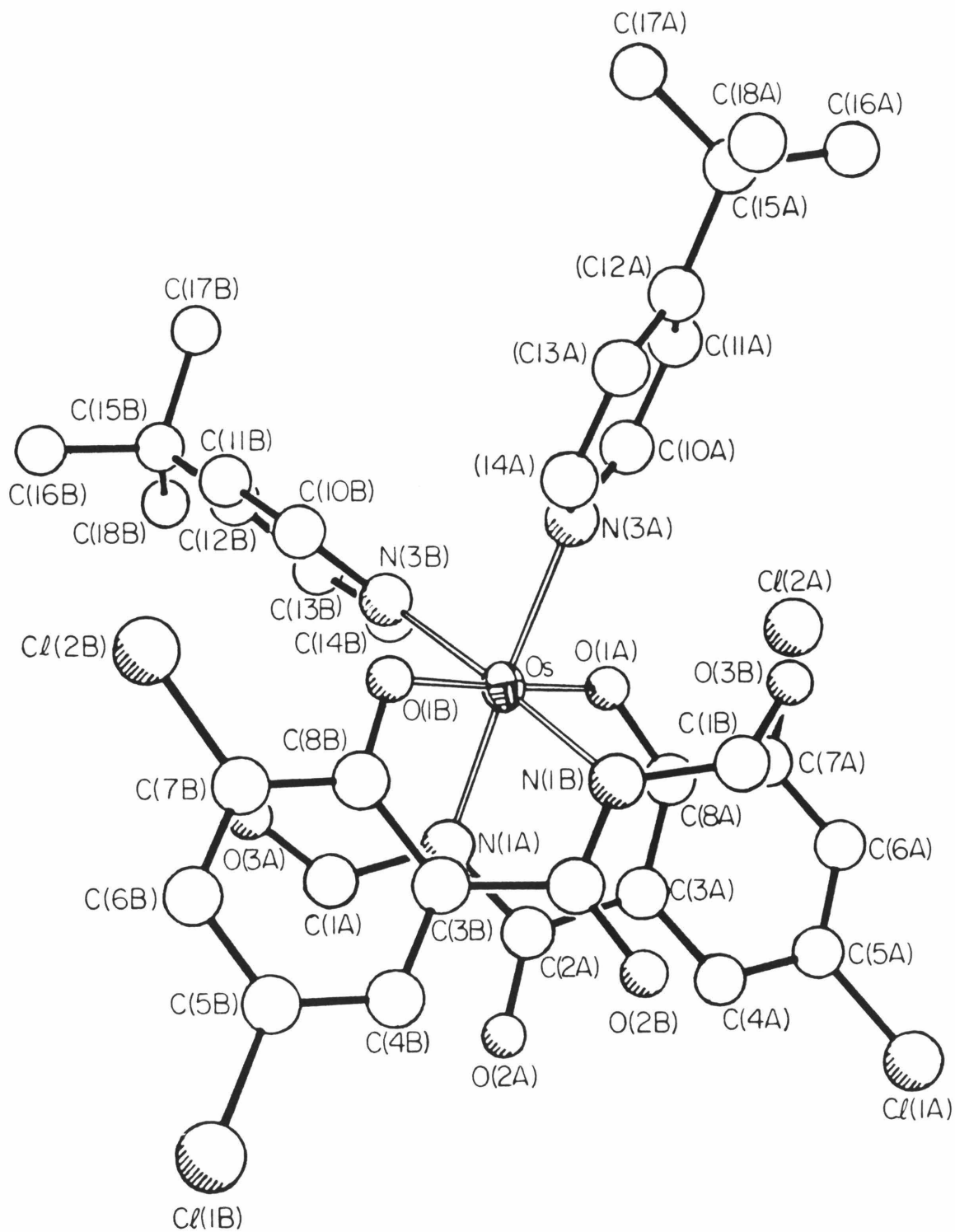
Figure 3.12. Molecular structure of cis-α-Os(η²-Fo-CHBA)₂(t-Bupy)₂, **9.**
Atoms labeled "B" are symmetry-related to those labeled "A".

Table 3.7. Bond distances for cis-α-Os(η²-Fo-CHBA)₂(t-Bupy)₂, 9 (Å).

Atoms	Distance	Atoms	Distance
Os–O(1A)	1.941(4)	Cl(1A)–C(5A)	1.742(6)
Os–N(1A)	2.027(4)	Cl(2A)–C(7A)	1.735(5)
Os–N(3A)	2.119(4)	N(1A)–C(1A)	1.393(4)
O(1A)–C(8A)	1.343(6)	N(1A)–C(2A)	1.403(6)
O(2A)–C(2A)	1.209(6)	N(3A)–C(10A)	1.339(7)
O(3A)–C(1A)	1.202(6)	N(3A)–C(14A)	1.329(10)
C(1A)–H(1A)	1.01 (5)	C(10A)–C(11A)	1.366(9)
C(2A)–C(3A)	1.498(6)	C(11A)–C(12A)	1.377(12)
C(3A)–C(4A)	1.399(7)	C(12A)–C(13A)	1.380(8)
C(3A)–C(8A)	1.407(6)	C(13A)–C(14A)	1.377(9)
C(4A)–C(5A)	1.371(7)	C(12A)–C(15A)	1.531(8)
C(5A)–C(6A)	1.374(7)	C(15A)–C(16A)	1.539(8)
C(6A)–C(7A)	1.365(7)	C(15A)–C(17A)	1.531(7)
C(7A)–C(8A)	1.407(6)	C(15A)–C(18A)	1.509(14)

Table 3.8. Bond angles for <u>cis</u>-α-Os(η ^{2}-Fo-CHBA)$_2$(<u>t</u>-Bupy)$_2$, 9 (deg).

Atoms	Angle	Atoms	Angle
O(1A)-Os-N(1A)	86.8(2)	N(1A)-Os-N(1B)	86.4(2)
O(1A)-Os-N(3A)	91.4(2)	N(1A)-Os-N(3B)	91.9(2)
O(1A)-Os-N(1B)	95.0(2)	N(3A)-Os-N(3B)	89.9(2)
O(1A)-Os-N(3B)	86.8(2)	N(1A)-Os-N(3A)	177.4(1)
O(1A)-Os-O(1B)	177.4(2)	Os-O(1A)-C(8A)	121.9(3)
Os-N(1A)-C(1A)	123.6(4)	Os-N(3A)-C(10A)	122.3(5)
Os-N(1A)-C(2A)	120.8(2)	Os-N(3A)-C(14A)	121.7(3)
C(1A)-N(1A)-C(2A)	115.0(4)	C(4A)-C(5A)-Cl(1A)	118.5(4)
N(1A)-C(1A)-O(3A)	124.2(5)	C(6A)-C(5A)-Cl(1A)	119.5(4)
N(1A)-C(1A)-H(1A)	109.0(2)	C(4A)-C(5A)-C(6A)	122.0(5)
O(3A)-C(1A)-H(1A)	127.0(2)	C(5A)-C(6A)-C(7A)	118.0(5)
N(1A)-C(2A)-C(3A)	116.5(4)	C(6A)-C(7A)-Cl(2A)	119.7(4)
N(1A)-C(2A)-O(2A)	122.8(4)	C(8A)-C(7A)-Cl(2A)	117.7(4)
O(2A)-C(2A)-C(3A)	120.6(5)	C(5A)-C(7A)-C(8A)	122.6(4)
C(2A)-C(3A)-C(4A)	115.7(4)	C(3A)-C(8A)-O(1A)	123.6(4)
C(2A)-C(3A)-C(8A)	125.2(4)	C(3A)-C(8A)-C(7A)	117.9(4)
C(4A)-C(3A)-C(8A)	118.8(4)	O(1A)-C(8A)-C(7A)	118.5(4)
C(3A)-C(4A)-C(5A)	120.2(5)		
N(3A)-C(10A)-C(11A)	123.1(8)	C(10A)-N(3A)-C(14A)	115.9(5)
C(13A)-C(14A)-N(3A)	123.8(6)	C(12A)-C(15A)-C(16A)	109.9(6)
C(10A)-C(11A)-C(12A)	121.4(6)	C(12A)-C(15A)-C(17A)	107.2(5)
C(11A)-C(12A)-C(13A)	115.3(5)	C(12A)-C(15A)-C(18A)	112.4(5)
C(11A)-C(12A)-C(15A)	122.7(5)	C(16A)-C(15A)-C(17A)	109.8(5)
C(13A)-C(12A)-C(15A)	122.0(7)	C(16A)-C(15A)-C(18A)	107.9(5)
C(12A)-C(13A)-C(14A)	120.4(8)	C(17A)-C(15A)-C(18A)	109.7(7)

positions. The bond lengths and angles are all normal. The two carbon-nitrogen bonds in each imide group are equivalent within experimental error, as are the two carbon-oxygen bonds.

The structure of the trans isomer, 9',[17] is shown in Figure 3.13. The bond lengths (Table 3.9) and angles (Table 3.10) are essentially the same as found in the cis-α isomer. Both structures display a trans arrangement across the terminal carbon-nitrogen imide bond. In 9' this causes the two bidentate ligands to bend significantly out of the equatorial plane in order to avoid contact of the two formyl oxygens. However, the coordination sphere of the osmium is only slightly distorted from octahedral. The staggered configuration of the t-Bupy ligands is presumably due to crystal-packing effects (see page 77).

The deprotonated imide in 9 and 9' is expected to be a poorer σ-donor than the deprotonated amides in the parent tetradentate ligands. As shown in Table 3.13 (page 105), the electrochemical data support this. Compounds 9 and 9' are easier to reduce than 5, 7 or 8 by ca. 200-250 mV and are significantly harder to oxidize, showing no oxidation waves below +1.1 V vs. Fc^+/Fc. The ^1H NMR spectra of 9 and 9' are also consistent with less electron-rich metal centers. All of the osmium(IV) HBA complexes previously discussed showed very significant upfield shifts of the pyridine ortho and para protons, but not of the meta protons (Table 3.11).[4] This was attributed to a π-backbonding interaction[6] from osmium to the pyridine π^* orbital, $3B_1$.[5] In 9 and 9' the ortho and para signals are also shifted upfield, but to a much smaller extent. This would be consistent with a greatly weakened π-backbonding interaction.
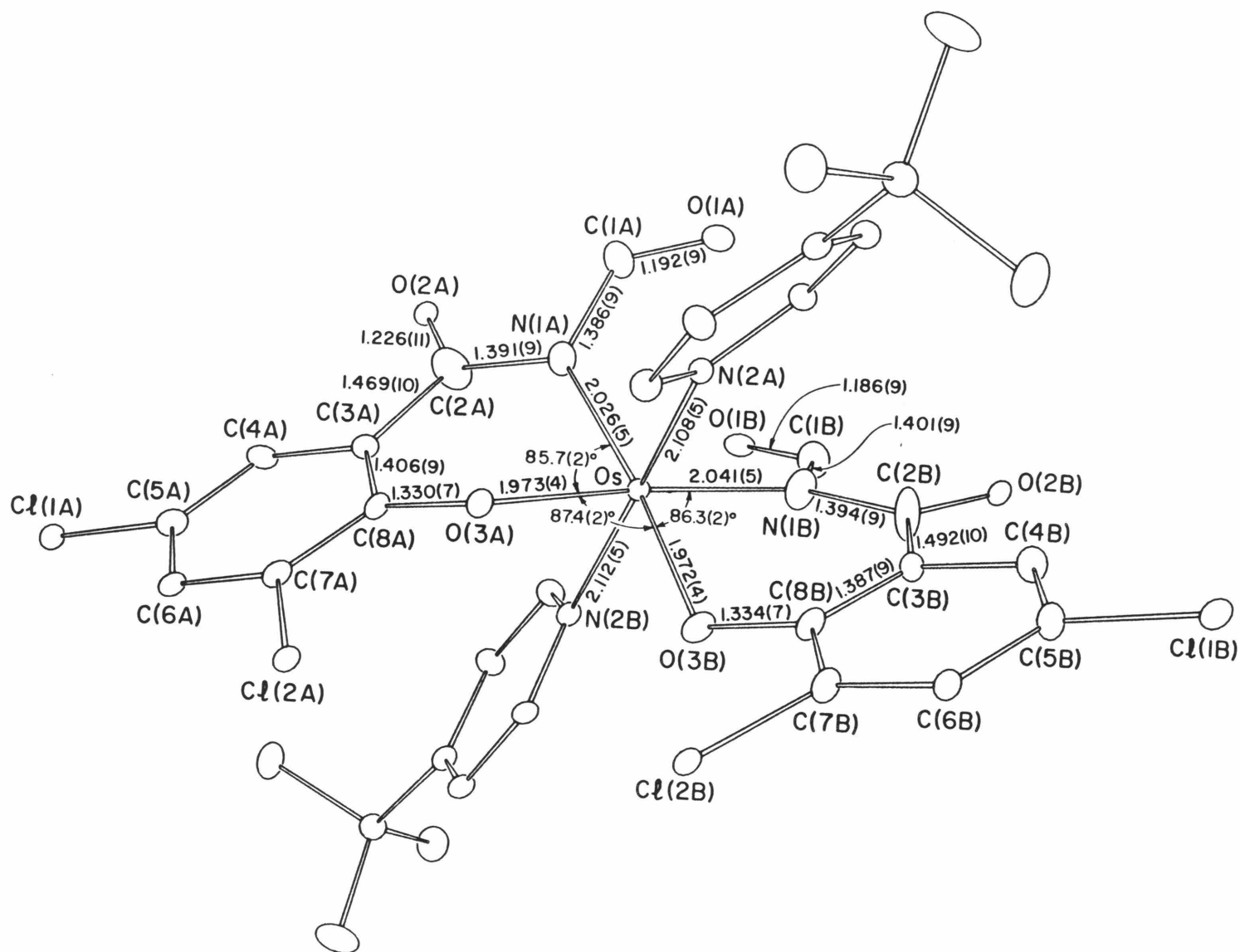
Figure 3.13. Molecular structure of <u>trans</u>-Os(η^2-Fo(CHBA)$_2$(<u>t</u>-Bupy)$_2$, **9'**.

Table 3.9. Bond distances for trans-Os($_\eta$²-Fo-CHBA)$_2$(t-Bupy)$_2$, **9** (Å).

Atoms	Distance	Atoms	Distance
Os–O(3A)	1.973(4)	Os–O(3B)	1.972(4)
Os–N(1A)	2.026(5)	Os–N(1B)	2.041(5)
Os–N(2A)	2.108(5)	Os–N(2B)	2.112(5)
Cl(1A)–C(5A)	1.745(8)	Cl(1B)–C(5B)	1.735(8)
Cl(2A)–C(7A)	1.730(7)	Cl(2B)–C(7B)	1.721(7)
O(3A)–C(8A)	1.330(7)	O(3B)–C(8B)	1.334(7)
O(2A)–C(2A)	1.225(11)	O(2B)–C(2B)	1.221(10)
O(1A)–C(1A)	1.192(9)	O(1B)–C(1B)	1.186(9)
N(1A)–C(1A)	1.386(9)	N(1B)–C(1B)	1.401(9)
N(1A)–C(2A)	1.391(9)	N(1B)–C(2B)	1.394(9)
N(2A)–C(9A)	1.358(8)	N(2B)–C(9B)	1.337(8)
N(2A)–C(13A)	1.337(8)	N(2B)–C(13B)	1.365(8)
C(2A)–C(3A)	1.469(10)	C(2B)–C(3B)	1.492(10)
C(3A)–C(4A)	1.401(10)	C(3B)–C(4B)	1.397(10)
C(3A)–C(8A)	1.406(9)	C(3B)–C(8B)	1.387(9)
C(4A)–C(5A)	1.358(10)	C(4B)–C(5B)	1.381(11)
C(5A)–C(6A)	1.396(10)	C(5B)–C(6B)	1.376(11)
C(6A)–C(7A)	1.376(10)	C(6B)–C(7B)	1.374(10)
C(7A)–C(8A)	1.403(9)	C(7B)–C(8B)	1.407(9)
C(9A)–C(10A)	1.362(9)	C(9B)–C(10B)	1.379(9)
C(10A)–C(11A)	1.383(9)	C(10B)–C(11B)	1.399(9)
C(11A)–C(12A)	1.391(9)	C(11B)–C(12B)	1.371(9)
C(12A)–C(13A)	1.365(9)	C(12B)–C(13B)	1.376(10)
C(11A)–C(14A)	1.523(9)	C(11B)–C(14B)	1.526(9)
C(14A)–C(15A)	1.529(12)	C(14B)–C(15B)	1.536(11)
C(14A)–C(16A)	1.515(11)	C(14B)–C(16B)	1.522(13)
C(14A)–C(17A)	1.535(12)	C(14B)–C(17B)	1.520(12)

Table 3.10. Bond angles for trans-Os(η^2-Fo-CHBA)$_2$(t-Bupy)$_2$, 9' (deg).

Atoms	Angle	Atoms	Angle
O(3A)-Os-O(3B)	87.4(2)		
O(3A)-Os-N(1A)	85.7(2)	O(3A)-Os-N(1B)	173.6(2)
O(3A)-Os-N(2A)	85.0(2)	O(3A)-Os-N(2B)	87.7(2)
O(3B)-Os-N(1A)	173.0(2)	O(3B)-Os-N(1B)	86.3(2)
O(3B)-Os-N(2A)	87.3(2)	O(3B)-Os-N(2B)	85.9(2)
N(1A)-Os-N(1B)	100.7(2)	N(2A)-Os-N(2B)	170.2(2)
N(1A)-Os-N(2A)	91.9(2)	N(1A)-Os-N(2B)	94.0(2)
N(1B)-Os-N(2A)	95.7(2)	N(1B)-Os-N(2B)	90.9(2)
Os-O(3A)-C(8A)	122.0(4)	Os-O(3B)-C(8A)	121.8(4)
Os-N(1A)-C(1A)	122.9(4)	Os-N(1B)-C(1B)	122.7(4)
Os-N(1A)-C(2A)	122.3(5)	Os-N(1B)-C(2B)	123.9(4)
Os-N(2A)-C(9A)	125.6(4)	Os-N(2B)-C(9B)	125.5(4)
Os-N(2A)-C(13A)	116.8(4)	Os-N(2B)-C(13B)	116.5(4)
O(1A)-C(1A)-N(1A)	125.3(7)	O(1B)-C(1B)-N(1B)	124.8(7)
C(2A)-N(1A)-C(1A)	114.8(6)	C(2B)-N(1B)-C(1B)	113.3(6)
C(13A)-N(2A)-C(9A)	116.8(5)	C(13B)-N(2B)-C(9B)	117.0(5)
N(1A)-C(2A)-O(2A)	120.9(7)	N(1B)-C(2B)-O(2B)	121.2(7)
C(3A)-C(2A)-O(2A)	119.0(7)	C(3B)-C(2B)-O(2B)	119.1(7)
C(3A)-C(2A)-N(1A)	120.0(6)	C(3B)-C(2B)-N(1B)	119.7(6)
C(4A)-C(3A)-C(2A)	116.7(6)	C(4B)-C(3B)-C(2B)	115.6(6)
C(8A)-C(3A)-C(2A)	123.4(6)	C(8B)-C(3B)-C(2B)	124.0(6)
C(8A)-C(3A)-C(4A)	119.8(6)	C(8B)-C(3B)-C(4B)	120.4(6)
C(5A)-C(4A)-C(3A)	120.3(7)	C(5B)-C(4B)-C(3B)	119.8(7)

Table 3.10. Continued.

Atoms	Angle	Atoms	Angle
C(4A)-C(5A)-Cl(1A)	120.6(6)	C(4B)-C(5B)-Cl(1B)	118.6(6)
C(6A)-C(5A)-Cl(1A)	117.7(6)	C(6B)-C(5B)-Cl(1B)	120.4(6)
C(6A)-C(5A)-C(4A)	121.6(7)	C(6B)-C(5B)-C(4B)	121.0(7)
C(7A)-C(6A)-C(5A)	118.0(7)	C(7B)-C(6B)-C(5B)	119.0(7)
C(6A)-C(7A)-Cl(2A)	119.2(5)	C(6B)-C(7B)-Cl(2B)	119.4(5)
C(8A)-C(7A)-Cl(2A)	118.2(5)	C(8B)-C(7B)-Cl(2B)	118.6(5)
C(8A)-C(7A)-C(6A)	122.6(6)	C(8B)-C(7B)-C(6B)	121.9(6)
C(3A)-C(8A)-O(3A)	124.2(5)	C(3B)-C(8B)-O(3B)	123.2(5)
C(7A)-C(8A)-O(3A)	118.2(5)	C(7B)-C(8B)-O(3B)	118.9(5)
C(7A)-C(8A)-C(3A)	117.7(6)	C(7B)-C(8B)-C(3B)	117.9(6)
C(10A)-C(9A)-N(2A)	122.6(6)	C(10B)-C(9B)-N(2B)	123.1(6)
C(11A)-C(10A)-C(9A)	121.1(6)	C(11B)-C(10B)-C(9B)	120.3(6)
C(12A)-C(11A)-C(10A)	115.5(6)	C(12B)-C(11B)-C(10B)	115.9(6)
C(13A)-C(12A)-C(11A)	121.1(6)	C(13B)-C(12B)-C(11B)	121.8(6)
C(12A)-C(13A)-N(2A)	122.8(6)	C(12B)-C(13B)-N(2B)	121.7(6)
C(12A)-C(11A)-C(14A)	123.2(6)	C(12B)-C(11B)-C(14B)	123.3(6)
C(10A)-C(11A)-C(14A)	121.2(6)	C(10B)-C(11B)-C(14B)	120.7(6)
C(15A)-C(14A)-C(11A)	107.6(6)	C(15B)-C(14B)-C(11B)	111.9(6)
C(16A)-C(14A)-C(11A)	110.5(6)	C(16B)-C(14B)-C(11B)	110.5(6)
C(17A)-C(14A)-C(11A)	112.1(6)	C(17B)-C(14B)-C(11B)	107.1(6)
C(15A)-C(14A)-C(16A)	108.9(6)	C(15B)-C(14B)-C(16B)	108.6(7)
C(15A)-C(14A)-C(17A)	108.6(7)	C(15B)-C(14B)-C(17B)	109.1(6)
C(16A)-C(14A)-C(17A)	109.0(7)	C(16B)-C(14B)-C(17B)	109.6(7)

Table 3.11. 90-MHz ^{1}H NMR data for osmium complexes.

No.	Compound	Chelate Ligand		Pyridine				Other
		H_1	$H_2, H_3{}^b$	H_o	H_m	H_p	t-Bu	
1^c	(structure: ethylenediamine chelate, H_1 labels, −NH HN−)	3.70 s, 4	7.74, d, 2 7.54, d, 2					
3^c		3.88 s, 4	8.21, d, 2 7.27, d, 2					3.77 s, 2 $\Big)$ H_2
5^d	L = py	68.55 s, 4	14.93, d, 2 10.55, d, 2	−6.29, d, 4 $J_{o,m}=8$	7.73, dd, 4 $J_{m,o}=8$ $J_{m,p}=8$	−1.39, t, 2 $J_{p,m}=8$		
5^d	L = t-Bupy	69.78 s, 4	15.40, d, 2 10.78, d, 2	−7.26, d, 4 $J_{o,m}=7.5$	7.38, d, 4 $J_{m,o}=7.5$		0.18 s, 18	
7^d	(structure with H_1 labels, −N N−, Os)	−15.52 s, 2	5.38, d, 2 4.26, d, 2	−1.12, d, 4 $J_{o,m}=8$	7.38, dd, 4 $J_{m,o}=8$ $J_{m,p}=8$	−2.29, t, 2 $J_{p,m}=8$		
7^d	L = t-Bupy	−14.30 s, 2	5.61, d, 2 4.89, d, 2	−2.90, d, 4 $J_{o,m}=7.5$	7.11, d, 4 $J_{m,o}=7.5$		0.13 s, 18	
8a^{d,e}	(structure: H_b H_a, O−C−C−H_a, EtO, H_1 H_c H_a, −N N−, Os)	6.01 s, 2	10.48, d, 2 9.22, d, 2	−1.32, dd, 4 $J_{o,m}=7.5$ $J_{o,p}=1.5$	8.59, dd, 4 $J_{m,p}=8.5$ $J_{m,o}=7.5$	1.61, tt, 2 $J_{p,m}=8.5$ $J_{p,o}=1.5$		2.06, dd, 6 $\Big)$ H_a $J_{a,b}=J_{a,c}=8$ 7.54, dq, 2 $\Big)$ 6.08, eq, 2 $\Big)$ H_b, H_c $J_{b,c}=10$
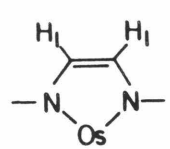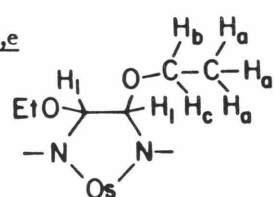
Table 3.11. Continued.

No.	Compound	Chelate Ligand		Pyridine				Other
		H_1	H_2, H_3[b]	H_o	H_m	H_p	t-Bu	
8b[d]		6.77 s, 2	10.91, d, 2 9.43, d, 2	-1.75, d, 4 $J_{o,m} = 7.5$	8.60, dd, 4 $J_{m,o} = 8$ $J_{m,p} = 8$	1.25, t, 2 $J_{p,m} = 7.5$		5.77 s, 6) CH_3
8c[d,e]		7.02 s, 2	10.60, d, 2 9.29, d, 2	-1.59, d, 4 $J_{o,m} = 7.5$	8.58, dd, 4 $J_{m,o} = 7.5$ $J_{m,p} = 7.5$	ca. 1.5		2.27, m, 4) H_a 7.43, dt, 2) 6.03, dt, 2) H_b, H_c $J_{a,b}=J_{a,c} = 7$) $J_{b,c} = 9.5$) 0.91, t, 6) CH_3 $J = 6$) 1.2-1.8, m, 20) $-CH_2-$
8d[f,e]		7.89 s, 2	11.09, d, 2 9.57, d, 2	-2.69, dd, 4 $J_{o,m} = 7.5$ $J_{o,p} = 1.5$	8.60, dd, 4 $J_{m,o} = 7.5$ $J_{m,p} = 7.5$	1.62, tt, 2 $J_{p,m} = 7.5$ $J_{p,o} = 1.5$		2.40, d, 6) 1.91, d, 6) H_a, H_b $J_{a,c}=J_{b,c} = 6$) 7.35, dq, 2) H_c $J_{c,a}=J_{c,b} = 6$)
8e[f,e]		8.04 s, 2	11.61, d, 2 9.82, d, 2	-2.86, dd, 4 $J_{o,m} = 7.5$ $J_{o,p} = 1.5$	8.34, dd, 4 $J_{m,o} = 7.5$ $J_{m,p} = 7.5$	0.17, tt, 2 $J_{p,m} = 7.5$ $J_{p,o} = 1.5$		8.49, d, 2) 7.35, d, 2) H_a, H_b $J_{a,b} = 11.5$) 7.57, d, 4) H_a $J_{c,d} = 7.5$) 7.1-7.4, m, 6) H_c, H_d
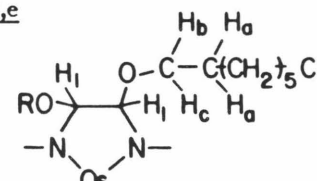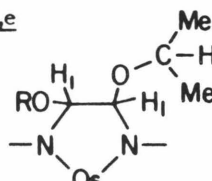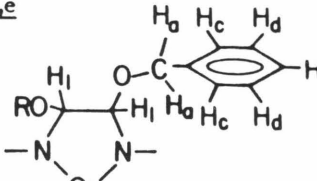
Table 3.11. Continued.

No.	Compound	Chelate Ligand		Pyridine				Other
		H_1	$H_2, H_3{}^b$	H_o	H_m	H_p	t-Bu	
8f$\underline{d}$	(RO, H$_1$, O–C(CH$_3$)$_3$, H, –N–Os–N– ring)	2.89 s, 2	9.08, d, 2 8.50, d, 2	0.79, dd, 4 $J_{o,m}=7.5$ $J_{o,p}=1.5$	8.76, dd, 4 $J_{m,o}=7.5$ $J_{m,p}=7.5$	2.85, tt, 2 $J_{p,m}=7.5$ $J_{p,o}=1.5$	2.43 s, 18) t-Bu	
8b*$\underline{d,g}$	(H$_b$, OCH$_3$, H$_c$O, H$_a$, –N–Os–N– ring)		14.43, d, 1 12.79, d, 1 10.67, d, 1 10.29, d, 1	-2.59, dd, 2 -6.85, dd, 2 $J_{o,m}=7.5$ $J_{o,p}=1.5$	8.94, dd, 2 7.83, dd, 2 $J_{m,o}=7.5$ $J_{m,p}=8.5$	-0.57, tt, 1 -1.00, tt, 1 $J_{p,m}=8.5$ $J_{p,o}=1.5$		8.59, s, 1) H$_a$ 16.87, d, 1) H$_b$ $J_{b,c}=3$) 7.57, d, 1) H$_c$ $J_{c,b}=3$) 4.87, s, 3) CH$_3$
8c*$\underline{d,g}$	(H$_d$, O–C(CH$_2$)$_6$CH$_3$, H$_b$, H$_c$O, H$_a$ H$_e$, –N–Os–N– ring)		14.46, d, 1 12.71, d, 1 10.63, d, 1 10.31, d, 1	-2.54, d, 2 -6.89, d, 2 $J_{o,m}=7$	8.88, dd, 2 7.79, dd, 2 $J_{m,o}=7$ $J_{m,p}=7$	-0.63, t, 1 -1.15, t, 1 $J_{p,m}=7$		8.47, s, 1) H$_a$ 7.88, d, 1) H$_b$ $J_{b,c}=3$) 17.18, d, 1) H$_c$ $J_{c,b}=3$) 6.20, m, 1) H$_d$, H$_e$ 5.17, m, 1) 0.78, t, 3) –CH$_3$ 0.5-1.4, m, 12) –CH$_2$–
8d*$\underline{d,e,g}$	(CH$_3$, O–C–H$_c$, H$_b$, H$_c$O, H$_a$ CH$_3$, –N–Os–N– ring)		14.25, d, 1 12.61, d, 1 10.50, d, 1 10.28, d, 1	-2.81, d, 2 -6.73, d, 2 $J_{m,o}=7$	8.76, dd, 2 7.78, dd, 2 $J_{m,o}=7$ $J_{m,p}=7$	-0.65, t, 1 -1.14, t, $J_{p,m}=7$		9.10, s, 1) H$_a$ 8.02, d, 1) H$_b$ $J_{b,c}=3$) 17.55, d, 1) H$_c$ $J_{c,b}=3$) 6.13, dq, 1) $J_{d,CH_3}=6$) H$_d$ 1.35, d, 3) –CH$_3$ 1.19, d, 3)

Table 3.11. Continued.

No.	Compound	Chelate Ligand		Pyridine				Other
		H_1	H_2, H_3[b]	H_o	H_m	H_p	t-Bu	
8f*[d,g] (structure: H_b, O–C(CH_3)_3, H_cO, H_a, –N, N–, Os)			14.45, d, 1 12.11, d, 1 10.48, d, 1 9.99, d, 1	-1.23, d, 2 -6.29, d, 2 $J_{o,m} = 7$	9.18, dd, 2 7.80, dd, 2 $J_{m,o} = 7$ $J_{m,p} = 7$	-0.81, t, 1 -0.08, t, 1 $J_{p,m} = 7$		5.44, s, 1) H_a 16.58, d, 1) H_b $J_{b,c} = 3$) 8.26, d, 1) H_c $J_{c,b} = 3$) 1.33, s, 9) t-Bu
9[d] (structure: O, H, C, N, Os, L = t-Bupy)			9.52, d, 2 7.65, d, 2	5.33, d, 4 $J_{o,m} = 7.5$	9.67, d, 4 $J_{m,o} = 7.5$		1.67 s, 18	10.44) s, 2) H_a
9'[d] L = py			7.96, d, 2 7.30, d, 2	4.92, d, 4 $J_{o,m} = 7.5$	9.08, d, 4 $J_{m,o} = 7.5$		1.42 s, 18	7.14) s, 2) H_a
9'[d] L = t-Bupy			8.11, d, 2 7.39, d, 2	5.23, d, 4 $J_{o,m} = 8$	9.20, dd, 4 $J_{m,o} = 8$ $J_{m,p} = 8$	6.26, t, 2 $J_{p,m} = 8$		7.28) s, 2) H_a
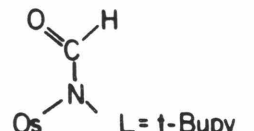
[a]The chemical shifts of the paramagnetic Os(IV) species are somewhat concentration dependent. The values reported here are uncorrected. Coupling constants are reported in Hz. [b]$J_{2,3} = J_{3,2} = 3$ Hz. [c]Ppm in d_6-acetone. [d]Ppm in $CDCl_3$. [e]Selective ^1H decoupling experiments have confirmed these assignments. [f]Ppm in CD_2Cl_2. [g]H_c readily exchanges on addition of D_2O which causes collapse of the H_b signal to a singlet.

Table 3.12. Selected 500-MHz ^{13}C NMR data.

No.	Compound	C_1 (Proton Coupled)	C_1 (H_1 or H_a Selectively Decoupled)[b]
7[a]		105.28, d $J_{C,H}$ = 187 Hz	105.28, s
8a[a]		51.76, d $J_{C,H}$ = 160 Hz	51.76, s
9[a]		196.46, d $J_{C,H}$ = 208 Hz	196.46, s

[a]δ in CDCl$_3$.

Table 3.13. Formal potentials of osmium compounds.

Compound	III/II[a]	IV/III[a]	V/IV[a]
5	-1.88	-0.65	(+0.70)[b]
5, L = t-Bupy	-1.96	-0.70	(+0.60)[b]
7	-1.76	-0.62	+0.37[c]
8b	-1.95	-0.64	(ca. +0.9)[b]
9	-1.88	-0.46	[d]
9'	-1.88	-0.39	[d]

[a]Potentials were measured in CH$_2$Cl$_2$ against the Fc$^+$/Fc couple (ca. 0.48 vs. SCE). [b]Peak potential for an irreversible oxidation. [c]7 also exhibits an irreversible oxidation at +0.92 V. [d]No oxidations are seen below +1.1 V.

In addition to the electrochemical synthesis of **9** and **9'**, a direct chemical route from **5** to **9'** was discovered. Oxidation of **5** in CH_2Cl_2 with tetrabutylammonium periodate in the presence of trifluoroacetic acid (TFA) produced the unrearranged product, **9**, in high yield.[2] The same method was found to convert **8** to **9'**. Both **9** and **9'** undergo acid catalyzed hydrolysis of the formyl groups to yield the corresponding primary amido complexes. These are catalysts for the electrochemical oxidation of alcohols (see Chapter 4).

Mechanistic Considerations for CHBA-Et Oxidation

At this point it might be helpful to suggest a mechanism for the oxidative conversions discussed above. Scheme 3.5 shows a mechanism for the electrochemical transformation of **5** to **8** which we believe is consistent with all of the data. One-electron oxidation of **5** would produce a cationic osmium(V) complex. This could then undergo reductive deprotonation to yield an osmium(III) monoimine complex which would be rapidly oxidized at the potential employed (+0.87 V vs. Fc^+/Fc). The resultant osmium(IV) cation could undergo a second reductive deprotonation to give complex **7**. One-electron oxidation of **7** would produce a compound which possesses carbonium ion character at the carbon atoms of the bridge. Nucleophilic attack at the bridge by alcohol followed by proton loss would lead to another osmium(III) monoimine complex. This neutral osmium(III) species would again be rapidly oxidized, and attack by a second molecule of alcohol would yield compound **8**.

The transient intermediate **6** could be produced on a second reaction pathway. TLC results indicate that **6** is neutral and contains the alcohol

Scheme 3.5. Proposed mechanism for conversion of **8** to **9**.
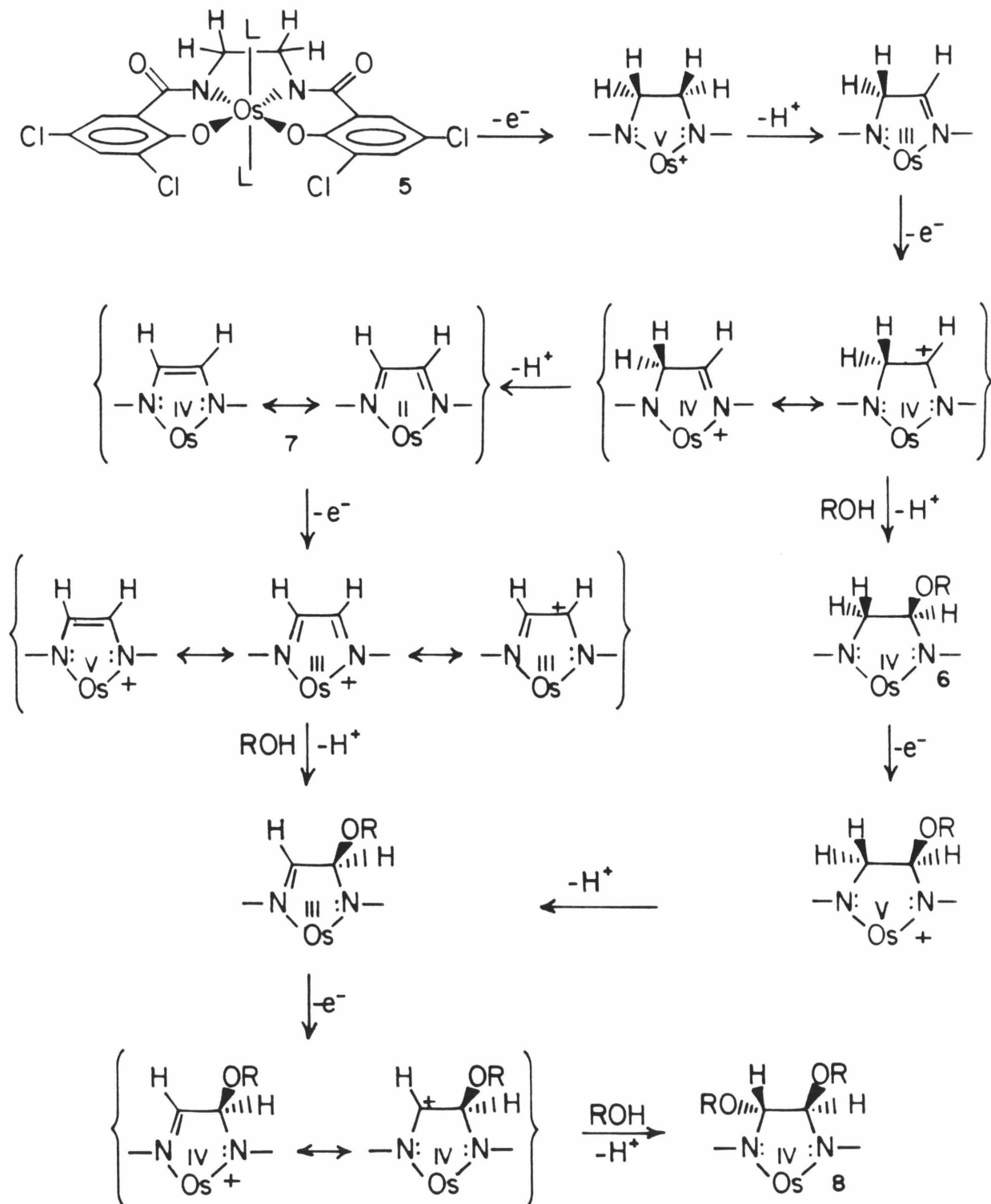
group.[2] Its color suggests that it is an osmium(IV) species. The pathway shown is consistent with these observations and it explains why **6** is formed during the oxidation of **5** but not **7**.

The process depicted in Scheme 3.5 involves oxidative dehydrogenation of the metallacyclopentane ring in **5**. A number of ligand oxidative dehydrogenations have been previously reported.[18-20] The oxidative functionalization of the unsaturated metallacycle in **7** is 100% stereoselective, yielding only the trans substituted compounds **8** and **8***.

The last step in the electrochemical oxidation of **5** to **9** and/or **9'** exhibits some interesting features. This is a rather complicated transformation which can perhaps be best understood by a historical treatment of the problem. As judged by TLC, the stereochemistry of the final product was found to be principally determined by the nature of the alcohol, ROH, used during the electrolysis, with a lesser dependence on the monodentate ligands, L.[2] For L = py the transformations were highly stereoselective. When R was methyl, ethyl, n-butyl, isopropyl, or benzyl, **9** was produced quantitatively. When R was tert-butyl, tert amyl, or H, **9'** appeared to be the major product. Substitution of t-Bupy for py lowered the selectivity. Thus, when L = t-Bupy and R = isopropyl, a mixture of **9** and **9'** was formed in the approximate ratio 7/3.

A mechanism which is consistent with the initial experimental observations is shown in Scheme 3.6. One-electron oxidation of **8** would produce an osmium(V) cation. This species could undergo a reductive dealkylation with ring cleavage to yield an osmium(III) monoimine complex. Oxidation, followed by a second dealkylation, would lead to **9** or **9'**.

Scheme 3.6. A mechanism for conversion of **8** to **9**.
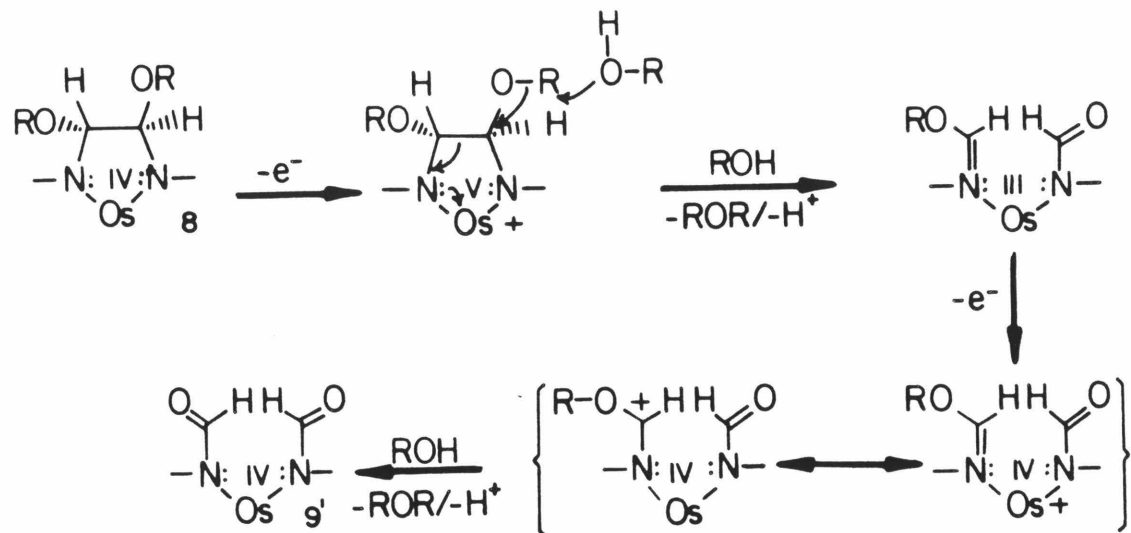
Several pieces of evidence support this mechanism. In one experiment **5** was electrolyzed in the presence of CD_3OD. The product, **9**, was isolated, examined by ^{1}H NMR and found to contain H at the formyl positions. This is consistent with the methylene protons on the bridge in **5** being carried through to the final product. According to the overall mechanism depicted in Schemes 3.5 and 3.6, the stoichiometric conversion of **5** to **9** or **9'** would require exactly six electrons. Experimentally, the charge consumed is variable, but it is always greater than or equal to six electrons per osmium atom. Also, in several experiments, between one and three equivalents of the ether ROR was detected.[2]

Isomerization to the cis-α isomer at the osmium(V) stage could account for the stereochemistry of the products. The distribution between **9** and **9'** would depend on the relative rate of isomerization vs. the rate of ring cleavage. If the rate of cleavage were significantly faster than the rate of isomerization

only the unrearranged product, **9'**, would be formed. If the rate of cleavage were slower, the isomerized product, **9**, would be produced. Based on the mechanism shown in Scheme 3.6, one would expect the rate of cleavage to be principally dependent on R. If the reaction were S_N1, the rate would be fast when R is a good leaving group (R = 3° alkyl or H) and slow when R is a poor leaving group (R = 1°, 2° alkyl). This is in agreement with the observed stereochemistry.

Complexes **9** and **9'** cannot be interconverted and, in fact, none of the osmium(IV) complexes described thus far show any tendency to rearrange. This suggested to us that the isomerization probably occurs at the osmium(V) stage. This has been supported by more recent results obtained with other HBA complexes. The osmium(IV) compound $Os(\eta^4\text{-CHBA-DCB})(\underline{t}\text{-Bupy})_2$ is formed solely as the trans isomer but upon oxidation to osmium(V) the complex forms an equilibrium mixture of the trans and cis-α isomers.[1,7] It has been shown that the HBA ligands are better donors in the cis-α configuration than in the planar equatorial arrangement. Therefore, oxidation of **8** to the osmium(V) cation could induce both the isomerization and the ring cleavage reaction. Isomerization prior to cleavage of the carbon-carbon bond would also restrict the number of isomers formed and thereby explain the fact that only two of the possible five diastereomers are produced. Finally, results presented in Chapter 4 indicate that there is no apparent electronic driving force for the isomerization once the carbon-carbon bond has been cleaved.[2]

Based on the mechanism described above, one piece of data appeared to be anomalous. If the rate of ring cleavage were determined by the stability of the leaving group R^+, one would expect the benzyl derivative to behave more

like the 3° alkyls and H, but instead it gives the same result as the 1° and 2° alkyls. In the electrochemical synthesis of **9** and **9'** from **5**, R is necessarily the same on the alcohol in solution as on the ligand bridge. Since the nature of both alkyl groups could be important in determining the stereochemistry, we undertook several experiments in order to gain a better understanding of the conversion from **8** to **9** or **9'**.

A series of compounds, **8** and **8***, was synthesized chemically from **7** (L = py) using methanol, ethanol, n-octanol, isopropanol, benzyl alcohol and t-butanol. These materials were isolated, purified and characterized by ^{1}H NMR (Table 3.11) and elemental analyses. Each compound in the series was then electrolyzed with the same alcohol in solution. This was intended to give a clearer picture of how the isomer distribution varies as a function of the alkyl group on the ligand bridge. After the electrolysis was complete the ratio of **9** to **9'** in the anolyte solution was determined quantitatively by high pressure liquid chromatography (HPLC).[21]

The results (Table 3.14) clearly demonstrate that the isomer distribution is not principally determined by the nature of R on the ligand bridge. With ethanol in solution the rearranged product **9** is formed regardless of which alkoxide is on the bridge. With t-butanol in solution the isomer distribution is again reasonably constant for the series of intermediate **8** complexes. It appears that, to a first approximation, the stereochemistry of the reaction is dependent on the nature of the alcohol in solution rather than the alkyl group on the ligand. A secondary effect is apparently exerted by the presence of **9** hydroxyl group on the bridge.

One surprising aspect of these results is that the use of t-butanol in

Table 3.14. Isomer distribution in electrolysis of **8** and **8***.[a]
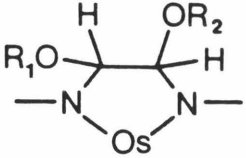
| | | % **9**/% **9'**[b] | |
		ROH = EtOH	ROH = t-BuOH
8b	$R_1=R_2=Me$	100/0	63/37
8c	$R_1=R_2=$n-octyl	100/0	69/31
8d	$R_1=R_2=$i-Pr	100/0	79/21
8e	$R_1=R_2=$benzyl	100/0	61/39
8f	$R_1=R_2=$t-Bu	100/0	79/21
8b*	$R_1=Me, R_2=H$	100/0	37/63
8f*	$R_1=$t-Bu, $R_2=H$	91/9	41/59

[a]Control potential oxidation of **8** or **8*** (0.1 mM) in CH_2Cl_2 at +0.87 V vs. Fc^+/Fc in the presence of ROH (0.5 M). [b]Ratio determined by HPLC with a detection limit of ca. 5%.

solution does not produce **9'** as the major product. In earlier experiments, the electrolysis of **5** in the presence of t-butanol, t-amyl alcohol or H_2O appeared to yield predominantly **9'**. This discrepancy could stem from several sources. First, the TLC analysis used in the earlier experiments is only a qualitative measure, while the HPLC method used in the later experiments is quantitative. When the oxidation of **5** was rerun in the presence of t-butanol, and the products checked by HPLC, the ratio of **9** to **9'** was found to be 31/69. This is still more **9'** than expected, based on the results in Table 3.14, but oxidation of **5** in the presence of t-butanol generates a significant quantity of **8f*** in addition to **8f**. This would increase the yield of **9'**.

The results in Table 3.14 are not inconsistent with the general features

of the mechanism proposed above, but the origin of the stereochemical control must be reexamined. Several explanations for the dependency of isomer distribution on the alcohol in solution have been considered. The following is perhaps the best explanation. Oxidation of **8** to the osmium(V) cation could be followed by coordination of ROH to the osmium center. Such coordination could stabilize the oxidized species and retard the rate of ring cleavage, thus favoring the isomerized product **9**. The use of _t_-butanol, which is a poorer ligand for steric reasons, would yield less isomerized product and more **9'**. Two additional pieces of data fit this mechanism. The results in Table 3.15 show that increased alcohol concentration leads to more isomerized

Table 3.15. Isomer distribution in electrolysis of **8**.[a]

Compound		ROH in Solution	9/9'[b]
8b	$R_1=R_2=Me$	0.5 M, EtOH	100/0
8b	$R_1=R_2=Me$	0.1 M, EtOH	98/2
8b	$R_1=R_2=Me$	0.02 M, EtOH	76/24
8d	$R_1=R_2=Me$	0.1 M, i-PrOH	87/13
8d	$R_1=R_2=i-Pr$	H_2O (<0.18 M)	30/70

[a]Controlled potential oxidation of **8** (0.1 mM) in CH_2Cl_2 at +0.87 V vs. Fc+/Fc. [b]Ratio determined by HPLC.

product as expected. Also isopropanol appears to be a poorer ligand than ethanol while H_2O is worse still. Finally, it has been shown that the first oxidation of intermediate **8** by cyclic voltammetry is irreversible, but it

becomes reversible on addition of ROH or H_2O. Ethanol is more effective in this respect than either t-butanol or water.

These results indicate that the presence of ROH or H_2O somehow stabilizes the osmium(V) cation, perhaps through coordination. Surprisingly, the anodic peak potentials are unchanged on addition of ROH or H_2O. If coordination occurred, one would expect at least some change in the potential. The fact that it doesn't change could be coincidental, since the observed peak potential of an irreversible oxidation can be lower than the true formal potential. Alternatively, the stabilization imparted by the presence of alcohols could arise from more subtle effects such as stabilization of a charged species by a more polar environment. In any case, the factors which determine the stereochemistry could involve very small energy differences. This fact, coupled with the complexity of the system, precludes any definitive conclusion about the stereochemical control based on the available data.

Yet another experiment has called into question the basic mechanism, depicted in Scheme 3.6, for the conversion of **8** to **9** or **9'**. As mentioned earlier, one to three equivalents of ether, ROR, were detected by HPLC in several experiments after conversion of **5** to **9** in the presence of benzyl alcohol.[2] This appeared to support the contention that the alkyl group on the ligand bridge left as R^+ to form ROR with alcohol in solution. During the later series of experiments the n-octyl derivative, **8c**, was electrolyzed in the presence of benzyl alcohol and a gas chromatographic analysis was employed to test for the benzyl-octyl ether.[21] None of the ether was detected. Instead, ca. 35% of the octyl groups were found as n-octanol. The presence of benzyl ether in the earlier experiments has since been shown to arise

from acid catalyzed dehydration of benzyl alcohol.[21] The more recent results suggest that perhaps a different mechanism is operative in which the alkoxide rather than the alkyl group is eliminated.

One such mechanism is shown in Scheme 3.7. The osmium(V) cation, produced by one-electron oxidation of **8**, could again undergo a ring cleavage reaction but without loss of the alkyl group. Attack at the resultant carbonium ion by alcohol produces an acetal while attack by H_2O yields a hemiacetal. The formation of both species is reversible, but the hemiacetal can go on to the formyl group by loss of ROH.[22] Oxidation of this osmium (III) monoimine followed by the same sequence of events would lead to **9** or **9'**. With the assymetric complex, **8***, the first formed carbonium ion could simply undergo deprotonation of the hydroxyl group to yield the formyl. Since the isomerization apparently occurs prior to the carbon-carbon bond cleavage, the same stereochemical considerations apply here as were discussed above. Appropriate ^{18}O labeling experiments could presumably distinguish between the two mechanisms in Schemes 3.6 and 3.7.

Scheme 3.7. Proposed mechanism for conversion of **8** to **9**.
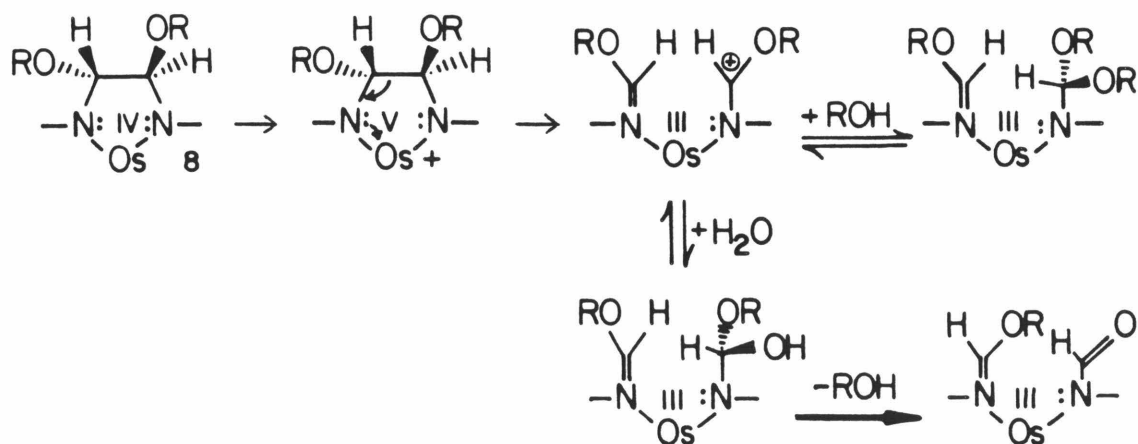
An interesting contrast appears in the mechanism for the ligand oxidation. The osmium(V) cation produced by one-electron oxidation of **5** undergoes a carbon-hydrogen bond cleavage reaction, but the analogous osmium(V) cation produced by oxidation of **8** chooses to cleave the carbon-carbon bond. Each reaction is completely selective in this respect. The presence of the alkoxides somehow promotes the ring cleavage. The carbonium ion formed by carbon-carbon bond cleavage is clearly stabilized by the alkoxide substituent, but the alternative reaction, loss of a proton, would also form a stabilized carbonium ion. Interaction of the alkoxide lone pairs with the adjacent carbon orbitals may promote carbon-carbon over carbon-hydrogen bond cleavage.

Conclusions

The irreversible oxidation of complex 5 has been examined in some detail. Controlled potential electrolysis of 5 in the presence of water or alcohol proceeds through a series of transformations in which the ethane backbone of the ligand is oxidized in a selective and stepwise fashion. Several of the intermediates were isolated, independently synthesized and characterized. The ethane bridge in 5 undergoes an oxidative dehydrogenation to yield the complex $Os(\eta^4\text{-CHBA-ethylene})(py)_2$, 7. The electrochemical and structural data suggest that the unsaturated metallacyclopentene ring in 7 provides some resonance stabilization of the complex. Complex 7 exhibits an unusual band in its IR spectrum at ca. 3650 cm^{-1} which could be due to a low energy electronic transition.

In the second isolated intermediate, 8, the unsaturated bridge of 7 has been selectively oxidized to a trans-1,2-diether. The related trans-1-hydroxy-2-alkoxy complex, 8*, demonstrates that asymmetry in these paramagnetic osmium(IV) complexes is clearly evident in their NMR spectra. Further oxidation of 8 or 8* cleaves the carbon-carbon bond of the ligand bridge with loss of the alkoxy and/or hydroxy groups to yield two bidentate ligands in which each amide nitrogen bears a formyl group. The cleavage product is formed as two diastereomers, 9 and 9', which differ only in the coordination geometry at the metal center. The diastereomeric distribution is determined primarily by the alcohol in solution.

All of the characterized complexes in this system are paramagnetic osmium(IV) species which have well resolved NMR spectra. The ^{1}H NMR data suggest that some π-backbonding from osmium to pyridine may be

operative. The electrochemical data indicate that the osmium(IV) centers are remarkably electron-rich by virtue of the CHBA ligand systems. The compounds are inert towards substitution of the chelate and pyridine ligands.

The mechanistic aspects of the electrochemical ligand oxidation process have been addressed and a consistent mechanism has been proposed. The mechanism involves a sequence in which each removal of an electron from the osmium complex is followed by a chemical reaction. Attempts have been made to elucidate the unique stereochemical features in the conversion of **8** to **9** or **9'**. The stereochemical control appears to be quite subtle and the available data do not permit a definitive conclusion regarding its source.

These studies demonstrate that the ethane bridge in the H_4CHBA-Et ligand is unsuitable for use in strongly oxidizing systems. Replacement of the ethane bridge with a dichlorobenzene bridge has permitted the synthesis of highly oxidized osmium and cobalt complexes.[1,7,23] This work has followed the oxidative transformation of the ligand in considerable detail and has uncovered some interesting mechanistic steps. Several unique structural and spectroscopic features have been discovered in the isolated complexes.

Experimental

General Considerations

Materials. All solvents were reagent grade (Aldrich, Baker, Mallinckrodt, M.C.B. or U.S.I.) and were used as received unless otherwise noted. Benzyl alcohol (99%, Aldrich), 4-tert-butylpyridine (99%, Aldrich), tert-butyl alcohol (reagent, Baker), 2,3-dichloro-5,6-dicyano-1,4-benzoquinone (98%, Aldrich), ethanol (absolute, U.S.I.), hydrogen peroxide (30% Superoxol, Baker), isopropyl alcohol (reagent, Baker), methanol (reagent, Baker), n-octanol (99%, Aldrich), periodic acid (Alfa), pyridine (reagent, Mallinckrodt), tetrabutylammonium hydroxide (25% in MeOH, M.C.B.) and triphenylphosphine (99%, Aldrich) were all used as received. Analytical and preparatory thin layer chromatography plates, 250 and 1000 μm, respectively, were silica gel GF (Analtech).

Physical Measurements. ^{1}H NMR spectra were measured at 90 MHz on a Varian EM 390 or a JEOL FX-90Q spectrometer. ^{13}C NMR spectra[24] were measured at 500 MHz on a Bruker WM-500 spectrometer. ^{1}H and ^{13}C chemical shifts are reported in ppm δ vs. Me$_4$Si with the solvent (CDCl$_3$, δ = 7.25; CD$_2$Cl$_2$, δ = 5.35; d$_6$-acetone, δ = 2.05) as internal standard. Infrared spectra were taken as Nujol mulls on KBr windows and were recorded on a Beckman IR 4240 spectrophotometer unless otherwise noted. Elemental analyses were obtained at the Caltech Analytical Facility. All electro-chemical experiments were carried out by S. L. Gipson at Caltech. Details of these procedures can be found in reference 1 or will appear in the near future.

X-ray Crystallography

Details on the data collection and structure determination of **8b*** can be found in reference 25.

Data Collection and Structure Determination of **7**.[8] A crystal 0.037 x 0.095 x 0.238 mm of Os(η^4-CHBA-ethylene)(t-Bupy)$_2$·½ CH_2Cl_2 was obtained by slow crystallization from CH_2Cl_2/hexane. Oscillation and Weissenberg photographs indicated that the space group was triclinic. The intensity data were collected on a locally modified Syntex P2$_1$ diffractometer with MoKα radiation (λ = 0.71073 Å). The unit cell parameters were obtained by least-squares refinement of the orientation matrix using fifteen 2θ values. Three check reflections, remeasured after each block of 97 reflections, indicated a linear decay of less than 1% over the 204 h of data collection. The total number of unique data was 5092, of which 3660 had intensities greater than $3\sigma_F$. The details of the data collection are summarized in Table 3.16.

The atomic position of the Os atom was derived from the Patterson map. Subsequent Fourier and difference maps revealed all non-hydrogen atoms. Atomic scattering factors were taken from reference 26. The anomolous dispersion factors for osmium and chlorine were included. A difference map, calculated after all non-hydrogen atoms had been located, revealed the presence of a molecule of dichloromethane solvent. At this stage, hydrogen atoms were placed at a distance of 0.95 Å from their respective carbon or oxygen atoms by assuming ideal geometry, and were not refined. The hydrogen atoms were given isotropic Gaussian amplitudes of 5.0 Å^2, except for methyl and solvent hydrogens which were given Gaussian amplitudes of 3.0 Å^2.

Several cycles of full-matrix least-squares refinement minimizing $\Sigma w\left(F_0^2 - (F_c/k)^2 \right)^2$ on all non-hydrogen parameters yielded $R_F = 0.045$, $R_{3\sigma} = 0.034$, and $S = 1.81;$[27] final shift/errors <0.10; data-to-parameter ratio $= 11.3$. All calculations were carried out on a VAX 11/780 computer using the CRYM system of programs.[28]

Data Collection and Structure Determination of 9. A long crystal of 9 (L = t-Bupy) was obtained by slow crystallization from CH_2Cl_2/hexane. Diffractometer data (Nicolet diffractometer, graphite monochromator, $MoK\alpha$ radiation) indicated monoclinic symmetry and space group C2/c (Table 3.16). The six check reflections indicated no decomposition, and following an empirical correction for absorption, the data were reduced to F_0^2. Details of the data collection are summarized in Table 3.16.

Solution of the structure was by the Patterson map, and refinement on $|F|$. The solvent molecule, CH_2Cl_2, is disordered, and attempts to model it and refine the remainder of the structure gave $R_F = 0.031$ and $S' = \left(\Sigma w(\Delta F)^2 / \Sigma w F_0^2 \right)^{\frac{1}{2}} = 1.60$; final average shift/error $= 0.02$, the maximum deviation in final ΔP map is 0.59 e/$\overset{o}{A}^3$. The data collection and refinement was carried out by Crystalytics Co.

Data Collection and Structure Determination of 9'.[17] A thin needle-like crystal of 9' (L = t-Bupy) was obtained from a solution of CH_2Cl_2/EtOH. Oscillation and Weissenberg photographs showed symmetry no higher than $\overline{1}$. The unit cell parameters (Table 3.16) were determined from a refinement using fifteen 2θ values with $25^o < |2\theta| < 35^o$, averaged from centered values at both $+2\theta$ and -2θ. The intensity data were collected on a locally modified Syntex P2$_1$ diffractometer with graphite monochromator and

Table 3.16. Summary of data collection and refinement information.

	7	9	9'
formula	$C_{34}H_{34}OsN_4O_4Cl_4 \cdot \frac{1}{2}CH_2Cl_2$	$C_{34}H_{32}OsN_4O_6Cl_4 \cdot CH_2Cl_2$	$C_{34}H_{32}OsN_4O_6Cl_4$
formula weight	979.61	1009.60	924.67
space group	P$\bar{1}$	C2/c	P$\bar{1}$
a, Å	10.994(3)	19.907(6)	8.533(1)
b, Å	11.998(3)	28.850(7)	13.688(2)
c, Å	15.660(3)	9.445(3)	16.415(2)
σ, deg	99.88(2)	90	104.35(1)
β, deg	105.19(2)	131.79(2)	97.33(1)
γ, deg	95.83(2)	90	79.18(1)
v, Å^3	1940.5(8)	4044(2)	1817.8(4)
z	2	4	2
D_{calcd}, gcm^{-3}	1.520	1.66	1.69
crystal size, mm	0.037 x 0.095 x 0.238	0.11 x 0.20 x 0.80	0.10 x 0.23 x 0.42
λ, Å	0.71073	0.71073	0.71073
μ, mm^{-1}	3.396	3.60	3.86
scan type	θ-2θ	ω	θ-2θ
2θ limits	4-45°	3-43°, 43-55°	4-30°, 25-56°
scan rate, deg/min	2	6, 4	6, 2
scan width, deg	2	0.9	2.0
total collected refl	5583	--	9710
final refl	5092	4657	8315
refinement on	F^2	F	F^2
final no. of param.	451	264	442
final cycle[a]			
R_F	0.045 (4803)	--	0.051 (7989)
R_F'	0.034 (3660)	0.031 (3903)	0.043 (6871)
S	1.81 (5092)	1.60 (3903)	2.16 (8315)

[a]The number of contributing reflections is given in parentheses; see reference 27 for definitions.

MoKα radiation. The three check reflections indicated no decomposition, and the data were reduced to F_0^2 as above. The form factors[26] of Os and Cl were corrected for anomalous dispersion.

Solution and refinement of the structure proceeded smoothly; the position of the Os atom was derived from the Patterson map, and the Fourier map map phased on the Os atom revealed the remainder of the structure. The hydrogen atoms were introduced into the model with fixed coordinates at idealized positions (the methyl hydrogen atoms from ΔF maps) and fixed Gaussian amplitudes of $U = 0.10 \ \overset{\circ}{A}^2$. Full-matrix least-squares refinement of the non-hydrogen atoms with anisotropic U_{ij}'s, using all reflections with $I > 0$, yielded $R_F = 0.051$, $R_F' = 0.043$, and $S = 2.16$;[27] final average shift/error = 0.04 in last cycle. Maximum deviation in the final $\Delta\rho$ map is 2.5 $e/\overset{\circ}{A}^3$. All calculations were carried out on a VAX 11/780 computer using the CRYM system of programs.[28]

Syntheses

All reactions were carried out in air unless otherwise noted.[29] $K_2[Os(\eta^4\text{-CHBA-Et})(O)_2]$, 2, and $Os(\eta^4\text{-CHBA-Et})(py)_2$, 5, were prepared as described in Chapter 2.

$\underline{Os(\eta^4\text{-CHBA-Et})(\text{t-Bupy})_2, \ 5.}^3$ $K_2[Os(\eta^4\text{-CHBA-Et})(O)_2] \cdot (H_2O)_4$, 2 (0.540 g), was dissolved in 4-$\underline{tert}$-butylpyridine (15 mL) and H_2O (10 mL). Triphenylphosphine (0.445 g, 2.5 equiv) was added and the inhomogeneous mixture was heated with stirring at 60°C for 20 min. The reaction was accompanied by a color change to deep red-orange. The solution was

evaporated to dryness while heating and the residue was then warmed under vacuum for an additional 6 h to insure complete removal of the t-Bupy and H_2O. The dry residue was washed with CH_2Cl_2 (20 mL) to remove the phosphines. The reduced intermediate, 4, was collected as a red-brown solid which was then redissolved in THF (50 mL) and H_2O (20 mL). To this solution was added 30% H_2O_2 (ca. 20 mL) in THF (20 mL) while cooling in a $0^{\circ}C$ bath. The solution was stirred at room temperature for ca. 15 min or until the color change to deep royal blue was complete. Addition of methanol (20 mL) followed by slow removal of the THF yielded the product as a dark blue microcrystalline solid (0.511 g, 84% based on 2). An analytical sample was obtained by purification on a preparatory TLC plate using CH_2Cl_2/THF (3/2) followed by recrystallization from CH_2Cl_2/pentane: ^{1}H NMR (Table 3.11); Anal. calcd. for $C_{34}H_{34}Cl_4N_4O_4Os$: C, 45.54; H, 3.83; N, 6.26. Found: C, 45.56; H, 3.83; N, 6.23.

Os(η^4-CHBA-ethylene)(py)$_2$, 7.[3] Os(η^4-CHBA-Et)(py)$_2$, 5 (100 mg), was dissolved in THF (50 mL) and placed in a 250-mL round-bottom flask containing silica gel (15 g). The mixture was stirred and heated at reflux for 1 h and then evaporated to dryness. The dry silica was heated at $120^{\circ}C$ for 1 h and then placed on top of a small quantity of clean silica gel in a short column. Elution with CH_2Cl_2/acetone (4/1) removed the bulk of the product as a bright yellow band. Some starting material, 5, and some of the corresponding Os(III) salt, 4, remained on the column. Second and third fractions of the product were obtained by again heating the dry silica at $120^{\circ}C$ for 1 h and eluting on a short column as before. Filtration and removal of solvent from the combined fractions yielded the product as a dark gold-brown micro-

crystalline solid (91 mg, 91%). An analytical sample was obtained by recrys-
tallization from $CHCl_3$/hexane: IR (Figs. 3.6 and 3.7); ^1H and ^{13}C NMR
(Tables 3.11 and 3.12, Fig. 3.11); Anal. calcd. for $C_{26}H_{16}Cl_4N_4O_4Os$: C,
40.01; H, 2.07; N, 7.18. Found: C, 39.93; H, 2.10; N, 7.18.

Os(η^4-CHBA-ethylene)(t-Bupy)$_2$, **7**.[3] Os(η^4-CHBA-Et)(t-Bupy)$_2$, **5** (100
mg), was heated on silica gel as described for the unsubstituted pyridine
adduct of **7**. The product was removed from the silica as a bright yellow band
by elution with CH_2Cl_2/acetone (9/1). Three fractions were collected as
before and recrystallization from CH_2Cl_2 yielded the product as a very dark
brown microcrystalline solid (61 mg, 61%): ^1H NMR (Table 3.11); Anal. calcd.
for $C_{34}C_{32}Cl_4N_4O_4Os$: C, 45.75; H, 3.61; N, 6.28. Found: C, 45.53; H,
3.63; N, 6.18.

Os(η^4-CHBA-t-1,2-diEtO-Et)(py)$_2$, **8a**.[3] Os(η^4-CHBA-ethylene)(py)$_2$,
7 (100 mg), was dissolved in absolute ethanol (20 mL) and dry CH_2Cl_2 (20 mL).
Addition of dichlorodicyanobenzoquinone (DDQ) (90 mg) caused an immediate
color change to deep royal blue. The solution was stirred for 20 min and then
evaporated to dryness. The product was extracted into CH_2Cl_2 and purified
on a short silica gel column by elution with CH_2Cl_2/acetone (9/1). After
recrystallization from CH_2Cl_2/pentane the product was obtained as a dark
blue microcrystalline solid (76 mg, 68%): IR (nujol) 1612 (sh), 1604 (s), 1598
(s), 1578 (s) 1539 (m), 1287 (vs), 1057 (s), 862 (s), 784 (s), 742 (s) cm^{-1}; ^1H
and ^{13}C NMR (Tables 3.11 and 3.12); Anal. calcd. for $C_{30}H_{26}Cl_4N_4O_6Os$:
C, 41.39; H, 3.01; N, 6.44. Found: C, 41.23; H, 2.96; N, 6.43.

Os(η^4-CHBA-t-1,2-diMeO-Et)(py)$_2$, **8b**.[3] Os(η^4-CHBA-ethylene)(py)$_2$,

7 (100 mg), was dissolved in absolute methanol (20 mL) and dry CH_2Cl_2 (20 mL). The solution was treated with DDQ (90 mg) as for **8a** and the crude product was purified on two successive short silica gel columns. Recrystallization from CH_2Cl_2/pentane yielded the product as a dark blue powder. NMR established the structure of the product but also showed the presence of a small impurity (< 10%). The impurity was separated from the product on a preparatory thin layer chromatography plate using CH_2Cl_2/THF (5/1). ^{1}H NMR indicated that the impurity was an asymmetrically substituted compound with one hydroxy and one methoxy group on the ligand bridge. This compound, **8b***, was the first in this series with inequivalent NMR signals for the two pyridine ligands and the two aromatic rings in the chelate ligand. It was therefore deliberately synthesized as discussed below. After removal of the impurity, the major product, **8b**, was again recrystallized form CH_2Cl_2/pentane (43 mg, 40%): ^{1}H NMR (Table 3.11); Anal. calcd. for $C_{28}H_{22}Cl_4N_4O_6Os$: C, 39.92; H, 2.63; N, 6.65. Found: C, 39.94; H, 2.69; N, 6.61.

Os(η^4-CHBA-t-1,2-diRO-Et)(py)$_2$, **8c** (R = n-octyl).^{3} Complex 7 (90 mg) was dissolved in dry CH_2Cl_2 (20 mL) and n-octanol (10 mL). The solution was treated with DDQ (90 mg) as described for **8a**. After purification on a short silica gel column followed by recrystallization from CH_2Cl_2/hexane the product was obtained as a dark blue powder (102 mg, 85%): ^{1}H NMR (Table 3.11); Anal. calcd. for $C_{42}H_{50}Cl_4N_4O_6Os$: C, 48.56; H, 4.85; N, 5.39. Found: C, 48.83; H, 4.88; N, 5.40.

Os(η^4-CHBA-t-1,2-diRO-Et)(py)$_2$, **8d** (R = i-Pr).^{3} Complex 7 (90 mg) was dissolved in dry CH_2Cl_2 (20 mL) and isopropanol (20 mL). DDQ (90

mg) was added and the reaction was stirred at room temperature for 1 h. The product was isolated and purified on a silica gel as described for **8a**. Recrystallization from CH_2Cl_2/hexane yielded the dark blue product as a crystalline solid (80 mg, 77%): ^{1}H NMR (Table 3.11); Anal. calcd. for $C_{32}H_{30}Cl_4N_4O_6Os$: C, 42.77; H, 3.37; N, 6.23. Found: C, 43.06; H, 3.44; N, 6.20.

Os(η^4-CHBA-t-1,2-diRO-Et)(py)$_2$, **8e** (R = benzyl).[3] Complex 7 (100 mg) was dissolved in dry CH_2Cl_2 (20 mL) and benzyl alcohol (6 mL). DDQ (100 mg) was added and the reaction was stirred for 0.5 h. The CH_2Cl_2 was removed by evaporation and the excess benzyl alcohol was removed under vacuum while heating. The product was extracted into CH_2Cl_2 and purified on two successive short silica gel columns by elution with CH_2Cl_2/acetone (97/3). An analytical sample was obtained by recrystallization from CH_2Cl_2/hexane: yield 116 mg (91%); ^{1}H NMR (Table 3.11); Anal. calcd. for $C_{40}H_{30}Cl_4N_4O_6Os$: C, 48.30; H, 3.04; N, 5.63. Found: C, 48.44; H, 3.12; N, 5.56.

Os(η^4-CHBA-t-1,2-diRO-Et)(py)$_2$, **8f** (R = t-Bu).[3] t-Butanol was refluxed for 12 h over CaH_2 and then distilled under N_2. Intermediate 7 was freshly recrystallized from CH_2Cl_2/hexane and dried for 12 h at 80°C under vacuum. Complex 7 (100 mg) was dissolved in dry CH_2Cl_2 (20 mL) and dry t-butanol (20 mL). Predried DDQ (90 mg) was added and the reaction was stirred under N_2 for 1 h. The CH_2Cl_2 and excess t-butanol were removed under vacuum and the product was purified on two successive short silica gel columns by elution with CH_2Cl_2/acetone (9/1). An analytical sample was obtained by recrystallization from CH_2Cl_2/hexane followed by heating at 80°C

under vacuum for 24 h: yield 60 mg (50.5%); IR (nujol) 1610 (s), 1595 (s), 1570 (s), 1539 (m), 1303 (sh), 1291 (vs), 1190 (s), 1049 (s), 993 (s), 868 (s), 792 (s), 741 (s) cm^{-1}; ^{1}H NMR (Table 3.11); Anal. calcd. for $C_{34}H_{34}Cl_4N_4O_6Os$: C, 44.07; H, 3.70; N, 6.05. Found: C, 44.15; H, 3.73; N, 5.98.

Os(η^4-CHBA-t-1-OH-2-MeO-Et)(py)$_2$, 8b*.[3] Os(η^4-CHBA-ethylene)-(py)$_2$, 7 (100 mg), was dissolved in a mixture of CH_2Cl_2 (24 mL), absolute methanol (18 mL) and H_2O (3 mL). The solution was oxidized with DDQ (90 mg) as described for 8a and 8b. The crude product was extracted into CH_2Cl_2 and washed down a short silica gel column to separate out the quinones. TLC indicated that the crude product contained three blue compounds in the approximate ratio of 1/2/1. The three were separated on a preparatory thin layer chromatography plate using CH_2Cl_2/THF (4/1). One of the minor components was shown by NMR to be the dimethoxy substitute compound, 8b. The major component proved to be the desired product, 8b*, and the other minor component was presumably the dihydroxy substituted compound. The product was recrystallized from CH_2Cl_2/pentane and obtained as a dark blue microcrystalline solid (35 mg, 33%): IR (nujol) 3230 (s broad, ν(O-H)), 1609 (vs, ν(C=O)), 1585 (m), 1561 (vs), 1530 (m), 1283 (vs), 1069 (s), 868 (s), 782 (s), 733 (s) cm^{-1}; ^{1}H NMR (Table 3.11); Anal. calcd. for $C_{27}H_{20}Cl_4N_4O_6Os$: C, 39.14; H, 2.43; N, 6.76. Found: C, 38.97; H, 2.56; N, 6.55.

Os(η^4-CHBA-t-1-OH-2-RO-Et)(py)$_2$, 8c* (R = n-octyl).[3] Complex 8c* was formed as a minor product (10-15%) in the synthesis of 8c and was isolated from the silica gel column purification of 8c. The asymmetric product was recrystallized from CH_2Cl_2/hexane: ^{1}H NMR (Table 3.11).

$\underline{Os(\eta^4\text{-CHBA-t-1-OH-2-RO-Et})(py)_2}$, **8d*** (R = i-Pr).[3] Complex **8d***
was formed as a minor product (ca. 20%) in the synthesis of **8d** and was
isolated from the silica gel purification of **8d**. Complex **8d*** was purified on a
second column by elution with CH_2Cl_2/acetone (4/1) and recrystallized from
CH_2Cl_2/hexane: ^{1}H NMR (Table 3.11).

$\underline{Os(\eta^4\text{-CHBA-t-OH-2-RO-Et})(py)_2}$, **8f*** (R = t-Bu).[3] Complex **8f*** was
formed as a minor product (30-40%) in the synthesis of **8f**. The two products
were separated on a short silica gel column and the asymmetric compound
was then purified on a second column by elution with CH_2Cl_2/acetone (85/15).
An analytical sample was obtained by recrystallization from CH_2Cl_2/hexane:
^{1}H NMR (Table 3.11); Anal. calcd. for $C_{30}H_{26}Cl_4N_4O_6Os$: C, 41.39; H,
3.01; N, 6.44. Found: C, 41.63; H, 3.05; N, 6.37.

$\underline{Cis\text{-}\alpha\text{-}Os(\eta^2\text{-Fo-CHBA})_2(py)_2}$, **9**.[3] Method A.[31] $Os(\eta^4\text{-CHBA-Et})(py)_2$
(40 mg, 0.051 mmol), was dissolved in CH_2Cl_2 (25 mL) containing TBAP (0.1
M) and a 1° or 2° alcohol (methanol, n-butanol, isopropanol or
benzyl alcohol) (1 M). The solution was electrolyzed in a three-compartment
electrochemical cell at a BPG anode at +1.40 V vs. Ag/AgCl until the current
had decayed to < 5% of its initial value and TLC indicated that the reaction
was complete. The anolyte was transferred to a beaker and ether (65 mL)
was slowly added. The precipitated TBAP was removed by filtration and the
solvents were evaporated from the filtrate. The resulting oil was dissolved in
acetone (25 mL) and the product was precipitated by addition of H_2O (50 mL).
The dark blue product was redissolved in CH_2Cl_2, dried over $MgSO_4$ and
precipitated with hexane: yield 30 mg (72%): IR (nujol) 1682 [vs, ν(C=O)],
1645 [vs, ν(C=O)], 1611 (m, py), 1579 (m), 1272 (vs), 1218 (s), 1119 (s), 1072

(m, py), 1051 (w, py), 1018 (w, py), 869 (s), 797 (m), 785 (m), 749 (s) cm^{-1};

Anal. calcd. for $C_{26}H_{16}Cl_4N_4O_6Os$: C, 38.44; H, 1.99; N, 6.90. Found: C, 38.41; H, 2.06; N, 6.88.

Method B.[31] Os(η^4-CHBA-ethylene(py)$_2$, 7 (8 mg), was dissolved in CH_2Cl_2 (20 mL) containing TBAP (0.1 M) and isopropanol (0.5 M). The solution was electrolyzed according to the procedure described in method (A) to give the desired product, 9, and a trace of 9'.

Cis-α-Os(η^2-Fo-CHBA)$_2$(t-Bupy)$_2$, 9.[3,31] Os(η^4-CHBA-Et)(t-Bupy)$_2$, 5 (50 mg, 0.050 mmol), was oxidized in the presence of methanol or isopropanol in the same manner used for the pyridine adduct of 9. The product, which was isolated as before, contained significant amounts of the trans isomer, 9'. The two compounds were separated on a preparative TLC plate (2000 μM, silica gel) by elution with CH_2Cl_2/THF (30/1). The product, 9 (32 mg, 62%), was isolated as a dark blue powder from CH_2Cl_2/ hexane. An analytical sample was obtained by slow crystallization from CH_2Cl_2/hexane: ^{1}H and ^{13}C NMR (Tables 3.11 and 3.12); Anal. calcd. for $C_{34}H_{32}Cl_4N_4O_6Os$: C, 44.15; H, 3.49; N, 6.06. Found: C, 44.07; H, 3.68; N, 5.76.

Trans-Os(η^2-Fo-CHBA)$_2$(py)$_2$, 9'.[3] Method A.[31] Os(η^4-CHBA-Et)- (py)$_2$, 5, was oxidized by the same method used in the synthesis of 9 except that the CH_2Cl_2 contained t-butanol (1 M), t-amyl alcohol (1 M)or was saturated with water, TLC indicated that the product was formed in high yield but difficulty in purification and isolation produced a low yield (<30%) of the dark blue product: ^{1}H NMR (Table 3.11); Anal. calcd. for $C_{26}H_{16}Cl_4N_4O_6Os$: C, 38.44; H, 1.99; N, 6.90. Found: C, 38.63; H, 2.16;

N, 6.79.

Method B.[2] $Os(\eta^4\text{-CHBA-Et})(py)_2$, **5** (8 mg, 0.01 mmol) was dissolved in CH_2Cl_2 (10 mL) containing methanol (0.5 M) and trifluoroacetic acid (2 M). To this solution was added a CH_2Cl_2 solution of tetrabutylammonium periodate (0.1 M) which had been prepared from tetrabutylammonium hydroxide and pedriodic acid. TLC again indicated that **9'** was produced in high yield.

Trans-$Os(\eta^2\text{-Fo-CHBA})_2(t\text{-Bupy})_2$, **9'**.[3] Method A.[31] $Os(\eta^4\text{-CHBA-Et})\text{-}(t\text{-Bupy})_2$, **5** (25 mg) was oxidized in the presence of tert-butanol (0.5 M) using the same procedure as for the pyridine adducts of **9** and **9'**. TLC showed that the reaction was clean and that the product was formed in high yield. The high solubility of the dark blue compound led to a much lower yield of isolated material after recrystallization from boiling cyclohexane: yield 15 mg (58%); ^{1}H NMR (Table 3.11); IR (nujol) 1702 (s, ν(C=O)), 1688 (s, ν(C=O)), 1640 (vs, ν(C=O)), 1633 (vs, ν(C=O)), 1585 (m), 1278 (vs), 1217 (s), 1067 (m, t-Bupy), 1036 (m, t-Bupy), 874 (m), 795 (m), 784 (m), 735 (s) cm^{-1}; Anal. calcd. for $C_{34}H_{32}Cl_4N_4O_6Os$: C, 44.15; H, 3.49; N, 6.06. Found: C, 44.02; H, 3.53; N, 5.93.

Method B. A.[31] $Os(\eta^4\text{-CHBA-t-1,2-diEtO-Et})(t\text{-Bupy})$, **8a** (10 mg), was dissolved in 10 mL of CH_2Cl_2 containing 1 drop of trifluoroacetic acid. An excess of tetrabutylammonium periodate was added as a CH_2Cl_2 solution. TLC indicated quantitative conversion of **8a** to **9'**.

References and Notes

(1) Anson, F. C.; Christie J. A.; Collins, T. J.; Coots, R. J.; Furutani, T. T.; Gipson, S. L.; Keech, J. T.; Krafft, T. E.; Santarsiero, B. D.; Spies, G. H. J. Am. Chem. Soc. 1984, 106, 4460.

(2) Gipson, S. L. See reference 1.

(3) Ligand names are: 1,2-bis(3,5-dichloro-2-hydroxybenzamido)ethane, H_4CHBA-Et; 1,2-bis(3,5-dichloro-2-hydroxybenzamido)ethylene, H_4CHBA-ethylene; 1,2-bis(3,5-dichloro-2-hydroxybenzamido)-trans-1,2-dialkoxyethane, H_4CHBA-t-1,2-diRO-Et; 1,2-bis(3,5-dichloro-2-hydroxybenzamido)-trans-1-hydroxy-2-alkoxyethane, H_4CHBA-t-1-OH-2-RO-Et; N-formyl-3,5-dichloro-2-hydroxybenzamide, H_2Fo-CHBA.

(4) Paramagnetically shifted NMR spectra have been previously observed for Os(IV) complexes. (a) Pawson, D.; Griffith, W. P. J. Chem. Soc., Dalton Trans. 1975, 417. (b) Randall, E. W.; Shaw, D. J. Chem. Soc., A 1969, 2867. (c) Chatt, J.; Leigh, G. J.; Mingos, D. M. P.; Paske, R. J. Ibid. 1968, 2636. (d) Chatt, J.; Leigh, G. J.; Mingos, D. M. P.; Randall, E. W.; Shaw, D. Chem. Commun. 1968, 419.

(5) Jorgensen, W. L.; Salem, L. "The Organic Chemist's Book of Orbitals"; Academic Press: New York, 1973, p. 265.

(6) See Chapter 2 (page 42) for a brief discussion of π-backbonding in this and similar systems.

(7) Gipson, S. L.; Keech, J. T.; Peake, G. T. Unpublished results.

(8) The X-ray crystal structure determination of 7 was performed by Dr. R. J. Coots at Caltech.

(9)   Cotton, F. A.; Wilkinson, G. "Advanced Inorganic Chemistry"; 4th ed.;
        John Wiley and Sons: New York, 1980, pp. 644-652 and 912-913.

(10)   Silverstein, R. M.; Bassler, G. C.; Morrill, T. C. "Spectrometric
        Identification of Organic Compounds"; John Wiley and Sons: New
        York, 1974, pp. 91-95.

(11)   (a) Magnuson, R. H.; Lay, P. A.; Taube, H. J. Am. Chem. Soc. 1983,
        105, 2507. (b) Creutz, C.; Taube, H. Ibid. 1973, 95, 1086. (c)
        Magnuson, R. H.; Taube, H. Ibid. 1972, 94, 7213. (d) Creutz, C.;
        Taube, H. Ibid. 1969, 91, 3988. (e) Richardson, D. E.; Sen, J. P.;
        Buhr, J. D.; Taube, H. Inorg. Chem. 1982, 21, 3136.

(12)   The solution IR spectrum was recorded on a Mattson Sirius 100
        spectrophotometer.

(13)   The X-ray crystal structure determination of 8b* was performed by G.
        H. Spies at Caltech. See reference 25.

(14)   Silverstein, R. M.; Bassler, G. C.; Morrill, T. C. "Spectrometric
        Identification of Organic Compounds"; John Wiley and Sons: New
        York, 1974, pp. 174-176.

(15)   Gordon, A. J.; Ford, R. A. "The Chemist's Companion"; John Wiley
        and Sons: New York, 1972, pp. 272-274.

(16)   The X-ray crystal structure determination of 9 was carried out by
        Crystalytics Co.

(17)   The X-ray crystal structure determination of 9' was performed by T. T.
        Furutani and Dr. W. P. Schaefer at Caltech. See reference 1.

(18)   For example, see: (a) Lay, P. A.; Sargeson, A. M.; Skelton, B. W.;
        White, A. H. J. Am. Chem. Soc. 1982, 104, 6161. (b) Ridd, M. J.;

Keene, F. R. Ibid. 1981, 103, 5733. (c) Thompson, M. S.; Meyer, T. J. Ibid. 1981, 103, 5577. (d) Brown, G. M.; Weaver, T. R.; Keene, F. R.; Meyer, T. J. Inorg. C hem. 1976, 15, 190.

(19) For a recent review of α,α-diimine complexes including ligand oxidations see: Van Koten, G.; Vrieze, K. Adv. Organomet. Chem. 1982, 21, 151.

(20) Oxidation of methylene units in polypeptide systems has been reported. (a) Rybka, J. S.; Margerum, D. W. Inorg. Chem. 1981, 20, 1453. (b) Kirschenbaum, L. J.; Rush, J. D. J. Am. Chem. Soc. 1984, 106, 1003.

(21) Gipson, S. L. Unpublished results.

(22) March, J. "Advanced Organic Chemistry"; 2nd ed.; McGraw-Hill: New York, 1977.

(23) Anson, F. C.; Collins, T. J.; Coots, R. J.; Gipson, S. L.; Richmond, T. G. J. Am. Chem. Soc. 1984, 106, 5037.

(24) ^{13}C NMR spectra were recorded at the Southern California Regional NMR facility.

(25) Spies, G. H. Ph.D. Thesis, California Institute of Technology, October, 1984.

(26) Atomic scattering factors were taken from: "International Tables for X-ray Crystallography"; Witton: Birmingham, 1974; Vol. IV, pp. 72-97.

(27) The goodness-of-fit $S = \left(\Sigma w \Delta^2/(n-v) \right)^{1/2}$, n = number of reflections, v = number of parameters; $R_F = \Sigma |\Delta F|/\Sigma |F_o|$ (based on reflections with I > o), $\Delta F = |F_o| - |F_c|$, $R_F^! = R_F$ (based on reflections with $I > 3\sigma_I$).

(28)   The CRYM computing system was used (Duchamp, D. J., California Institute of Technology).

(29)   Although the complexes reported here are generally stable species, appropriate precautions should be taken when working with osmium complexes, since evolution of toxic OsO_4 is possible.[30]

(30)   Malin, J. M. Inorg. Synth. 1980, 20, 61.

(31)   The electrochemical synthesis and initial isolation of the product was carried out by S. L. Gipson. See reference 1.

CHAPTER 4

Osmium Complexes Bearing Bidentate N-Coordinated

Primary Organic Amide Ligands. Catalysts for

the Electrochemical Oxidation of Alcohols

Introduction

The discovery of the catalyst was made by Stephen Gipson. Most of the work on the catalytic system and all of the electrochemistry reported here were also performed by Steve. Due to the complexity and the collaborative nature of this project, a considerable portion of his work is reported in this chapter for the sake of continuity.

The electrochemical oxidation of $Os(\eta^4\text{-CHBA-Et})(py)_2$, **5**, in the presence of alcohol leads to a complex series of reactions in which the bridge of the CHBA-Et ligand is oxidized (see Chapter 3).[1] The final products of the ligand oxidation, <u>cis</u>-α- and <u>trans</u>-$Os(\eta^2\text{-Fo-CHBA})_2(py)_2$, **9** and **9'**,[2] can be converted to active catalysts for the electrochemical oxidation of alcohols. The catalytic system selectively oxidizes benzyl alcohol to benzaldehyde with no further oxidation to benzoic acid or to benzyl esters. Turnover numbers of over one hundred can be attained with benzyl alcohol, but the activity with other alcohols is much lower. Nevertheless, the high selectivity of the system is an important feature which encouraged us to pursue its study.

The catalysts, **11** and **11'**, are osmium(IV) complexes which bear two bidentate N-coordinated primary amido ligands and two pyridine ligands. An X-ray crystal structure of one of the compounds, **11'**, is reported. Attempts were made to directly synthesize the compounds by coordinating the appropriate bidentate ligands to osmium. This led to the production of several additional complexes which show the same type of catalytic activity as **11** and **11'**. The synthesis, characterization and properties of the osmium compounds and significant features of the catalytic system are reported in this chapter.

Results and Discussion

N-Coordinated Primary Amide Complexes of Osmium(IV)

Electrochemical oxidation of $Os(\eta^4\text{-CHBA-Et})(py)_2$, **5**, is irreversible on the cyclic voltammetry time scale, even at fast scan rates.[3] Upon oxidation by one electron the complex apparently undergoes a very rapid irreversible chemical change. An attempt was made to improve the reversibility of the oxidation by adding alcohol to the system. It was thought that the oxidized osmium complex might preferentially oxidize the alcohol rather than undergo decomposition. The addition of alcohol alters the fate of the osmium complex, but it does not produce a reversible osmium(V/IV) couple. With alcohol or water present the oxidation of **5** proceeds through a series of osmium complexes in which the ethane bridge of the ligand is oxidized in a selective and stepwise fashion (see Chapter 3).[1]

Little or no catalytic alcohol oxidation is observed during the ligand oxidation process, but the discovery was made that the final osmium oxidation products, cis-α- and trans-$Os(\eta^4\text{-Fo-CHBA})_2(py)_2$, **9** and **9'**, can be converted to active catalysts for the electrochemical oxidation of alcohols.[4] On one occasion, after oxidation of **5** to **9**, the anolyte solution containing **9**, TBAP, benzyl alcohol and acid was allowed to stand for several weeks. A cyclic voltammogram of the solution showed the presence of a large catalytic current at ca. +1.0 V vs. Fc^+/Fc (Fig. 4.1). TLC indicated that a new osmium complex, **11**, had been formed quantitatively.

The conversion of **5** to **11** can be effected by oxidizing **5** to **9** in the presence of any primary or secondary alcohol and then refluxing the anolyte
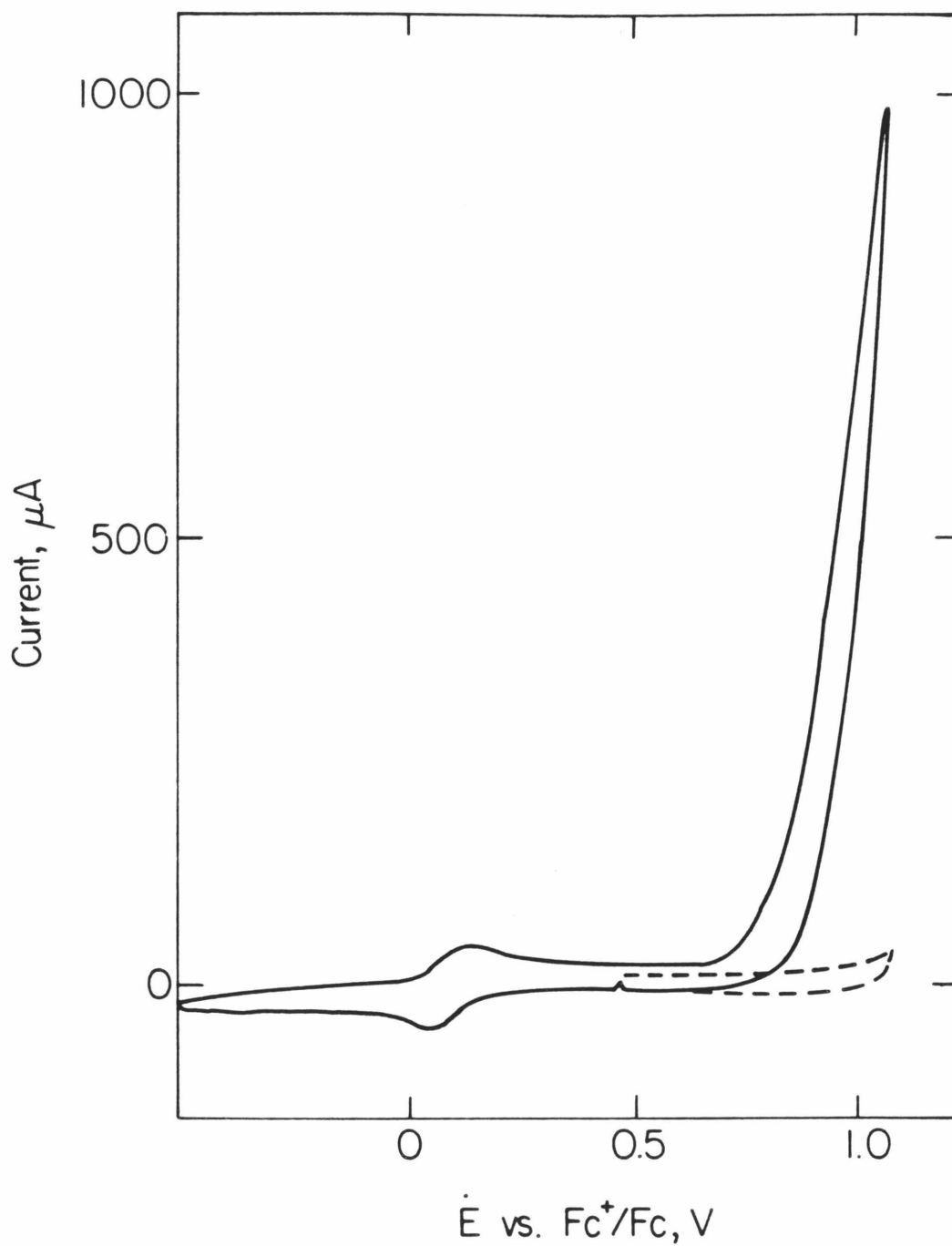
Figure 4.1.   Cyclic voltammogram of 1 mM **11** and 1 M benzyl alcohol in CH_2Cl_2, 0.1 M TBAP at 0.174 cm^2 BPG electrode. Scan rate = 200 mV s^{-1}. The dotted line shows the response with no alcohol present.

solution for 24 h.[4] When **5** is oxidized in the presence of a tertiary alcohol or water, **9'** is produced. Reflux of this anolyte solution produces **11'** which also shows catalytic activity. The compounds **11** and **11'** can be separated from the supporting electrolyte and purified by column chromatography.

Cyclic voltammograms of **11** or **11'** [4] in the absence of added alcohol show no catalytic current. Addition of benzyl alcohol gives rise to large anodic currents as shown in Figure 4.1. No catalytic activity is observed in the absence of the osmium compounds. The catalytic wave observed in the presence of benzyl alcohol corresponds to the oxidation of benzyl alcohol to benzaldehyde (vide infra). Over one hundred turnovers of benzyl alcohol can be achieved by controlled potential electrolysis. The benzaldehyde produced is not further oxidized to benzoic acid or to benzyl benzoate. Although the present system has serious limitations, its high selectivity is potentially an important feature which prompted closer investigation of the osmium complexes involved.

The catalysts **11** and **11'** can be produced directly from **5** without isolation of the intermediates, as described above. Alternatively, they can be obtained by heating pure **9** or **9'** in the presence of acid.[4] In both cases the conversion from **9/9'** to **11/11'** involves a selective and stepwise acid catalyzed hydrolytic cleavage of the two formyl N-C bonds (Scheme 4.1). Thus, each organic imido ligand is converted to a primary organic amido ligand. Cleavage of the second carbonyl N-C bond and the metal-ligand bonds does not readily occur. The coordination geometry at the metal center is unaffected by the reaction. TLC shows the presence of one intermediate, **10** or **10'**, whose R_f is between that of the starting material and the product.

Scheme 4.1. The conversion of **9** to **11** and **9'** to **11'**.
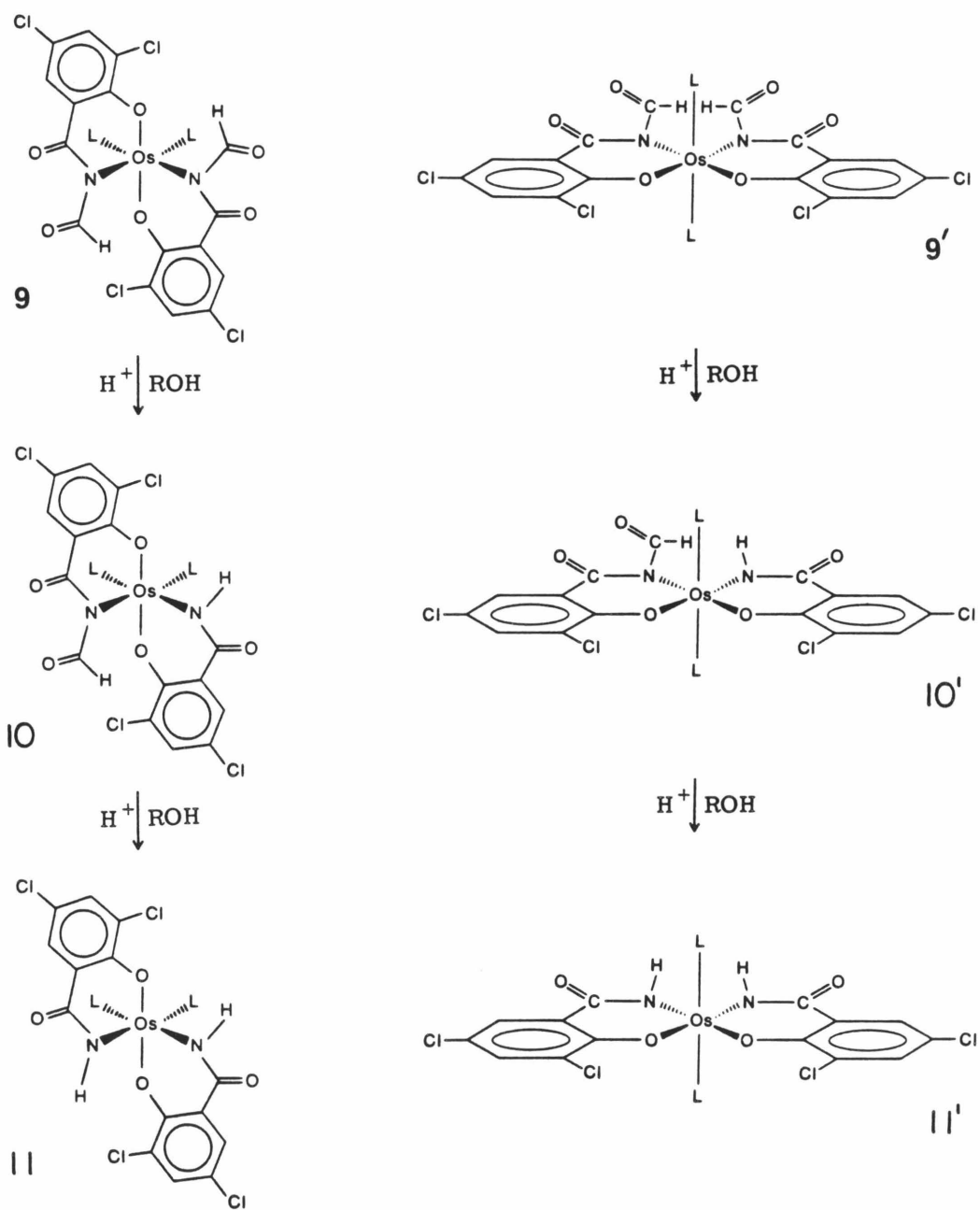
Compounds 10 and 10' have not been isolated or characterized, but are presumed to be the mono imido mono amido compounds as shown.

Both 11 and 11' are deep blue neutral osmium(IV) compounds. They have been characterized by IR, ^{1}H NMR and elemental analysis. In addition, an X-ray crystal structure of compound 11' has been performed. Poor solubility of the pyridine adducts prompted synthesis of the t-Bupy derivatives which exhibit well-resolved paramagnetically shifted NMR spectra (see Table 4.3, page 161).[5] The signals for the t-Bupy ortho protons are shifted upfield. This feature has been shown in the ^{1}H NMR spectra of all the osmium(IV) complexes discussed in Chapters 2 and 3 and has been attributed to an osmium-pyridine $\pi*$ interaction (see Chapter 2, pages 40 and 42).[6]

The X-ray crystal structure of 11' is shown in Figure 4.2.[7] This is the first example of an N-coordinated primary amide complex of osmium(IV). The coordination geometry in 11' is the same as in the parent complex 9', which has also been structurally characterized (see Chapter 3, page 97). The osmium lies at the center of a slightly distorted octahedron with the two bidentate ligands in the equatorial plane and eclipsed t-Bupy ligands in the axial positions. Bond lengths (Table 4.1) and angles (Table 4.2) in the structure are all normal.

The primary amido hydrogens could not be located, due to limitations in the quality of the structure and because of close proximity to the osmium atom. This raises the possibility that the bidentate ligands could be coordinated through O-bound oxyimine groups rather than N-bound primary amides (Fig. 4.3). Bond lengths and angles in the structure would fit either formulation. The IR spectrum shows a strong band in the carbonyl region which seems to be

Figure 4.2   Molecular structure of <u>trans</u>-Os(η^2-CHBA)$_2$(<u>t</u>-Bupy)$_2$, **11'**.
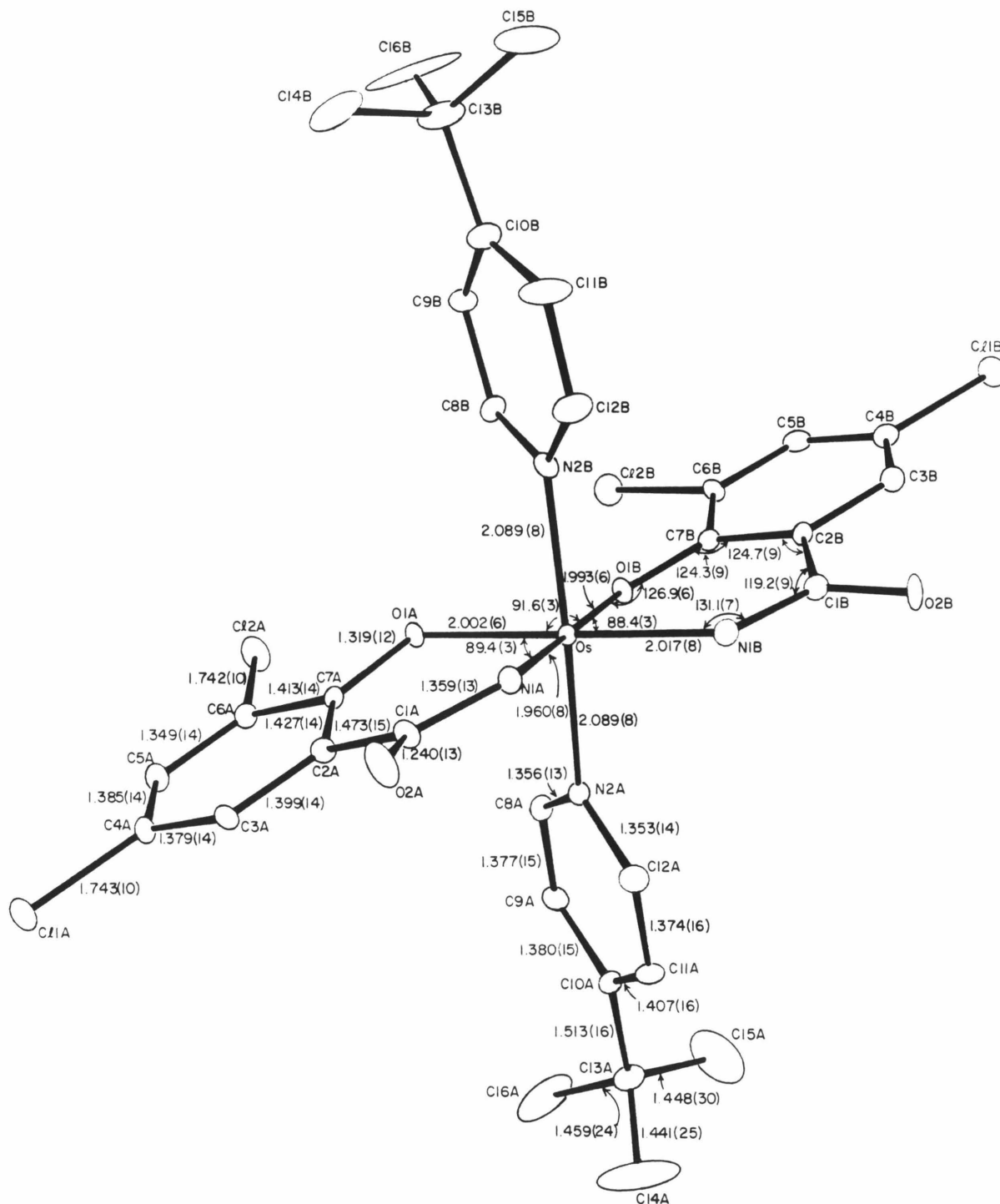
Table. 4.1. Bond distances for <u>trans</u>-Os(η^2-CHBA)$_2$($\underline{t}$-Bupy)$_2$, 11' ($\overset{o}{A}$).

Atoms	Distance	Atoms	Distance
Os-O(1A)	2.002(6)	Os-O(1B)	1.993(6)
Os-N(1A)	1.960(8)	Os-N(1B)	2.017(8)
Os-N(2A)	2.089(8)	Os-N(2B)	2.089(8)
Cl(1A)-C(4A)	1.743(10)	Cl(1B)-C(4B)	1.751(12)
Cl(2A)-C(6A)	1.742(10)	Cl(2B)-C(6B)	1.732(11)
O(1A)-C(7A)	1.319(11)	O(1B)-C(7B)	1.310(12)
O(2A)-C(1A)	1.240(13)	O(2B)-C(1B)	1.268(13)
N(1A)-C(1A)	1.359(13)	N(1B)-C(1B)	1.330(14)
N(2A)-C(8A)	1.356(13)	N(2B)-C(8B)	1.344(13)
N(2A)-C(12A)	1.353(14)	N(2B)-C(12B)	1.333(15)
C(1A)-C(2A)	1.473(15)	C(1B)-C(2B)	1.480(15)
C(2A)-C(3A)	1.399(14)	C(2B)-C(3B)	1.406(15)
C(2A)-C(7A)	1.427(14)	C(2B)-C(7B)	1.444(15)
C(3A)-C(4A)	1.379(14)	C(3B)-C(4B)	1.370(16)
C(4A)-C(5A)	1.385(14)	C(4B)-C(5B)	1.403(16)
C(5A)-C(6A)	1.349(14)	C(5B)-C(6B)	1.365(15)
C(6A)-C(7A)	1.413(14)	C(6B)-C(7B)	1.385(15)
C(8A)-C(9A)	1.378(15)	C(8B)-C(9B)	1.374(15)
C(9A)-C(10A)	1.380(15)	C(9B)-C(10B)	1.381(16)
C(10A-C(11A)	1.407(16)	C(10B)-C(11B)	1.391(18)
C(10A)-C(13A)	1.513(16)	C(10B)-C(13B)	1.504(19)
C(11A)-C(12A)	1.374(16)	C(11B)-C(12B)	1.400(19)
C(13A)-C(14A)	1.442(25)	C(13B)-C(14B)	1.502(25)
C(13A)-C(15A)	1.448(30)	C(13B)-C(15B)	1.478(25)
C(13A)-C(16A)	1.460(24)	C(13B)-C(16B)	1.440(27)

Table 4.2. Bond angles for trans-Os(η^2-CHBA)$_2$(t-Bupy)$_2$, 11' (deg).

Atoms	Angle	Atoms	Angle
O(1A)–Os–O(1B)	91.6(2)		
O(1A)–Os–N(1A)	89.4(3)	O(1A)–Os–N(1B)	179.2(3)
O(1A)–Os–N(2A)	87.1(3)	O(1A)–Os–N(2B)	87.3(3)
O(1B)–Os–N(1A)	178.7(3)	O(1B)–Os–N(1B)	88.4(3)
O(1B)–Os–N(2A)	86.3(3)	O(1B)–Os–N(2B)	86.6(3)
N(1A)–Os–N(1B)	90.6(3)	N(2A)–Os–N(2B)	170.8(3)
N(1A)–Os–N(2A)	94.6(3)	N(1A)–Os–N(2B)	92.6(3)
N(1B)–Os–N(2A)	93.7(3)	N(1B)–Os–N(2B)	91.9(3)
Os–O(1A)–C(7A)	124.2(6)	Os–O(1B)–C(7B)	126.9(6)
Os–N(1A)–C(1A)	129.7(7)	Os–N(1B)–C(1B)	131.1(7)
Os–N(2A)–C(8A)	117.3(6)	Os–N(2B)–C(8B)	118.0(7)
Os–N(2A)–C(12A)	125.6(7)	Os–N(2B)–C(12B)	125.1(7)
C(12A)–N(2A)–C(8A)	116.6(9)	C(12B)–N(2B)–C(8B)	116.5(9)
N(1A)–C(1A)–O(2A)	120.1(10)	N(1B)–C(1B)–O(2B)	123.3(10)
C(2A)–C(1A)–O(2A)	120.1(10)	C(2B)–C(1B)–O(2B)	117.5(9)
C(2A)–C(1A)–N(1A)	119.8(9)	C(2B)–C(1B)–N(1B)	119.2(9)
C(3A)–C(2A)–C(1A)	115.2(9)	C(3B)–C(2B)–C(1B)	115.6(9)
C(7A)–C(2A)–C(1A)	123.8(9)	C(7B)–C(2B)–C(1B)	124.7(9)
C(7A)–C(2A)–C(3A)	120.8(9)	C(7B)–C(2B)–C(3B)	119.6(9)
C(4A)–C(3A)–C(2A)	119.7(9)	C(4B)–C(3B)–C(2B)	119.3(10)
C(3A)–C(4A)–Cl(1A)	119.5(8)	C(3B)–C(4B)–Cl(1B)	118.9(9)
C(5A)–C(4A)–Cl(1A)	119.3(8)	C(5B)–C(4B)–Cl(1B)	119.0(9)

Table 4.2. Continued.

| Atoms	Angle	Atoms	Angle
C(5A)–C(4A)–C(3A)	121.2(9)	C(5B)–C(4B)–C(3B)	122.0(11)
C(6A)–C(5A)–C(4A)	118.7(9)	C(6B)–C(5B)–C(4B)	118.5(10)
C(5A)–C(6A)–Cl(2A)	119.0(8)	C(5B)–C(6B)–Cl(2B)	118.1(8)
C(7A)–C(6A)–Cl(2A)	116.7(7)	C(7B)–C(6B)–Cl(2B)	118.8(8)
C(7A)–C(6A)–C(5A)	124.3(9)	C(7B)–C(6B)–C(5B)	123.0(10)
C(2A)–C(7A)–O(1A)	125.5(9)	C(2B)–C(7B)–O(1B)	124.3(9)
C(6A)–C(7A)–O(1A)	119.2(9)	C(6B)–C(7B)–O(1B)	118.2(9)
C(6A)–C(7A)–C(2A)	115.2(9)	C(6B)–C(7B)–C(2B)	117.6(9)
C(9A)–C(8A)–N(2A)	122.7(9)	C(9B)–C(8B)–N(2B)	123.0(10)
C(10A)–C(9A)–C(8A)	121.2(10)	C(10B)–C(9B)–C(8B)	121.9(10)
C(11A)–C(10A)–C(9A)	115.9(10)	C(11B)–C(10B)–C(9B)	114.9(11)
C(13A)–C(10A)–C(9A)	121.7(10)	C(13B)–C(10B)–C(9B)	122.7(11)
C(13A)–C(10A)–C(11A)	122.4(10)	C(13B)–C(10B)–C(11B)	122.4(11)
C(12A)–C(11A)–C(10A)	120.5(10)	C(12B)–C(11B)–C(10B)	120.5(12)
C(11A)–C(12A)–N(2A)	123.1(10)	C(11B)–C(12B)–N(2B)	123.0(11)
C(14A)–C(13A)–C(10A)	113.3(12)	C(14B)–C(13B)–C(10B)	108.1(12)
C(15A)–C(13A)–C(10A)	107.2(14)	C(15B)–C(13B)–C(10B)	110.7(13)
C(16A)–C(13A)–C(10A)	113.4(12)	C(16B)–C(13B)–C(10B)	112.8(14)
C(15A)–C(13A)–C(14A)	112.4(16)	C(15B)–C(13B)–C(14B)	104.4(14)
C(16A)–C(13A)–C(14A)	101.8(14)	C(16B)–C(13B)–C(14B)	109.4(15)
C(16A)–C(13A)–C(15A)	108.8(16)	C(16B)–C(13B)–C(15B)	111.2(15)
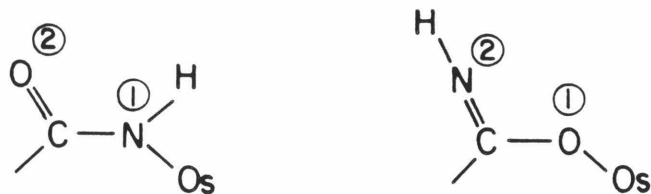
Figure 4.3

most consistent with the amide structure, but since the intensity of imine stretches is variable,[8] the IR data are not totally conclusive. The chemical properties of the complex clearly favor the amide formulation. Imines are susceptible to acid or base catalyzed hydrolysis of the carbon-nitrogen double bond,[9] but 11 and 11' are stable in the presence of strong acid.

The amide formulation has been confirmed by reexamining the X-ray data. The reported structure was refined with appropriate form factors for the amide structure. The atoms in position 1 were assigned a nitrogen form factor and the atoms in position 2 an oxygen form factor. This produced normal isotropic thermal parameters for the atoms in question (oxygens = 3.98 and 4.35; nitrogens = 2.61 and 3.33). The same data were then refined with the form factors switched: oxygen for atom 1 and nitrogen for atom 2. This resulted in abnormal values for the four atoms (position 1 = 1.85 and 2.05; position 2 = 5.02 and 5.94). By refining nitrogen as though it were oxygen the nitrogen electron cloud is essentially spread over too large an area. Therefore the thermal parameter increases. Conversely, by refining oxygen as though it were nitrogen, the oxygen electron cloud is forced into too small an area and the thermal parameter decreases. Thus, the structural data clearly support nitrogen coordination of the amide group.

Compound 11, although not structurally characterized, is formulated as the cis-α isomer shown in Scheme 4.1. The coordination geometry is presumed to be the same as in the parent compound 9, since the analogous conversion of 9' to 11' occurs with no isomerization. The NMR data, however, are also consistent with a cis-α configuration in which the amides are trans and the phenoxides cis or with a trans configuration bearing trans amides and trans phenoxides.

The electrochemical syntheses of compounds 11 and 11' from 5 are somewhat inconvenient and are not completely reproducible. We therefore sought a more direct chemical route to the catalysts by coordinating the appropriate bidentate ligand to osmium. The bidentate ligand in 11 and 11' is simply deprotonated 3,5-dichloro-2-hydroxybenzamide (H_2CHBA) or 3,5-dichlorosalicylamide which can be readily obtained in very high yield by chlorination of salicylamide. The ligand has been characterized by IR, ^1H NMR and elemental analysis.

Coordination of two of the bidentate ligands to osmium was achieved by the same method used for the tetradentate HBA ligands (Scheme 4.2). A blue methanol solution of potassium osmate was added at room temperature to an acetone solution containing two equivalents of the ligand. The reaction is quantitative and after recrystallization more than 90% of the product is obtained as a golden-brown powder. The diamagnetic osmium(VI) salt has been characterized by IR, ^1H NMR (Table 4.3, page 161) and elemental analysis. The IR spectrum shows a large band at 820 cm^{-1} which is attributed to the trans dioxo ligands. ^{18}O labeling has confirmed the assignment. Together the IR, NMR and elemental analysis data require equatorial

Scheme 4.2. Coordination of H₂CHBA to osmium.
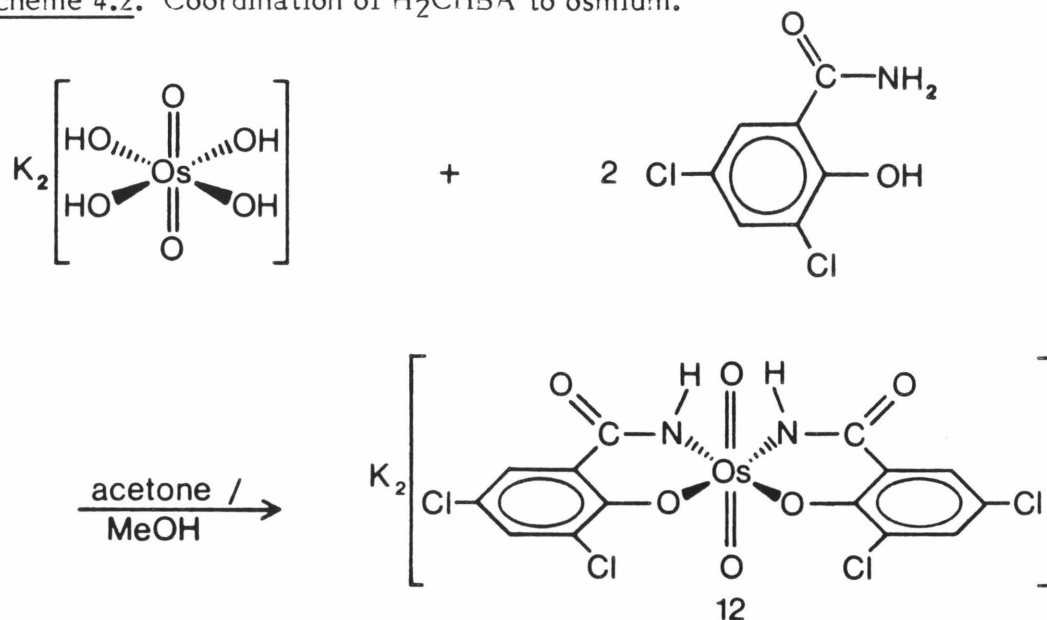
coordination of the two bidentate ligands to osmium, each as a dianion. Here

again the question arises concerning the mode of coordination of the deprotonated

amide (Fig. 4.3). Although not definitive, the IR data and the stability of **12**

to hydrolysis conditions imply coordination through nitrogen. The relative

orientation of the two bidentate ligands, cis vs. trans nitrogens, cannot be

determined based on the spectral data, but the cis configuration is supported

by the fact that compound **11'** can be produced directly from **12** (vide infra).

The conversion of **12** to **11** and/or **11'** was pursued by phosphine

reduction of **12** in the presence of pyridine followed by oxidation with H_2O_2

(Scheme 4.3). This general method was successfully employed in the synthesis

of Os(η^4-CHBA-Et)(py)$_2$, **5** (see Chapter 2, page 35), but the reaction had

required considerable fine tuning before high yields were obtained. The

reduction with **12** proved to be more complex. Mixtures of up to four com-

pounds are formed in significant quantities and the product distribution is

Scheme 4.3. Synthesis of **11'**, **13**, **14** and **15**.
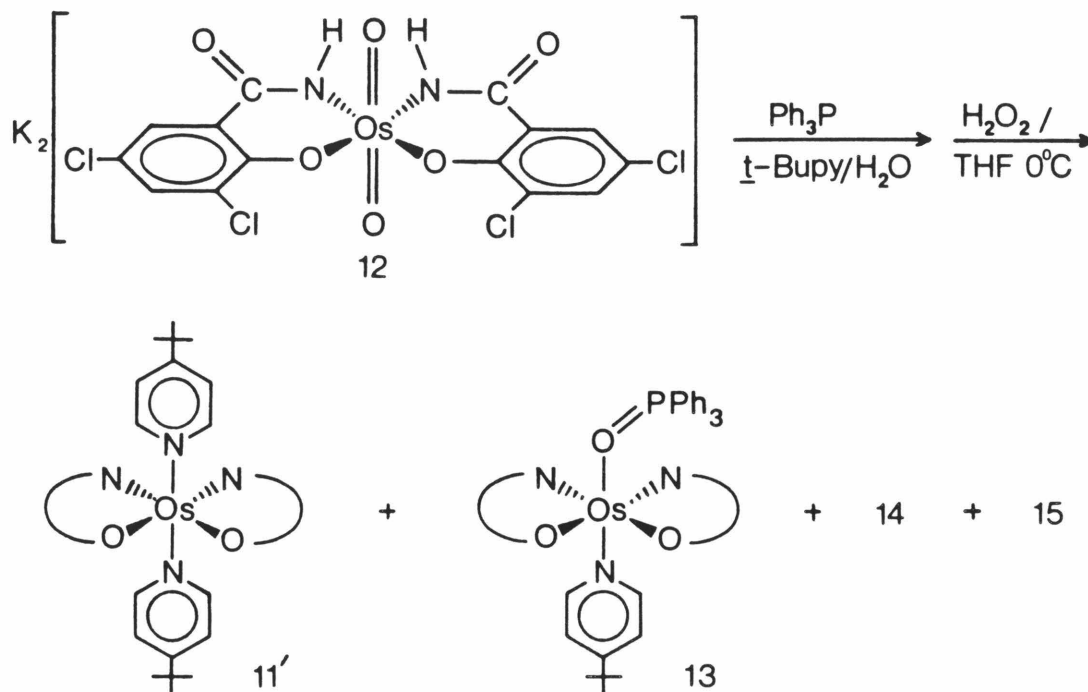
temperature-dependent. If the reduction is run at the same temperature used

in the production of **5** (ca. 60°C) significant decomposition occurs and very

little product can be isolated. At room temperature the reaction is cleaner

and ca. 40% of **11'** is formed in addition to two new compounds, **15** and **14**.

When the reaction was run at 0°C, it appeared that **11'** was formed in still

higher yield with only one side product, **14**, but closer examination by TLC

revealed that the major product was not **11'** but yet another compound, **13**.

The temperature-dependence of the product distribution is summarized in

Figure 4.4. The products of the reaction can be separated and purified by

column and thin layer chromatography. The maximum isolated yield of **11'**

(ca. 30%) was obtained at room temperature and its identity was established

by ^{1}H NMR and IR. None of compound **11** is observed in these reactions.
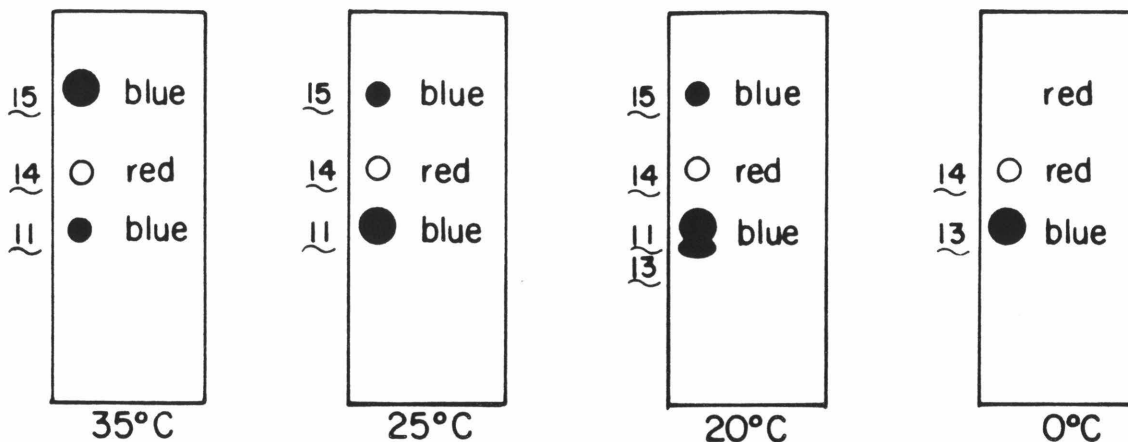
Figure 4.4.   Product distribution as judged by TLC for the reaction of 12 with Ph₃P and pyridine.

The deep violet-blue compound $\underline{trans}$-Os(η^2-CHBA)$_2$($\underline{t}$-Bupy)(Ph$_3$P=O), 13, was isolated as a microcrystalline solid after separation by column chromatography and recrystallization from CH_2Cl_2/hexane. The maximum isolated yield of 13 (42%) was obtained when the reduction was run at 0°C. The structure of the neutral paramagnetic osmium(IV) complex was established by IR, ^{1}H NMR and elemental analysis. The IR spectrum displays strong phosphine oxide bands at 1125, 1080 and 724 cm^{-1}. The ^{1}H NMR spectrum shows the presence of one Ph$_3$P=O, one $\underline{t}$-Bupy and two CHBA ligands (Table 4.3, page 161). The equivalence of the CHBA ligands requires that they occupy the equatorial positions. The 500-MHz proton spectrum clearly separates the ortho, meta and para signals of the Ph$_3$P=O ligand and shows their respective coupling (Fig. 4.5). The ortho and metal protons are coupled to the phosphorus by 13.0 and 3.5 Hz, respectively. Coupling to the para proton is not observed. The ortho signal is therefore a doublet of
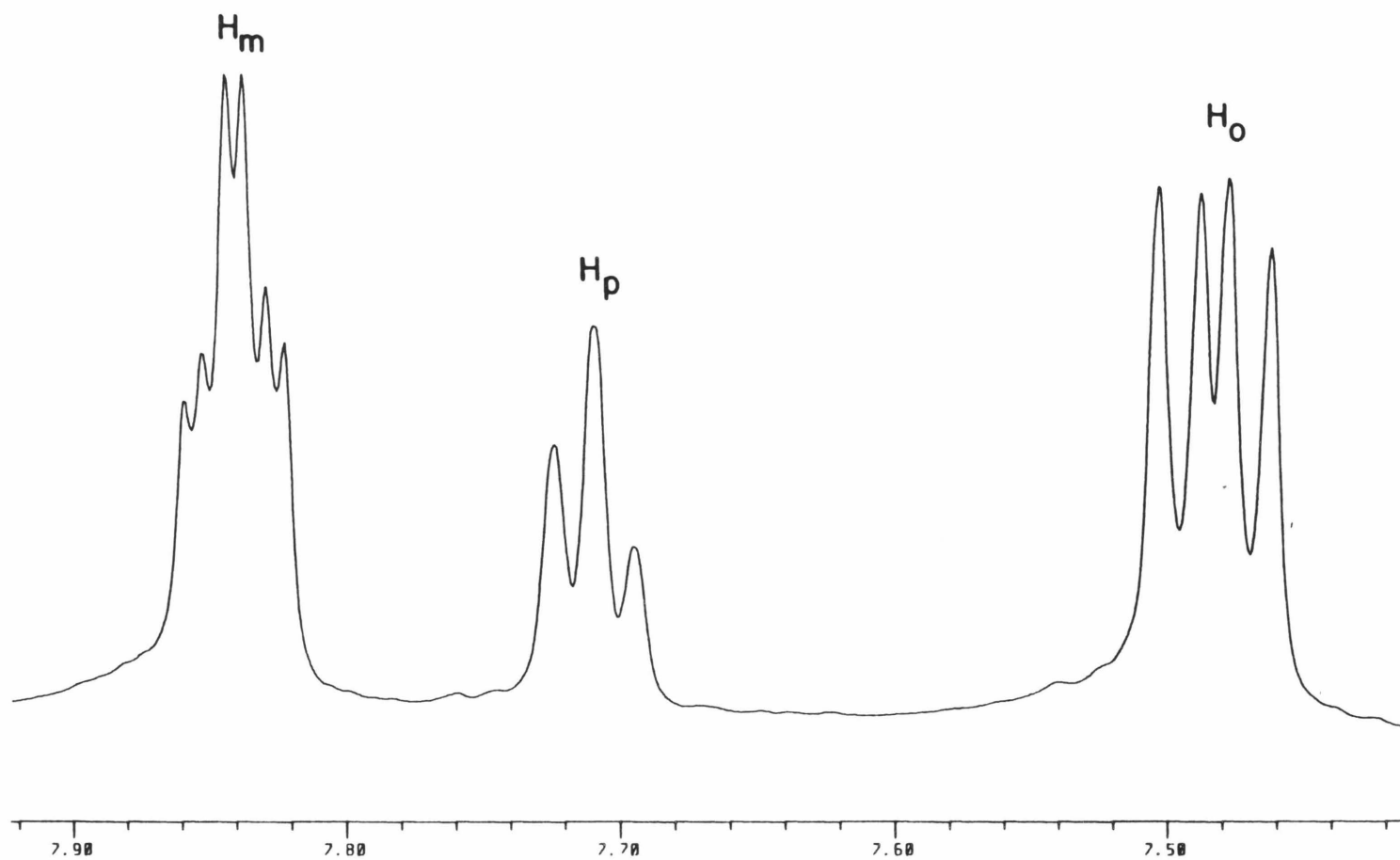
Figure 4.5. Triphenylphosphine oxide signals in the 500-MHz ^{1}H NMR spectrum of <u>trans</u>-Os(η^2-CHBA)$_2$(<u>t</u>-Bupy)(Ph$_3$P=O), 13.

doublets, the meta a doublet of doublets of doublets and the para a triplet. Selective proton decoupling has confirmed the assignment. The cis orientation of the amido nitrogens shown in Scheme 4.3 is inferred from the structure of compound 11', since both 11' and 13 were derived from the same parent complex, 12. However, the cis configuration is not required by the spectral data.

The purple-red compound 14 was isolated from the reaction mixtures by column chromatography and purified with difficulty by repeated chromatographic separations and recrystallizations. The yield of 14 was not optimized. Characterization of the complex by IR, ^{1}H NMR and elemental analysis revealed the same composition as 13, but a different coordination geometry. The IR spectrum is virtually identical to that of 13 with the phosphine oxide bands appearing at 1122, 1066 and 725 cm^{-1}. The ^{1}H NMR spectrum shows one Ph$_3$P=O, one t-Bupy and two inequivalent CHBA ligands with substantial downfield paramagnetic shifts of the two amide protons (56.63 and 41.38 ppm). The 500 MHz spectrum shows the same coupling in the Ph$_3$P=O ligand as seen for complex 13. The spectral data cannot discriminate among the cis-β and the two cis-α geometries, since each would

cis-α   cis-α   cis-β

Figure 4.6

give rise to inequivalent bidentate ligands (Fig. 4.6). Attempts to obtain structural quality crystals have not been successful. Both 13 and 14 exhibit catalytic activity similar to that of 11 and 11'.
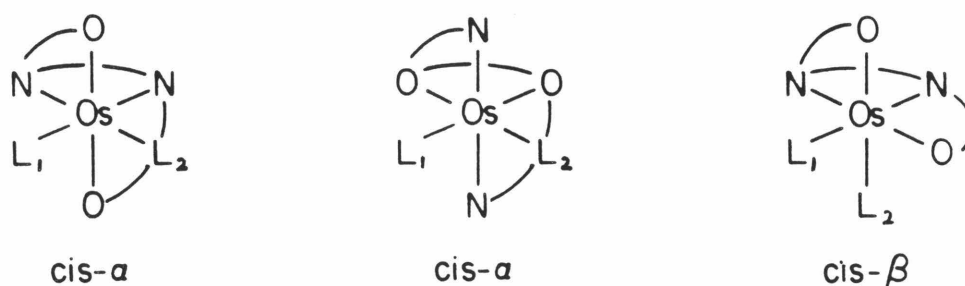
The final species produced in the reduction of 12 is the deep blue complex 15, which can be obtained as a microcrystalline solid after separation and purification by chromatography. The IR spectrum displays t-Bupy bands but no phosphine or phosphine oxide bands. The 90 MHz ^{1}H NMR spectrum (Fig. 4.7) suggests that the complex bears two inequivalent t-Bupy groups and two inequivalent CHBA ligands. Two singlets appear for the pyridine t-Bu groups at 1.37 (9H) and 1.43 (9H) ppm. The four inequivalent aromatic protons of the CHBA ligands are doublets (J = 3 Hz) at 6.87, 7.04, 7.15 and 7.37 ppm. The t-Bupy ortho and meta protons for one ring are seen as two doublets which are coupled to each other (J = 7.5 Hz) at 6.95 (2H) and 8.23 (2H) ppm. The ortho and para protons for the other t-Bupy ring appear as four broad peaks at 5.91, ca. 7.1, 7.59 and ca. 8.3 ppm. Each integrates for a single proton. The most reasonable explanation for this is that hindered rotation of one ring renders the four ortho and meta protons inequivalent. Each signal should still be a doublet because of ortho-metal coupling. At higher field strengths the four clearly appear as doublets (J = 7.5 Hz) (Fig. 4.8), although the signal at 8.24 ppm is partially obscured. Decoupling confirms that each proton is coupled to one of the other four. The protons at 5.83 and 8.24 ppm are coupled to each other and the two at 7.09 and 7.57 are coupled to each other.

One possible explanation of these results is that 15 is cis-β-Os(η^2-CHBA)$_2$(t-Bupy)$_2$, a different isomer of the compounds 11 and 11'. The IR
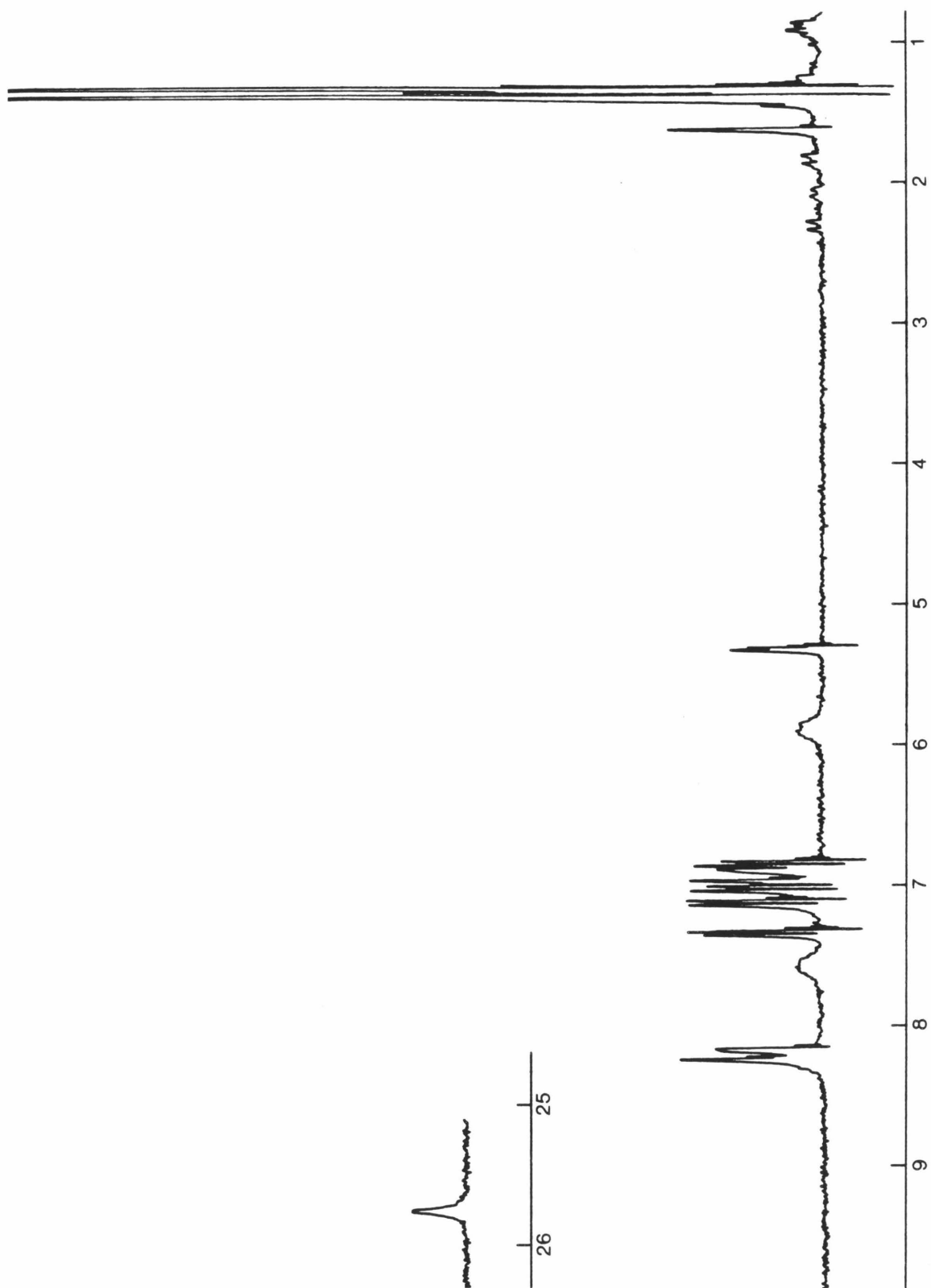
Figure 4.7. 90-MHz ^{1}H NMR spectrum of **15** (CD$_2$Cl$_2$).
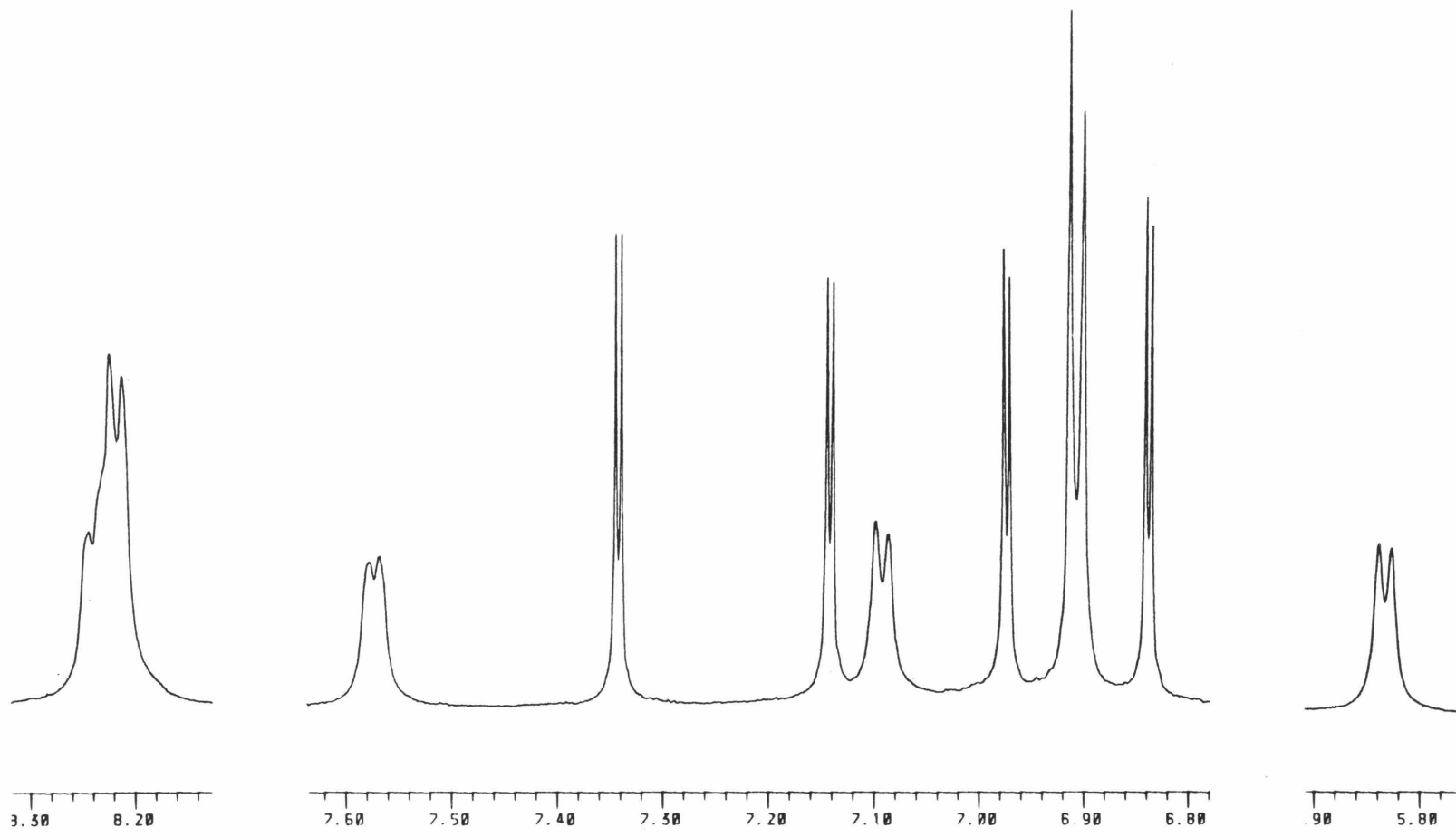
Figure 4.8. 500-MHz ^{1}H NMR spectrum of **15** (CD$_2$Cl$_2$) showing region from 5.8 to 8.3 ppm.

spectrum of 15 is nearly identical to those of 11 and 11', and the elemental

analysis is consistent with this formulation, but no good explanation for the

hindered rotation of one t-Bupy ring is apparent in the cis-β structure. The

cyclic voltammogram of 15 suggests an alternative structure. Whereas the

other osmium(IV) CHBA complexes, 11, 11', 13 and 14, exhibit a a single

reversible osmium(IV/III) reduction near -0.8 V, 15 shows two reversible waves

at -0.70 and -1.05. The potential of the second reduction is significantly

more positive than expected for an osmium(III/II) couple. Furthermore, the

peak current for each wave is exactly half of the value expected for a

monomeric complex. These facts point to a dimeric structure for 15.

The dimer shown in Figure 4.9 bears two inequivalent sets of bidentate

ligands and two inequivalent types of t-Bupy rings and it provides an

explanation for the hindered rotation of one type of ring. The axial pyridines

rotate freely, but molecular models indicate that rotation of the two
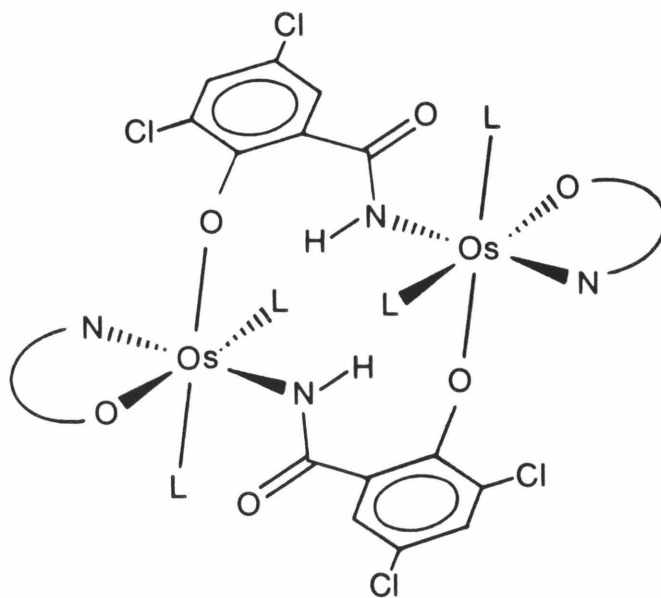
Figure 4.9. A possible dimeric structure for 15.

equatorial rings would be significantly hindered. A variable temperature NMR experiment was run at 200 MHz in an attempt to induce rapid rotation of the hindered rings. As the temperature was raised, the four small doublets broadened into the baseline, but the compound decomposed (ca. 100°C) before coalescence was complete. A solution molecular weight determination employing the "Duck Method" was attempted, but the results were inconclusive. Several attempts to obtain structural quality crystals were unsuccessful. Compound 15 shows little catalytic activity in cyclic voltammetry experiments and almost none in controlled potential oxidations.

The primary amide complexes 11, 11', 13 and 14 exhibit acid-base chemistry which is unique among the osmium compounds described in this thesis and is apparently involved in the catalysis by these species. The compounds can be twice protonated by strong acid. It is a protonated form of the catalysts 11 and 11' which is formed in their syntheses, although they are more easily isolated and handled as neutral compounds. In the conversion of 9/9' to 11/11', perchloric acid is added to the reaction, and in the direct synthesis of 11 or 11' from 5, protons are generated during the ligand oxidation process (see Chapter 3).

The twice protonated form of 11 has been isolated from the electrochemical reaction mixture as a perchlorate salt after its direct formation from 5. The reaction mixture was evaporated to dryness to give a residue which contained the catalyst and a large quantity of the THAP supporting electrolyte. This residue was then washed with benzene to remove the THAP. The compound was eventually isolated as a dark blue powder, recrystallized and characterized by IR and elemental analysis. Structural

quality crystals could not be obtained and low solubility precluded the use of NMR. The IR spectrum shows strong perchlorate bands and the carbonyl region is substantially different than that for the neutral compound. The elemental analysis confirms the presence of two perchlorate ions per osmium. We believe that the most likely sites for protonation are the carbonyl oxygens as shown in Figure 4.10.
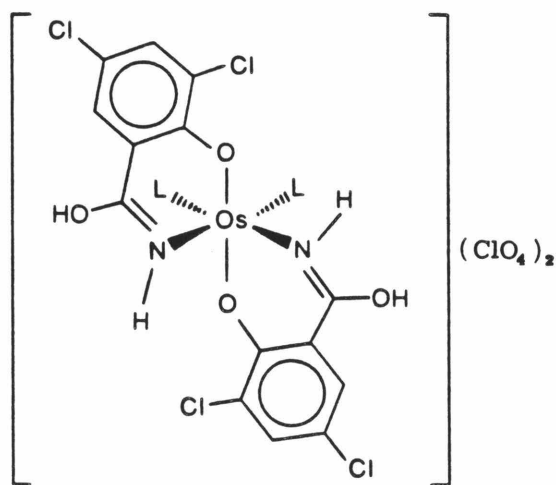
Figure 4.10. Proposed structure of protonated 11.

Isolation and characterization of other protonated species has proven difficult. The diprotonated compounds are strong acids which do not handle well. None of the monoprotonated salts have been isolated in pure form. Although NMR spectra of several of the protonated compounds have been obtained the exact stoichiometry of the species could not be confirmed by elemental analysis. As expected, sequential addition of acid to NMR samples of the neutral compounds causes a gradual shift of the signals, since the discreet species are in rapid equilibrium.

The visible spectrum of trans-Os(η^2-CHBA)$_2$(t-Bupy)(Ph$_3$P=O), **13**, in CH$_2$Cl$_2$ was monitored during the addition of small aliquots of HBF$_4$·Et$_2$O (Fig. 4.11). The experiment clearly indicates the formation of two distinct species during the addition. This supports the contention that **13**, and the other bidentate CHBA osmium complexes, exist in neutral, monoprotonated or diprotonated forms. In each case the conversion from the neutral to the diprotonated species is accompanied by a color change to brilliant turquoise-blue.
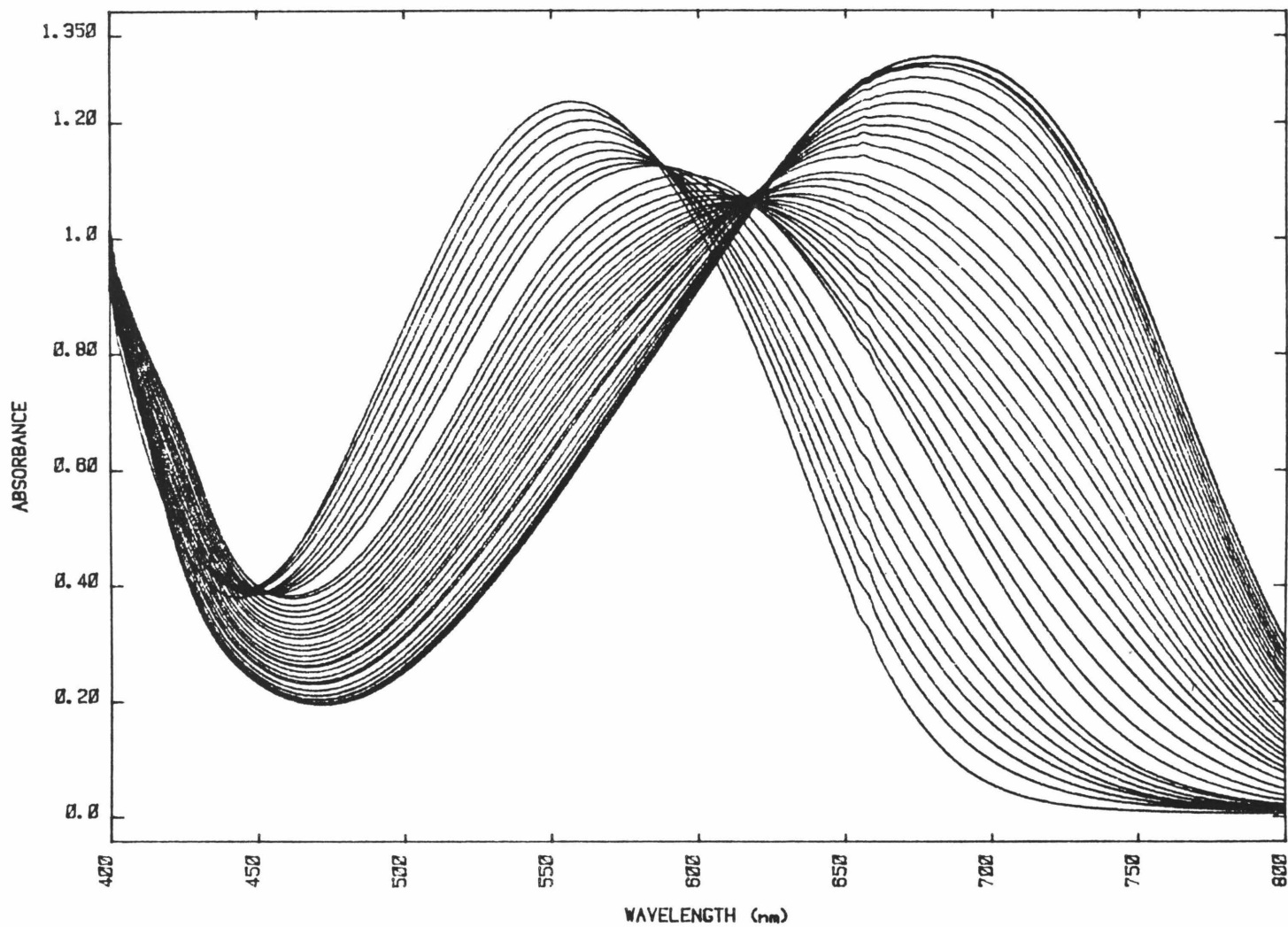
Figure 4.11.   Visible spectrum of trans-Os(η²-CHBA)(t-Bupy)(Ph₃P=O), **13,** in CH₂Cl₂ during the gradual addition of 9 equivalents of HBF₄·Et₂O in THF.

Table 4.3. 90 MHz ^1H NMR data for osmium complexes of H_2CHBA.[a]

Compound	Chelate Ligand		Pyridine			Other
	H_1 (amido)	H_2, H_3 (aromatic)[b]	H_o	H_m	t-Bu	
3,5-dichloro-2-hydroxybenzamide (H_2CHBA)[c]	13.72, s, 2 broad	7.87, d, 2 7.40, d, 2				
12[c]	9.50, s, 2 broad	8.08, d, 2 7.22, d, 2				3.68, s, 2) H_2O
11[d] L = t-Bupy	44.80, s, 2 broad	10.37, d, 2 8.97, d, 2	2.17, d, 4 $J_{o,m} = 7.5$	9.10, d, 4 $J_{m,o} = 7.5$	1.20, s, 18	
11'[d] L = t-Bupy	31.70, s, 2 broad	8.62, d, 2 8.04, d, 2	0.52, d, 4 $J_{o,m} = 7.5$	8.53, d, 4 $J_{m,o} = 7.5$	1.19, s, 18	
13[d,e]	26.64, s, 2 broad	9.32, d, 2 8.48, d, 2	-5.95, d, 2 $J_{o,m} = 7.5$	8.95, d, 2 $J_{m,o} = 7.5$	0.91, s, 9	7.33-7.95) $Ph_3P=O$ m, 15)
14[d,e]	56.63, s, 1 41.38, s, 1	10.11, d, 1 8.82, d, 1 8.78, d, 1 7.15, d, 1	-0.58, d, 2 $J_{o,m} = 7.5$	9.97, d, 2 $J_{m,o} = 7.5$	1.80, s, 9	7.60-8.35) $Ph_3P=O$ m, 15)
15[f,g]	25.75, s, 2 broad	7.37, d, 2 7.15, d, 2 7.04, d, 2 6.87, d, 2	6.95, d, 2 $J_{o,m} = 7.5$	8.23, d, 4 $J_{o,m} = 7.5$	1.43, s, 18 1.37, s, 18	8.30, d, 1) H_o,H_m) 5.91, d, 1)) 2nd J = 7.5)) t-Bupy 7.59, d, 1)) ring 7.10, d, 1) H_o,H_m) J = 7.5)

[a]The cheical shifts of the paramagentic Os(IV) species are somewhat concentration dependent. The values reported here are uncorrected. Coupling constants are reported in Hz. [b]$J_{2,3} = J_{3,2} = 3$ Hz, [c]Ppm in d_6-acetone. [d]Ppm in $CDCl_3$. [e]500 MHz ^1H decoupling of the $Ph_3P=O$ signals is discussed on page 150. [f]Ppm in CD_2Cl_2. [g]Appropriate ^1H decoupling at 400 MHz confirms these assignments.

Catalytic Alcohol Oxidation

The electrochemical results discussed below were performed solely by Stephen Gipson. A brief overview of his work on the catalysis is included here, since it provided the impetus for much of the chemistry contained in this thesis.

The complexes **11**, **11'**, **13** and **14** are all catalysts for the electrochemical oxidation of alcohols. The cyclic voltammograms of the four compounds in the absence of alcohols are similar. Each shows a reversible osmium(IV/III) couple between -0.67 and -0.95 V vs. Fc^+/Fc and an irreversible oxidation between +0.52 and +0.69 V (Table 4.4). The

Table 4.4. Formal potentials of osmium catalysts.

Compound	IV/III[a]	V/IV[a]
11 cis-α-Os(η^2-CHBA)$_2$(py)$_2$	-0.67	(+0.66)[b]
11 cis-α-Os(η^2-CHBA)$_2$(t-Bupy)$_2$	-0.71	(+0.69)[b]
11' trans-α-Os(η^2-CHBA)$_2$(t-Bupy)$_2$	-0.71	(+0.60)[b]
13 trans-α-Os(η^2-CHBA)$_2$(t-Bupy)(Ph$_3$P=O)	-0.91	(+0.54)[b]
14 cis-Os(η^2-CHBA)$_2$(t-Bupy)(Ph$_3$P=O)	-0.95	(+0.52)[b]

[a]Potentials were measured in CH_2Cl_2 against the Fc^+/Fc couple (ca. +0.48 vs. SCE). [b]Peak potential for an irreversible oxidation.

electrochemistry of the protonated species is markedly different. For example, in the cyclic voltammogram of protonated **11**, the osmium(IV/III) couple appears at +0.10 V vs. Fc^+/Fc and no anodic activity is seen below

+1.2 V. These potential shifts are consistent with a change from neutral to cationic osmium(IV) species.

Addition of benzyl alcohol to solutions of the protonated species results in large anodic currents which arise from oxidation of the benzyl alcohol to benzaldehyde. The potential of the reversible reduction is unaffected. The catalytic current also appears in the cyclic voltammograms of the neutral compounds when benzyl alcohol is present. For example, with neutral 11 if one first scans cathodic, the reversible osmium(IV/III) couple is seen at -0.67 V and the irreversible oxidation is seen at +0.66 V followed immediately by a large anodic wave. However, on the second scan only the reversible couple of protonated 11 is observed at +0.10 V in addition to the catalytic wave. The protonation occurs because acid is generated in the alcohol oxidation process.

These results demonstrate that the oxidation occurs equally well when the neutral osmium compound or the diprotnated form is the major species in solution. This suggests that the monoprotonated form may be the active species, since it would be present in equilibrium with either the neutral or dicationic species. Several pieces of data are consistent with this. In the first scan with the neutral compounds, the irreversible osmium(V/IV) oxidation can be seen at a lower potential than the catalytic wave, indicating that this oxidation is not directly involved in the catalysis. The diprotonated compounds show no anodic activity in the potential range where the catalytic alcohol oxidation occurs. High acid concentration has also been shown to hinder the alcohol oxidation. Of course it is possible that more than one species in the system is catalytic. Additional study of this point would be

difficult because of equilibrium between the three forms and because pH control and measurement in CH_2Cl_2 are difficult.

Controlled potential oxidation of benzyl alcohol in the presence of the catalysts results in the selective oxidation of benzyl alcohol to benzaldehyde. The production of benzaldehyde was quantified by an HPLC analysis after derivatization with benzoyl hydrazine. No further oxidation of the benzaldehyde to benzoic acid or benzyl benzoate occurs. The system displays no activity for the oxidation of aldehydes or ketones even when they are present in high concentrations. Over one hundred turnovers of benzyl alcohol to benzaldehyde can be achieved by controlled potential electrolysis.

Several important features of the catalytic system are summarized in Tables 4.5 and 4.6. The catalyst lifetimes are determined by monitoring the decrease in catalyst concentration as a function of charge consumed and extrapolating to zero. The catalyst concentration is measured by UV-visible spectroscopy. Current efficiencies are not corrected for charge consumed in the catalyst decomposition process. The results in Table 4.5 show that a high relative concentration of alcohol to catalyst is required for significant catalysis to occur. Increasing the catalyst concentration substantially lowers the lifetime, as does decreasing the alcohol concentration. With no alcohol present the catalyst decomposition requires only about three electrons per osmium. Turnover numbers with alcohols other than benzyl alcohol are quite low (Table 4.6). Current efficiencies are also low here, since the catalyst decomposition accounts for a larger share of the charge consumed. In the oxidation of cyclohexanol and 1-heptanol the products have been identified as the corresponding carbonyl compounds, hexanal and cyclohexanone.

Table 4.5. Effect of concentrations on catalyst lifetime.

[11]	BzOH	Potential[a]	Lifetime	Current Efficiency
0.6 mmol	0.5 M	+0.97 V	254 e^-/Os	97%
1.3	0.5	0.97	217	94
1.6	0.5	1.07	159	96
5.6	0.5	0.97	91	high
1.3	1.0	0.97	297	high
1.3	0.5	0.97	217	94
1.4	0.1	0.97	40	high
1.3	0	0.97	3	--

[a]Potentials were measured in CH_2Cl_2 against the Fc^+/Fc couple (ca. +0.48 V vs. SCE).

Table 4.6. Effect of alcohol on catalyst lifetime.[a]

[11]	Alcohol (0.5 M)	Lifetime	Current Efficiency
1.3 μmol	benzyl alcohol	217 e^-/Os	94%
1.3	1-heptanol	14	70%
1.3	cyclohexanol	10	68%
1.3	t-2-hexen-1-ol	8	--
1.3	allyl alcohol	6	--

[a]Oxidation at +0.97 V vs. Fc^+/Fc.

Table 4.7. Comparative lifetimes of osmium catalysts.[a]

Catalyst	Lifetime	Current Efficiency
11 cis-α-Os(η^2-CHBA)$_2$(py)$_2$	217 e^-/Os	94%
11' cis-α-Os(η^2-CHBA)$_2$(t-Bupy)$_2$	216	99
11' trans-Os(η^2-CHBA)$_2$(t-Bupy)$_2$	36	93
13 trans-Os(η^2-CHBA)$_2$(t-Bupy)(Ph$_3$P=O)	147	98
14 cis-Os(η^2-CHBA)$_2$(t-Bupy)(Ph$_3$P=O)	132	98

[a]Oxidation at +0.97 V vs. Fc^+/Fc in the presence of 0.5 M benzyl alcohol.

The results in Table 4.7 compare the lifetimes of the different catalysts under a given set of conditions. Substitution of t-Bupy for pyridine in 11 has no effect, but the change in coordination geometry from cis-α to trans greatly lowers the lifetime. Substitution of $Ph_3P=O$ for one t-Bupy also lowers the lifetime somewhat, but the different geometries in 13 and 14 have very little effect. The possibility always exists in a catalytic system that the active species is a very minor component which is not readily observed. In this case, the linear relationship between the concentration of the major species and the charge consumed argues against this possibility. Blank experiments have also demonstrated that osmium tetroxide is not the catalytic species.

Although the above system has obvious limitations, its high selectivity is a notable feature which could be exploited if longer catalyst lifetimes were attained. Numerous stoichiometric chemical methods exist for the conversion of primary alcohols to aldehydes, but electrochemical oxidations are generally not very selective for this reaction. Uncatalyzed anodic oxidation of primary alcohols produces aldehydes, acids and esters. The product distributions are dependent on the conditions but current efficiencies for production of aldehydes are generally low. A number of catalytic electrochemical systems which oxidize alcohols have recently been reported. These include systems which oxidize primary alcohols to esters and secondary alcohols to ketones. One system, based on $(trpy)(bpy)RuOH_2^{2+}/(trpy)(bpy)$-$RuO^{2+}$, does oxidize ethanol to acetaldehyde but aldehyde oxidation begins to compete when the ratio of alcohol to aldehyde reaches 40/1. By 100 turnovers the rate of alcohol and aldehyde oxidations are equal.

The electrocatalytic system we have reported here is the only one we know of which delivers such high current efficiencies for the oxidation of primary alcohols to aldehydes. With longer lifetimes these catalysts might be useful in this transformation and possibly in the oxidation of other substrates. More importantly, chiral analogs of long-lived catalysts might be capable of kinetic resolution of racemic alcohols. The potential in this area of oxidative kinetic resolution has been demonstrated by the Sharpless system for catalytic epoxidation of allylic alcohols. In the oxidation of alcohols a kinetic resolution system would preferentially oxidize one enantiomer of a racemic mixture such as sec-butanol, thus leaving the unreacted alcohol optically enriched.

In the osmium chemistry we have explored, all of the bidentate primary amido complexes of osmium(IV) and none of the tetradentate secondary amido complexes of osmium(IV) exhibit catalytic activity. All of these compounds are 16 e$^-$ species which are capable of coordinating alcohol and which have similar redox potentials, but several features are unique to the catalysts. One is the acid-base chemistry they display. The mechanism of the oxidation is unknown, but one possible reason for the difference between the catalysts and the other molecules is the cationic nature of the protonated catalysts. If direct coordination of alcohol to osmium is involved

$$cat. + ROH \rightleftharpoons cat. - OHCH_2R \qquad (4.1)$$

$$cat. - OHCH_2R \longrightarrow cat. + RCHO + 2H^+ + 2e^- \qquad (4.2)$$

in the oxidation (eqs. 4.1 and 4.2) then the cationic complexes would be much better catalysts by virtue of their higher affinity for alcohol.

Another unique feature of the catalysts is the bidentate nature of the CHBA ligand. Detachment and isomerization of a protonated amide (Fig. 4.12) would open another coordination site and encourage alcohl binding to the resultant 14 e$^-$ complex. This reaction is not available to the tetradentate ligand complexes. The ligand detachment process may also be involved in the irreversible catalyst deactivation. Finally, the presence of the primary amide group itself is unique to the catalysts and one can envisage mechanisms which involve attack by alcohol at the amide rather than the metal.
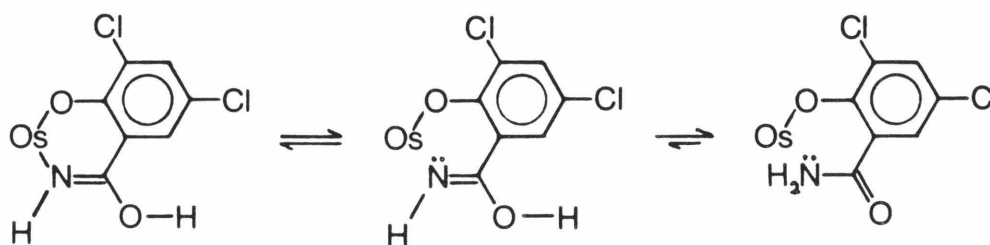
Figure 4.12. Detachment and isomerization of a protonated amide.

Attempts to develop better catalysts in the future must address some of these points. The importance of charge could be examined by alkylating the carbonyl groups on some of the osmium complexes which bear tetradentate CHBA ligands or developing related cationic osmium(IV) species with similar redox potentials. Since the detachment and isomerization of a protonated amide could be involved in both the catalysis and the catalyst degradation, the problem might be alleviated by building higher chelating ligands which incorporate the primary amide at the terminal positions. Loss

of the monodentate ligands might also be responsible for the catalyst destruction. This possibility could be examined by replacing the two pyridines with bipyridine or with diphosphine ligands. A greater understanding of the acid-base chemistry of the catalysts might be gained by working in aqueous solutions. One approach would be to covalently attach the catalysts to electrode surfaces. The feasibility of this has been demonstrated with the complex $Os(\eta^4\text{-CHBA-Et})(4\text{-vinylpyridine})_2$.

Conclusions

The discovery of a catalytic system for the electrochemical oxidation of alcohols was made after electrolyzing a solution of $Os(\eta^4\text{-CHBA-Et})(py)_2$, **5**, to yield <u>cis</u>-α- and <u>trans</u>-$Os(\eta^2\text{-Fo-CHBA})_2(py)$, **9** and **9'**. The catalysts were found to be the osmium(IV) compounds <u>cis</u>-α- and <u>trans</u>-$Os(\eta^2\text{-CHBA})_2(py)_2$, **11** and **11'**, in which the two bidentate primary amido ligands, $CHBA^{2-}$, are coordinated through nitrogen. These compounds are formed by selective stepwise hydrolysis of the to formyl groups in **9** and **9'**. The crystal structure of **11'** was the first example of an N-coordinated primary amido complex of osmium(IV).

Direct chemical synthesis of the catalysts was pursued by coordination of H_2CHBA to osmium. Two of the ligands readily coordinate to osmium(VI) as bidentate dianions in the complex $K_2\left[Os(\eta^2\text{-CHBA})_2(O)_2\right]$, **12**. Treatment of this material with Ph_3P and <u>t</u>-Bupy resulted in the formation of **11'**, **15** and the complexes <u>trans</u>- and <u>cis</u>-$Os(\eta^2\text{-CHBA})_2(\underline{t}\text{-Bupy})(Ph_3P=O)$, **13** and **14**, but not **11**. Compound **15** has been formulated as the osmium dimer $Os_2(\eta^2\text{-CHBA})_4(\underline{t}\text{-Bupy})_4$ in which rotation of the two <u>t</u>-Bupy rings is hindered. All of the complexes are osmium(IV) species which exhibit well resolved paramagnetically shifted NMR spectra.

The compounds **11**, **11'**, **13** and **14** are all catalysts for the electrochemical oxidation of alcohols. Each can undergo mono or diprotonation. This acid-base chemistry is unique among the osmium compounds described in this thesis, and may be involved in the catalysis. The identification of the active species and the mechanism of the oxidation are not known. Further synthetic and mechanistic work would be required for a

complete understanding of the catalysis.

The catalytic system selectively oxidizes benzyl alcohol to benzaldehyde without further oxidation to benzoic acid or benzyl esters. Under optimal condition approximately 150 molecules of benzyl alcohol are oxidized during the lifetime of the catalyst. Other primary alcohols are oxidized to aldehydes and secondary alcohols are oxidized to ketones but the catalytic activity with substrates other than benzyl alcohol is quite poor. Despite the serious limitations of the present system, its high selectivity for the production of aldehydes from primary alcohols is a feature which may warrant further investigation of this chemistry.

Experimental

General Considerations

Materials. All solvents were reagent grade (Aldrich, Baker, Mallinckrodt, M.C.B. or U.S.I.) and were used as received unless otherwise noted. 4-Tert-butylpyridine (reagent, Baker), Cl_2 (Matheson), glacial acetic acid (Aldrich), $H_2^{18}O$ (95%, Monsanto), H_2O_2 (30% Superoxol, Baker), salicylamide (99%, Aldrich), tetrafluoroboric acid (diethyl ether complex, Aldrich), trifluoromethanesulfonic acid (Alfa) and triphenylphosphine (99%, Aldrich) were all used as received. Analytical and preparatory thin layer chromatography plates, 250 and 1000 μM, respectively, were silica gel GF (Analtech).

Physical Measurements. ^{1}H NMR spectra were typically measured at 90 MHz on a Varian EM 390 or a JEOL FX 90-Q spectrometer. Several spectra were measured at 500 MHz on a Bruker WM-500 spectrometer[19] or at 400 MHz on a JEOL JNM-GX 400. Chemical shifts are reported in ppm δ vs. Me_4Si with the solvent ($CDCl_3$ δ = 7.25, CD_2Cl_2 δ = 5.35, $\underline{d}_6$-acetone δ = 2.05) as internal standard. Infrared spectra were taken as nujol mulls on KBr windows and were recorded on a Beckman IR 4240 spectrophotometer. UV-visible spectra were recorded on a Hewlett Packard 8450A spectrophotometer. Elemental analyses were obtained at the Caltech Analytical Facility and at Schwarzkopf Microanalytical Laboratory. All electrochemical experiments were carried out by S. L. Gipson at Caltech. Details of these procedures can be found in reference 1 or will appear in the near future.

Table 4.8. Data collection and refinement information for 11'.

formula	$C_{32}H_{32}Cl_4OsN_4O_4 \cdot \frac{1}{2} H_2O \cdot C_2H_5OH$
formula weight	923.73
space group	$P\bar{1}$
a, Å	10.439(4)
b, Å	12.606(4)
c, Å	15.136(3)
σ, deg	96.04(2)
β, deg	102.44(2)
γ, deg	101.09(2)
v, Å^3	1886.3(9)
Z	2
D_{calcd}, gcm^{-3}	1.643
λ, Å	0.71073
μ, mm^{-1}	3.714
scan type	$\theta - 2\theta$
2θ limits	$2\theta < 40°$
final cycle[a]	
R_F	0.046(3406)
R_F'	0.036(2897)
S	2.39

[a]The number of contributing reflections is given in parentheses; see reference 21 for definitions.

X-ray Crystallography

Data Collection and Structure Determination of 11'.[7] A suitable crystal was obtained by slow crystallization from $EtOH/H_2SO_4$. Oscillation and Weissenberg photographs showed symmetry no higher than $\bar{1}$. The intensity data were collected on a locally modified Syntex $P2_1$ diffractometer with MoK_α radiation ($\lambda = 0.71073$ Å). The unit cell parameters were obtained by least-squares refinement of the orientation matrix using fifteen 2θ values. Three standard reflections, remeasured after each block of 97 reflections, indicated a linear decay of ca. 1% over the exposure time of 142 h. The data were corrected for decay and for absorption; averaging gave 3531 reflections, 3406 with $I > 0$ and 2897 with $I > 3\sigma(I)$.

The position of the osmium atom was derived from a Patterson map, and the subsequent difference Fourier maps indicated the locations of the remaining non-hydrogen atoms of the ligands. Form factors and atomic scattering factors were taken from reference 20. The disordered solvent molecules were placed into positions derived from difference Fourier maps. The hydrogen atoms were placed in calculated positions and were not refined. Several cycles of full-matrix least-squares refinement minimizing $\Sigma w(F_o^2 - (F_c/k)^2)^2$ on all non-hydrogen parameters yielded $R_F = 0.046$, $R_{3\sigma} = 0.036$ and $S = 2.39$.[21] All calculations were carried out on a VAX 11/780 computer using the CRYM system of programs.[22]

Syntheses

All reactions were carried out in air.[23] $Os(\eta^4\text{-CHBA-Et})(py)_2$, 5, was prepared as described in Chapters 2 and 3 and $K_2[Os(OH)_4(O)_2]$ was obtained

by literature methods.[24]

<u>3,5-Dichloro-2-hydroxybenxzamide (H$_2$CHBA)</u>. Salicylamide (5.00 g) was dissolved in glacial acetic acid (220 mL) and the solution warmed to 70°C. Chlorine gas was bubbled through the solution until a yellow color persisted (ca. 0.5 h). The acetic acid was removed under vacuum, and the residue was washed with water and collected by filtration. Recrystallization from acetone/ H$_2$O yielded the product as a white microcrystalline solid (6.98 g, 93%): IR (nujol) 3457 (s, ν_{as}(NH)), 3344 (m, ν_s(NH)), 3215 (m broad, ν(OH)), 1668 (vs, amide I, ν(C=O)), 1620 (s, amide II), 1577 (m), 1259 (s), 1200 (m), 1161 (m), 848 (s), 804 (s), 745 (s) cm^{-1}; ^{1}H NMR (Table 4.3); Anal. calcd. for C$_7$H$_5$Cl$_2$N$_1$O$_2$: C, 40.81; H, 2.45; N, 6.80. Found: C, 40.82; H, 2.53; N, 6.71.

<u>K$_2$[Os(η^2-CHBA)(O)$_2$]·1.3 (H$_2$O), 12</u>.[2] Addition of a blue methanol solution of K$_2$[Os(OH)$_4$)(O)$_2$] (0.100 g in 25 mL) to a colorless acetone solution containing 2.2 equiv of pure H$_2$CHBA (0.123 g in 20 mL) produced an immediate color change to deep orange. The solution was stirred at room temperature for 15 min, then evaporated to dryness to give a quantitative yield of the product. After recrystallization from acetone/CH$_2$Cl$_2$ the orange microcrystalline product was dried under vacuum at 80°C for 7 h. NMR showed the presence of ca. 1.3 molecules of H$_2$O per molecule of complex: yield 184 mg (93%); IR (nujol) 1630 (s), 1592 (s), 1565 (s), 1535 (m), 1300 (s), 1235 (s), 1141 (m), 870 (m), 820 (vs, ν_{as}(OsO$_2$)) cm^{-1}; ^{1}H NMR (Table 4.3); Anal. calcd. for C$_{14}$H$_6$Cl$_4$K$_2$N$_2$O$_6$Os·1.3 (H$_2$O): C, 22.98; H, 1.18; N, 3.83. Found: C, 22.93; H, 1.16; N, 3.83. Incorporation of ^{18}O was effected by allowing the compound to stand with H$_2$^{18}O/acetone for 24 h; IR (nujol)

788 $\left(\text{vs}, \nu_{as}(\text{Os}\,^{18}\text{O})\right)$ cm^{-1}.

$\underline{\text{Trans-Os}(\eta^2\text{-CHBA})_2(\text{t-Bupy})_2, \mathbf{11'}}$.[2] $K_2\left(\text{Os}(\eta^2\text{-CHBA})_2(\text{O})_2\right)\cdot(\text{H}_2\text{O})_4$, 12 (0.100 g), was dissolved in H$_2$O (10 mL) and treated with 2.5 equiv of triphenylphosphine (0.085 g) in $\underline{\text{t}}$-Bupy (1.5 mL). The inhomogeneous mixture was stirred at room temperature for 20 min which produced a color change to deep red-orange. THF (ca. 15 mL) was added and the resultant homogeneous solution was cooled to 0°C. After slow addition of H$_2$O$_2$ (6 mL) at 0°C, the reaction was stirred at room temperature for an additional 20 min. The THF was removed by evaporation which yielded a two-phase mixture. The organic phase was separated, dried over MgSO$_4$, filtered and evaporated to dryness. Removal of the excess $\underline{\text{t}}$-Bupy required heating under vacuum. The residue was dissolved in a minimum of CH$_2$Cl$_2$, placed on a silica gel column and separated by elution with acetone/CH$_2$Cl$_2$. The first fraction (blue) contained compound 15, the second fraction (red) compound 14 and the last fraction (blue) the desired product, 11', which was isolated as a dark blue powder (68 mg, 29%). An analytical sample was obtained by purification on a preparatory TLC plate (60% acetone/40% hexane) followed by recrystallization from CH$_2$Cl$_2$/hexane: IR (nujol) 1618 $\left(\text{s}, \nu(\text{C=O})\right)$, 1598 (s), 1578 (m), 1535 (m), 1502 (m), 1289 (s), 1142 (m), 1067 (m, $\underline{\text{t}}$-Bupy), 1040 (m, $\underline{\text{t}}$-Bupy), 874 (m), 843 (m), 801 (m) cm^{-1}; ^{1}H NMR (Table 4.3); Anal. calcd. for C$_{32}$H$_{32}$Cl$_4$N$_4$O$_4$Os: C, 44.25; H, 3.71; N, 6.45. Found: C, 44.13; H, 3.68; N, 6.31.

$\underline{\text{Trans-Os}(\eta^2\text{-CHBA})_2(\text{t-Bupy})(\text{Ph}_3\text{P=O}), \mathbf{13}}$.[2] $K_2\left(\text{Os}(\eta^2\text{-CHBA})_2(\text{O})_2\right)\cdot$ (H$_2$O)$_4$, 12 (0.425 g), was dissolved in H$_2$O (40 mL) and treated with 2 equiv of triphenylphosphine (0.290 g) in $\underline{\text{t}}$-Bupy (4 mL) as described above for the

synthesis of **11**. The reduced intermediate was oxidized with H_2O_2 (15 mL) and the product mixture was handled according to the procedure employed for **11'**. The column separation was effected by first eluting with CH_2Cl_2 and then gradually increasing the acetone content of the elutant. The first fraction contained compound **14** and the second yielded compound **13** as a dark blue powder (233 mg, 42%). An analytical sample was obtained by purification on a preparatory TLC plate (60% acetone/40% hexane) followed by recrystallization from CH_2Cl_2/hexane: IR (nujol) 1627 $\left[s, \nu(C=O) \right]$, 1590 (s), 1573 (s), 1530 (m), 1500 (w), 1288 (s), 1125 $\left[s, \nu(P=O) \right]$, 1080 (m, $Ph_3P=O$), 1060 (m, t-Bupy), 1025 (m, t-Bupy), 724 (m, $Ph_3P=O$) cm^{-1}; ^{1}H NMR (Table 4.3); Anal. calcd. for $C_{41}H_{34}Cl_4N_3O_5Os$: C, 48.67; H, 3.39; N, 4.15. Found: C, 48.16; H, 3.30; N, 4.10.

Cis-Os(η^2-CHBA)$_2$(t-Bupy)(Ph$_3$P=O), **14**.[2] Compound **14** was produced as a side product in the above syntheses of **11'** and **13**. The yield was variable (10-30%) and was not optimized. The initial column separations of the product mixtures yielded a red fraction which contained **14**. This fraction contained a significant quantity of organic impurities and its evaporation produced a red oil. The oil was converted to a red powder by vigorous stirring with hexane. The compound was then purified by two successive silica gel columns, each followed by recrystallization from CH_2Cl_2/hexane. An analytical sample was obtained by further purification on two successive preparatory TLC plates (60% acetone/40% hexane) followed by slow crystallization from CH_2Cl_2/ hexane and drying under vacuum at 80°C for 18 h: IR (nujol) 1615 $\left[s, \nu(C=O) \right]$, 1598 (sh), 1576 (s), 1536 (m), 1502 (w), 1282 (s), 1122 $\left[s, \nu(P=O) \right]$, 1066 (s, $Ph_3P=O$), 1023 (m, t-Bupy), 725 (m, $Ph_3P=O$) cm^{-1}; ^{1}H NMR (Table 4.3);

Anal. calcd. for $C_{41}H_{34}Cl_4N_3O_5Os$: C, 48.67; H, 3.39; N, 4.15. Found: C, 48.16; H, 3.40; N, 4.21.

$\underline{Os_2(\eta^2\text{-}CHBA)_4(\text{t-Bupy})_4}$, **15**.[2] Compound **15** is produced as a side product in the formation of **11** at room temperature. Although it becomes the major product at slightly elevated temperatures (ca. 35°C) its yield is variable (10-30%) and was not optimized. Compound **15** is contained in the first fraction during column separation of the product mixtures. Additional purification on a preparatory TLC plate (35% acetone/65% hexane) was required in order to separate the compound from residual phosphines and other impurities. Recrystallization from CH_2Cl_2/hexane yielded the product as a deep blue crystalline solid. After drying under vacuum at 80°C for 12 h, the elemental analysis was too high in carbon and hydrogen and too low in nitrogen to fit the formulation for $Os_2(\eta^2\text{-}CHBA)_4(\underline{\text{t-Bupy}})_4$. The TLC purification and recrystallization were repeated twice and the analysis rerun. NMR of the crystalline compound consistently showed the presence of ca. 0.2 molecules of hexane per osmium even after drying under vacuum at elevated temperature for extended periods of time: IR (nujol) 1618 [vs, ν(C=O)], 1608 (sh), 1599 (m), 1578 (m), 1533 (m), 1499 (m), 1279 (vs), 1170 (m), 1129 (m), 1062 (m, $\underline{\text{t-Bupy}}$), 1036 (m, $\underline{\text{t-Bupy}}$), 873 (m), 842 (m), 793 (m) cm^{-1}; ^{1}H NMR (Table 4.3); Anal. calcd. for $C_{64}H_{64}Cl_8N_8O_8Os_2 \cdot 0.4$ (hexane): C, 45.01; H, 3.96; N, 6.32. Found: C, 44.98; H, 3.81; N, 6.28.

$\underline{\text{Cis-}\alpha\text{-}Os(\underline{\eta}^2\text{-}CHBA)_2(\text{t-Bupy})_2}$, **11**. In the electrochemical synthesis of compounds **11** and **11'**, **5** was oxidized to **9** or **9'** as described in Chapter 2. The anolyte solution containing **9/9'**, alcohol, TBAP, and acid generated during the oxidation process, was heated under reflux for 24 h or until TLC indicated

that the conversion to **11/11'** was complete. The reaction mixture was neutralized, and the electrolyte precipitated by addition of ether and removed by filtration. The filtrate was evaporated to dryness, redissolved in acetone and the neutral product precipitated by addition of H_2O. The crude product, **11**, was purified on two successive silica gel columns by elution with $CH_2Cl_2/$ acetone and then recrystallized from CH_2Cl_2/hexane: IR (nujol) 1620 [vs, $\nu(C=O)$], 1580 (s), 1538 (m), 1502 (m), 1277 (s), 1137 (m), 1068 (m, t-Bupy), 1034 (m, t-Bupy), 868 (m), 836 (m), 785 (m) cm^{-1}; ^1H NMR (Table 4.3); Anal. calcd. for $C_{32}H_{32}Cl_4N_4O_4Os$: C, 44.25; H, 3.71; N, 6.45. Found: C, 43.94; H, 3.66; N, 6.33.

[Cis-α-Os(η^2-HCHBA)$_2$(py)$_2$](ClO$_4$)$_2$, Protonated **11**. The protonated compound, **11**, was generated by electrolysis and hydrolysis as described above. The reaction mixture was evaporated to dryness and the residue, containing the protonated product (ca. 80 mg) and THAP (ca. 2.3 g) was then stirred with benzene (ca. 250 mL) for 15 min. The mixture, which contained the product as a blue oil, was allowed to stand for 2 h and then decanted. The oily blue solid was washed with a second aliquot of benzene which was decanted after the mixture stood for 3 h. The blue solid was collected by filtration, dissolved in CH_2Cl_2/acetone and precipitated with hexane. The crystalline product was dried under vacuum for 16 h at 80°C (60 mg): IR (nujol) 1613 (m, py), 1590 (sh), 1578 (vs), 1535 (sh), 1520 (s), 1153 (vs, ClO$_4$), 1108 (vs, ClO$_4$); Anal. calcd. for $C_{24}H_{18}Cl_6N_4O_{12}Os$: C, 30.11; H, 1.90; N, 5.85; Cl, 22.22. Found: C, 30.57; H, 2.21; N, 5.88; Cl, 22.09.

References

(1) Anson, F. C.; Christie, J. A.; Collins, T. J.; Coots, R. J.; Furutani, T. T.; Gipson, S. L.; Keech, J. T.; Krafft, T. E.; Santarsiero, B. D.; Spies, G. H. J. Am. Chem. Soc. 1984, 106, 4460.

(2) Ligand names are: 1,2-bis(3,5-dichloro-2-hydroxybenzamido)ethane, H_4CHBA-Et; N-formyl-3,5-dichloro-2-hydroxybenzamide, H_2Fo-CHBA; 3,5-dichloro-2-hydroxybenzamide, H_2CHBA.

(3) Gipson, S. L. See reference 1.

(4) Gipson, S. L. Unpublished results.

(5) Paramagnetically shifted NMR spectra have been previously observed for Os(IV) complexes. (a) Pawson, D.; Griffith, W. P. J. Chem. Soc., Dalton Trans. 1975, 417. (b) Randall, E. W.; Shaw, D. J. Chem. Soc. A 1969, 2867. (c) Chatt, J.; Leigh, G. J.; Mingos, D. M. P.; Paske, R. J. Ibid. 1968, 2636. (d) Chatt, J.; Leigh, G. J.; Mingos, D. M. P.; Randall, E. W.; Shaw, D. Chem. Commun. 1968, 419.

(6) See Chapter 2 (page 42) for a brief discussion of π-backbonding in this and similar systems.

(7) The X-ray crystal structure determination of 11' was performed by Dr. R. J. Coots at Caltech.

(8) Silverstein, R. M.; Bassler, G. C.; Morrill, T. C. "Spectrometric Identification of Organic Compounds"; John Wiley and Sons: New York, 1974, p. 111.

(9) March, J. "Advanced Organic Chemistry"; 2nd ed.; McGraw-Hill: New York, 1977, p. 806.

(10) Nakamoto, K. "Infrared and Raman Spectra of Inorganic and

CoordinationCompounds"; 3rd ed.; John Wiley and Sons: New York, 1978, p. 335.

(11)   Proper care should be taken when working with perchlorate salts. Due to the possibility of violent explosions, dry samples in particular should only be handled in milligram quantities.

(12)   Nakamoto, K. "Infrared and Raman Spectra of Inorganic and Coordination Compounds"; 3rd ed.; John Wiley and Sons: New York, 1978, p. 242.

(13)   Harrison and Harrison, "Compendium of Organic Synthetic Methods"; John Wiley and Sons: New York, 1971, pp. 137-143.

(14)   Scholl, P. C.; Lentsch, S. E.; Van de Mark, M. R. Tetrahedron **1976**, **22**, 303, and references therein.

(15)   Shono, T.; Matsumura, Y.; Hayashi, J.; Mizoguchi, M. Tetrahedron Lett. **1979**, 165.

(16)   (a) Samuels, G. J.; Meyer, T. J. J. Am. Chem. Soc. **1981**, 103, 307. (b) Yoshida, J.; Nakai, R.; Kawabata, N. J. Org. Chem. **1980**, 45, 5269. (c) Shono, T.; Matsumura, Y.; Hayashi, J.; Mizoguchi, M. Tetrahedron Lett. **1979**, 165. (d) Shono, T.; Matsumura, Y.; Mizoguchi, M.; Hayashi, J. Ibid. **1979**, 3861. (e) Shono, T.; Matsumura, Y.; Hayashi, J.; Mizoguchi, M. Ibid. **1980**, 1867.

(17)   Moyer, B. A.; Thompson, M. S.; Meyer, T. J. J. Am. Chem. Soc. **1980**, 102, 2310.

(18)   (a) Martin, V. S.; Woodard, S. S.; Katsuki, T.; Yamada, Y.; Ikeda, M.; Sharpless, K. B. J. Am. Chem. Soc. **1981**, 103, 6237. (b) Gonnella, N. C.; Nakanishi, K.; Martin, V. S.; Sharpless, K. B. Ibid. **1982**, 104, 3775.

(19)   500-MHz NMR spectra were recorded at the Southern California Regional NMR facility.

(20)   Atomic Scattering factors were taken from: "International Tables for X-ray Crystallography"; Witton: Birmingham, 1974; Vol. IV, pp. 72-97.

(21)   The goodness-of-fit $S = \left(\Sigma w \Delta^2/(n-v) \right)^{1/2}$, n = number of reflections, v = number of parameters; $R_F = \Sigma |\Delta F|/\Sigma |F_o|$ (based on reflections with I > 0), $\Delta F = |F_o| - |F_c|$, $R_F' = R_F$ (based on reflections with $I > 3\sigma_I$).

(22)   The CRYM computing system was used (Duchamp, D. J., California Institute of Technology).

(23)   Although the complexes reported here are generally stable species, appropriate precautions should be taken when working with osmium complexes, since evolution of toxic OsO_4 is possible.[24]

(24)   Malin, J. M. Inorg. Synth. **1980**, _20_, 61.